Nigerian Journal of Polymer Science and Technology

Volume 15, 2020

ISSN: 1119-4111

A PUBLICATION OF THE POLYMER INSTITUTE OF NIGERIA

Nigerian Journal of Polymer Science and Technology
ISSN: 1119-4111 Volume 15, 2020

EDITORIAL BOARD

NATIONAL OFFICERS AND COUNCIL MEMBERS OF THE POLYMER INSTITUTE OF NIGERIA (PIN)

Engr. (Dr.) Innocent Akuvue, FPIN	Chairman, Board of Directors
Chief Alexis N. Ajuebon, FPIN	Immediate Past Board Chairman
Prof. P. A.P Mamza, FPIN, FICCON, FCSN	President
Dr. J. E Imanah, FPIN, FCSN	Immediate Past President
Prof B. T Nwufo, FPIN, FICCON	Secretary to the Board
Prof. (Mrs) C. D Igwebike-Ossi	Vice President (Operations)
Dr. F. O Biotidara, FPIN	Vice President (Finance)
Engr. (Dr.) F. P Momoh, FPIN	General Secretary
Engr. (Dr.) N. C Iheaturu	Assistant Secretary General
Prof. P. M Ejikeme, FCSN	Treasurer
Mr. Ishaya G. Kure	Ag. Publicity Secretary
Engr. (Dr.) G. O Ihekweme	Membership Secretary
Chief A. S. Ogunkoya	Lagos District
Prof. Onyewuchi Akaranta, FPIN	Port Harcourt District
Mr. Inegbedion Festus	Auchi District
Dr. Owen Egharevba	Benin District
Prof Emmanuel Osabohien	Warri District
Prof. Isaac Igwe, FPIN	Owerri District
Prof. Clement Gonah	Zaria District
Prof. (Mrs.) Clementina Igwebike-Ossi	Anambra/Enugu/Ebonyi District
Dr. Adeyanju Olusola	Jos District
Mr. Noble Alu	Abuja District
Dr. Abdullahi Usman Garin Gabas	Kano/Jigawa District
Dr. (Mrs) Doris Boryo	Adamawa/Bauchi/Gombe Chapter
Dr. (Mrs) C. Obele	Anambra Chapter

Prof. Victor Adeola Popoola, FPIN	Ondo/Ekiti Chapter
Mr. Godfrey Okorie	Oyo/Ogun Chapter
Prof. D.S Oguniyyi	Ilorin Chapter
Prof. S. Achi (Acting)	Kaduna Chapter
Prof. Olumuyiwa Turoti	Osun Chapter
Dr. Misbahu M. Ladan (Acting)	Sokoto/Kebbi/Zamfara Chapter
Dr. Micheal Eneji	Kogi/Niger Chapter

PAST & PRESENT PRESIDENT(S) OF THE POLYMER INSTITUTE OF NIGERIA

1. Chief Engr. K. Ogunade, FPIN	1989 – 1995
2. Ms. May Ikokwu, FPIN	1995 – 1998
3. Dr. T. O Odozi, FPIN	1998 – 2001
4. Dr. P. C. O Nzelu, FPIN	2001 – 2005
5. Dr. E. J Asore, FPIN	Oct., 2005 – Dec., 2005
6. Prof. B. T Nwufo, FPIN, FICCON	Dec., 2005 – Oct., 2011
7. Dr. J. E Imanah, FPIN, FCSN	2011 – 2015
8. Prof. P. A. P Mamza, FPIN, FICCON, FCSN	2015 – till date

CORRESPONDENCE

Editor-in-Chief
Prof. S. M Gumel, FCSN, FPIN, FCAI
(smgumel.chm@buk.edu.ng)

Published by:
POLYMER INSTITUTE OF NIGERIA

Nigerian Journal of polymer Science and Technology

Information to Authors

Scope of the Journal

The Journal is devoted to publishing original research and short communications in all aspects of Polymer Science and Technology (Engineering). Articles in the related discipline of Materials Science Technology will also be considered for publication.

Preparation of Manuscript

Manuscript should be written in the third person in an objective, formal and impersonal style. The SI system should be used for all scientific and laboratory data. The full stop should not be included in abbreviations, example m (not m.) ppm not (p.p.m.). All mathematical expressions should be included in the manuscript. Care should be taken to distinguish between capital and lowercase letters, between zero (0) and letter (O), between the numeral (1) and letter (I), etc. Mathematical expressions should fit into a single column when set in type. Fractional powers are preferred to root signs and should always be used in more elaborate formulas. The solids (/) should be used instead of the horizontal lines for fractions whenever possible. Numbers that identify mathematical expressions should be enclosed in parentheses. Refer to equations in the text as "Eq. (1)", etc., or "Equation (1)", etc., at the beginning of a sentence.

Content

All pages must be numbered consecutively. A manuscript would normally include a title, abstract, keywords, introduction, materials and methods, results and discussion, conclusions and references.

i. **Title page**: A short title which should be concise but informative must be provided. This should be followed by the names and full addresses of all authors. E-mail addresses of the corresponding authors must be included.
ii. **Abstract**: The abstract should not be more 220 words. It should give concise factual information about objectives of the work, the methods used, the results obtained and the conclusions reached.
iii. **Keywords**: The authors should list below the abstract keywords for information retrieval purposes. The keywords should identify with main point in the paper.
iv. **Abbreviations and Notations**: Nomenclature must be listed at the

beginning of the paper and should conform to the system of standard SI units. Acronyms and abbreviations should be spelt out in full at their first appearance in the text.

v. **Text**: Papers should be typed single column, with double line spacing on one side of the paper only with ample margins on all sides. The text should be divided into sections each with a separate heading, numbered consecutively. The section heading be typed on a separate line and should be bold.

vi. **Conclusionsand Recommendations**: The conclusions should summarise the findings, clearly stating the contributions and their relevance. Recommendations for implementation or for areas of further work on the subject matter should be made.

vii. **Acknowledgements**: These should be brief and relevant. The names of funding organizations should be written in full. Dedications are not permitted.

viii. **References**: References to publish work should be indicated at the appropriate place in the text, according to the Harvard system (i.e. using author(s)' name(s) and date), with a reference list in alphabetical order, at the end of the manuscript. All references in this list should be indicated at some point in the text and vice versa. Papers by more than two authors but with same first author should be listed by year sequence and alphabetically within each year.

Examples of layout of reference are given below:

Book

Onyeyili, I.O. (2003) Analysis of statistically Determine Structures. El' DemakPublishers, Enugu.

Thesis

Ihueze, C.C. (2005) Optimum Buckling Response Model of GRP Composites. Ph.D. Thesis, University of Nigeria, Nsukka.

Journal

Umerie, S.C., Ogbuagu, A.S., Ogbuagu, J.O. (2004) Stabilisation of palm oils by using Ficusexasprata leaves in local processing methods. *Bioresources Technology*, 94: 307-310.

Conference

Menkiti, M.C., Ugodulunwa, F.X.O., Onukwuli, O.D. (2007) studies on the coagulation and flocculation of coal washery effluent. *Proceedings of the 37th annual conference of the Nigerian Society of Chemical Engineers*, Enugu, 22-24 November, pp169-184.

ix. **Illustrations**: All figures whether line drawings, graphs or photographs should be given a figure number be Arabic numeral in ascending order as reference is first made to them in the text (e.g. Fig. 1). Tables are to be similarly numbered. Captions of figures should be below the respective figures while captions of table should be above the respective tables. The measured quantity with the units, usually in brackets, and the numerical scale should be given alongside the ordinate and abscissa of every graph. All illustrations including chemical structures should be placed in the appropriate places within the text.

x. **Submission of Manuscript**: Manuscript should be submitted to the Editor-in-Chief via pineditor2017@gmail.com.

xi. Manuscripts are considered for acceptance on the understanding that the work described is original and have not been published or submitted for consideration elsewhere and that the author has obtained necessary authorization for publication of the material submitted. Submission of a multi-authored manuscript implies the consent of all the participating authors. A processing fee of N3, 000.00 (Three thousand naira only) is charged per manuscript. Make payment to PIN National Account, Polymer Institute of Nigeria account number **0006664735** at Union Bank Plc. A publication fee for accepted manuscript of **NGN10, 000.00** (Ten Thousand Naira) is charged and should be remitted to Polymer Institute of Nigerian Account number **0006664735** at Union Bank Plc.

xii. **Copyright**: By submitting a manuscript, the authors agree that the copyright for the article is transferred to the Polymer Institute of Nigeria, if and when the article is accepted for publication.

xiii. **Disposal of Material**: Once published, all copies of the manuscript and correspondence will be held for three months before disposal. Authors must contact the Technical secretary if they wish to have any material returned

LIST OF APPROVED DISTRICTS/CHAPTERS OF THE INSTITUTE AND CONTACT INFORMATION ON THEIR CHAIRMEN

CHAPTER	NAME OF CHAIRMAN	PHONE NO.	EMAIL ADDRESS
ABUJA	Mr Noble Alu	08060038607	greengreenpower@yahoo.com
AUCHI	Mr Inegbedion Festus	07038274039	festusinegbedion@yahoo.com
BAUCHI/GOMBE/ ADAMAWA	Dr (Mrs) Doris Boryo E.A.	08037243593	deaboryo@yahoo.com
BENIN	Dr Owen Egharevba	07036858714	eowen@yahoo.com
ENUGU/EBONYI	Prof. (Mrs) Clementina Igwebike-Ossi	08037952401	clemdossi@yahoo.com
ILORIN	Prof. Ogunniyi D.S.	08035828764	dsogunniyi@yahoo.com dsogunniyi@hotmail.com
JOS	Gerald Kure	07032881237	geraldtel@yahoo.com geraldlarry82@gmail.com
KANO/JIGAWA	Dr. Abdullahi Usman Garin Gabas	08065610456	aasalisu@yahoo.com aasalisu.chm@buk.edu.ng
KOGI/NIGER	Dr Michael Eneji	07036552658	michaeleneji@yahoo.com
LAGOS	Chief A.S. Ogunkoya		ogunkoyaabiodun@yahoo.com
ONDO	Prof Babatope Babaniyi	08034718487	niyibabatope@gmail.com bbabatope@oauife.edu.ng
OWERRI	Prof. Isaac Igwe	08066355637	Zik3gh@gmail.com
PORT HARCOURT	Prof. Onyewuchi Akaranta	08033845642	onyewuchi.akaranta@uniport.edu.ng
WARRI	Prof. Emmanuel Osabohien	08036761310	eosabohien@delsu.edu.ng
ZARIA	Prof. Clement Gonah		
OSUN	Prof. Olumuyiwa Turoti	08033766099	muyiwaturotl@yahoo.co.uk
ANAMBRA	Dr. (Mrs.) C. Obele		angelobele1@yahoo.co.uk

TABLE OF CONTENT

Nigerian Journal of Polymer Science and Technology, 2020, Vol. 15, pp1-11

Received: 05/06/2020 Accepted: 24/07/2020

Fourier Transform Infrared Spectroscopic Analysis of Kaolin and Metakaolin used in Geopolymer Production

Odieka, A. E.[1], Onojake M. C.[*1,2] and Obuzor, G. U.[1]

[1]Department of Pure and Industrial Chemistry, University of Port Harcourt, P.M.B 5323, Choba, Port Harcourt, Nigeria.

[2]Centre for Marine Pollution Monitoring and Seafood Safety, University of Port Harcourt, P.M.B 5323, Choba, Port Harcourt, Nigeria

*Corresponding author: ononed@yahoo.com, mudiaga.onojake@uniport.edu.ng

Abstract

Characterizations of Kaolin and metakaolin samples obtained by the thermal treatment of raw clay at 650 ºC were carried out using Fourier Transform Infrared spectrophotometer. This enabled the investigation of the influence of curing conditions on the mechanical properties and microstructures of the geopolymers. Results of Kaolin samples gave characteristic peaks at 3682 cm^{-1}as OH stretching vibration, 2783–2106 cm^{-1} as organic impurities, 1084 cm^{-1} as Si-O-Si or Al-O-Si asymmetric stretch and 769.9 cm^{-1} as Al-O-Si inner surface vibration. Characteristic peaks obtained for metakaolin are 3592 cm^{-1} as OH stretch vibration, 2934–2206 cm^{-1} as organic impurities, 1845 cm^{-1} as H-O-H bending of water and 887cm^{-1} as Si-O and Al-O asymmetric stretch vibration. The metakaolin was used to produce geopolymers at 28 days cure which gave characteristic peaks at 3625 cm^{-1} as OH stretch vibration, 1693 cm^{-1} as OH bending, 756 cm^{-1} as symmetric Si-O-Si or Si-O-Al and 1005 cm^{-1} as Si-O and Al-O asymmetric stretch. These results were comparable with those of previous studies and showed excellent properties for geopolymers

.**Keywords**: Infrared Spectroscopy, geopolymer, alkaline reagent, Metakaolin, microstructures

1. Introduction

Geopolymerization involves the reaction of naturally existing silica-aluminates with an alkaline solution of high concentration. This process results in the formation of a geopolymer which is classified as an inorganic polymer having combined properties of cement, ceramic and polymer (Alehyen et al., 2017). Geopolymers are network or chains of mineral molecules linked with covalent bonds. They are inorganic alumino-silicate polymers (high molecular, macromolecules) formed in an alkaline environment which can serve as a green substitute to the conventional Portland cement by reason of its low carbon footprint.

The structures of geopolymers consist of a polymeric Si-O-Al framework, similar to the zeolites only that zeolites are crystalline whereas geopolymers are amorphous (Aleksandar, Ivan & Henk, 2017). On a nanometer scale, the microstructure of geopolymers consist of small alumino-silicate clusters with minute pores spread within a highly permeable (porous) network with cluster sizes range from 5 to 10nm which can harden at a low temperature (~25 – 80 ºC) in a relatively short amount of time (Romisuhani, Mustafa Al Bakri, & Nur Ain, 2015 , Huang & Han, 2011).

In recent time, studies on geopolymers have become noteworthy because of their excellent mechanical strength, thermal and chemical stability, long-term durability and their ability to behave as adhesives (Valeria & Kenneth, 2003; Bell, Gordon & Kriven, 2005). These properties make them economically viable alternatives used for the production of cement for various applications such as protective coats, high-tech ceramics, insulating foams with thermal stability, fireproof buildings, refractory adhesives (Davidovits, 2015; Richard, Riessen & Vickers, 2015).

Kaolin, a soft, chalk-like and lightweight sedimentary rock, has an earthy odour. It consists mainly of kaolinite, a hydrous aluminium silicate which is formed by the decomposition of potassium feldspars, aluminium silicates and granite (Varga, 2007). Kaolin contains quartz and mica, and less regularly, illite, montmorillonite, haematite, zircon, rutile, halloysite, kyanite and ilmenite. Clays that contain kaolin are the bedrock materials in the ceramic industry for pottery and also in the construction industry for a building. Kaolinite is used for the production of porcelain, electro-porcelain, tiles, chamotte, and bricks (Varga, 2007). Because of the wide applications of kaolinite, its structure and conversion (transformation) on heating has been studied intensely (Štubňa et al., 2006).

Kaolinite which is the main constituent of kaolin has a general structure that consists of Silicate sheets (SiO_4) bonded to aluminium hydroxide layer Al_2 $(OH)_4$ also referred to as gibbsite. The silicate and gibbsite layers are tightly bonded with weak bonds in the SS paired layer, that is, the interstitial layers are normal metals (Aroke, Abdulkarim, & Ogubunka, 2013). The chemical formula for kaolinite can be written as $Al_2Si_2O_5(OH)_4$ or $Si_2Al_2O_5(OH)_4$ which represents two-layer crystal (silicon-oxygen tetrahedral layer joined to alumina octahedral layer exist alternately). The first model of the structure designed by Brindley and Nakahira in 1959 is shown in Figure 1.

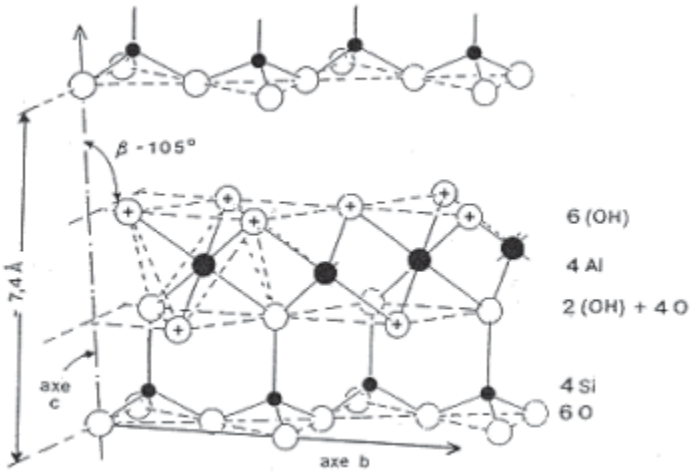

Figure 1: Crystallochemical structure of Kaolinite.

Many states in Nigeria have kaolin clay in abundance and can be sourced as wastes from quarry sites. Important occurrences have been reported in south-western Nigeria at Ubulu-Uku, Auchi, Ukwu-nzu, Ozanogogo, Sapele, and Ubiaja. Also, the Imo clay-shale and the Iyuku clay are important argillaceous bodies of interest in Southern Nigeria (Onyeobi et al., 2013).

Metakaolin is chemically composed of SiO_2, Al_2O_3, Fe_2O_3, MgO, CaO, Na_2O, K_2O and TiO_2. It is obtained by dihydroxylation and dehydrogenation of kaolinite crystals to a

partially disordered structure. This change is accompanied by a rise in the porosity, small shrinkage in the dimension of the sample, weight loss and change of mechanical and electrical properties (Varga, 2007). At a temperature range of 550-600 ºC endothermic dryness of kaolinite starts to produce chaotic metakaolin, but constant hydroxyl loss is perceived at 900 °C (Cadena,& Amigó-Borrás, 2011).

$$2Al_2Si_2O_5(OH)_4 \xrightarrow{550\text{-}650\ ^oC} \underset{\text{Metakaolin}}{2Al_2Si_2O_7} + 4H_2O$$

The Chemical equation for the dehydroxylation process is:

Metakaolin (MK_{650}) materials in geopolymerization differ distinctly in particle size, crystallinity and in purity compared with

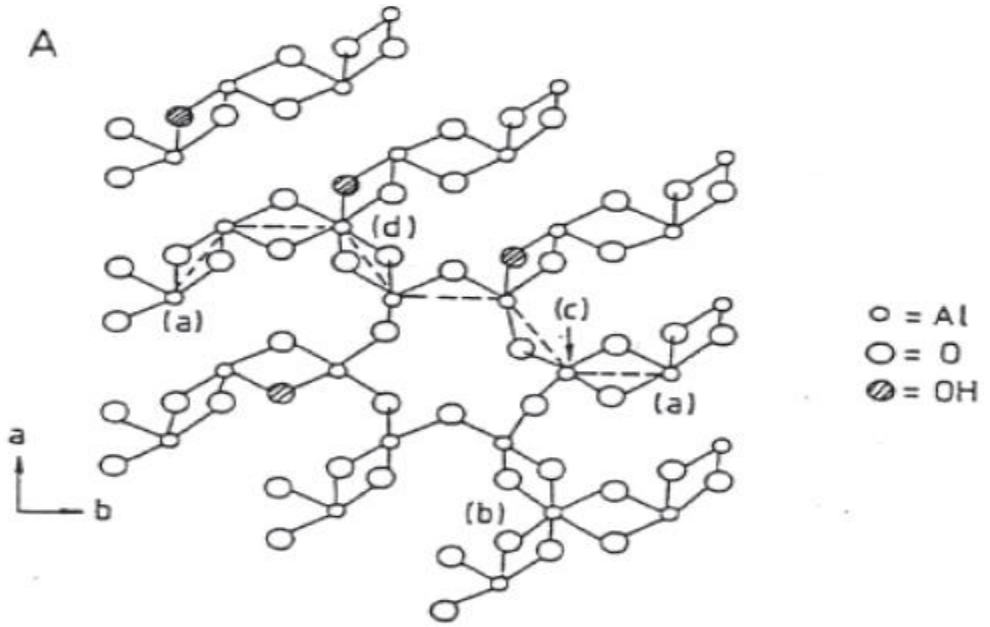

Figure 2: Structure of Metakaolin

Infrared (IR) spectroscopy has been a successful analytical technique and alternative method to XRD and other techniques for analyzing clay and other minerals (Janes & Peter, 2001). Fourier Transform Infrared spectroscopy (FTIR) is used frequently to examine the structure, bonding and chemical properties of clay materials (Madejova, 2003). Clay deposits vary in nature, which means that two deposits cannot have same minerals. Hence, identifying the functional group and fingerprint using FTIR spectra analysis is required. FTIR can give specific identification of minerals, unknown materials existing in a specimen and applied to minute quantities/amount of materials whether solid, liquid or gas. When the FTIR spectra do not provide an acceptable match, individual peaks of FTIR plot yield partial information about specimens (Pittiglio & Doner, 2003). The spectra of clays are generally divided into two (2) regions for ease of interpretation; the fingerprint regions with frequency (wave number) range of 400 to 1300 cm^{-1} and functional group region with frequency (wave number) range of 1300 to 4000 cm^{-1} for middle infrared analysis. The conventional method of frequency assignment is used to discuss results (Aroke et al., 2013).

The objective of this study is to utilize Kaolin clay to produce a Metakaolin-based geopolymeric materials and to characterize the starting materials (Kaolin and Metakaolin) in order to have a better comprehension of the composition and structure of the produced geopolymer. Characterisation of Kaolin and Metakaolin will lead to the production of a new geopolymer and also ascertain the possibility of its utilization in the production of low- cost energy-saving geopolymer ceramics.

2. Materials and Methods

2.1 Sample collection and preparation

Raw kaolin clay was obtained from Somak industries factory, Auchi, Edo State, Nigeria. The commercial grade Na_2SiO_3 was purchased from Redal Chemicals Nigeria, in Port Harcourt, Rivers State. 10g of raw clay in a crucible was placed in a pre-set muffle furnace at 650 ºC for one hour. The clay was removed, allowed to cool, labelled MK_{650} as the starting material (metakaolin) and stored for future usage. To **160g NaOH in a 500ml beaker was added 100ml water and stirred until the NaOH dissolved.** The solution was transferred into a 500ml volumetric flask, made up to volume with distilled water and allowed to cool. 250ml Na_2SiO_3 was added to 100ml of 8.0M NaOH solution in a 1L beaker. The mixture was stirred and transferred to a 500ml volumetric flask, thoroughly mixed and left for 24hrs before use as the reaction solvent which also serves as binder or activator for the geopolymer production.

2.1.1 Geopolymer Preparation

Three grams (3g) of metakaolin (MK_{650}) in a mixer was added to 1.2ml of the reaction solvent (activator) and thoroughly mixed to form a smooth paste. The paste was transferred to 140 x 40 x 40mm mould, vibrated for 10 minutes and covered with transparent polyethylene sheet to set at room temperature. The sample was removed from the mould after 3 days and allowed to cure in a sealed plastic bag for 28days.

2.2 Fourier Transformed Infrared Analysis (FTIR)

0.4g finely ground KBr was added 0.001g sample, thoroughly mixed and moulded into a disc. The disc was inserted into the sample compartment of the instrument. The IR spectrum was generated in transmission mode using an M 530 Buck scientific FTIR spectrophotometer with a wave number region of 4000 to 650 $cm^{-1.}$

3 Results and Discussion

3.1Results

The chemical composition of the raw starting material and produced geopolymer are shown in Tables 1, and 2. FTIR analyses of the kaolin (raw clay) and starting material (RK and MK*650*) with the produced geopolymer are shown in Tables 3. The result range from 756 – 3682 $cm^{-1.}$

Table 1: Assignment of IR bands for Kaolin (raw clay)

Wavenumber (cm^{-1})	RK	Assignment
3682	+	**Inner cage –OH stretch**
3546- 3285	+	**Si-OH and Al-OH stretch**
2783-2106	+	**Organic impurities**
1268	+	**Si – O Normal to plane stretching**
1084	+	**Si- O- Si & Al -O- Si Asymmetric stretch.**
856	+	Al-Fe-OH**deformations (Presence of illite)**
813	+	**Al – O bending vibration.**
769.9	+	Al-O-Si inner surface **vibration.**

RK = Raw kaolin

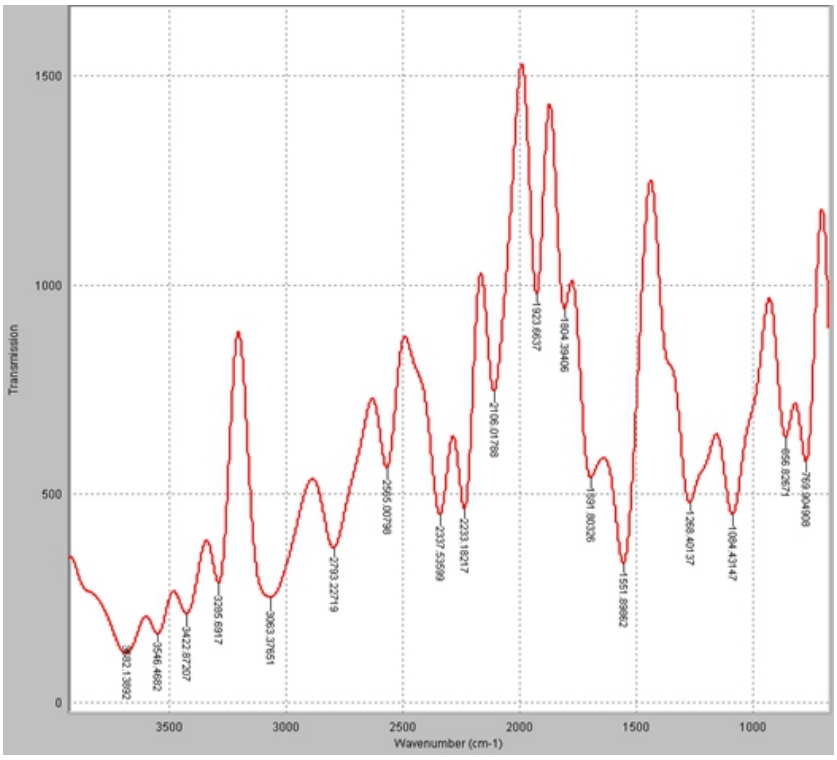

Figure 3: FTIR spectra of raw kaolin clay (RK)

Table 2: Assignment of IR bands for Metakaolin (MK_{650})

Wavenumber (cm^{-1})	MK_{650}	Assignment
3682	+	Al -OH stretch
3592	+	Weak -OH stretch
3425	+	OH stretch of absorbed water.
2934-2206	+	C-H stretch and sharp peak for carbonates
1845	+	H- O- H bending of water
1151	+	Si –O stretch
887	+	Main peak in the fingerprint region Indicating a strong peak of Si-O &Al-O Asymmetric stretch vibration

MK_{650} = Metakaolin (calcined clay).

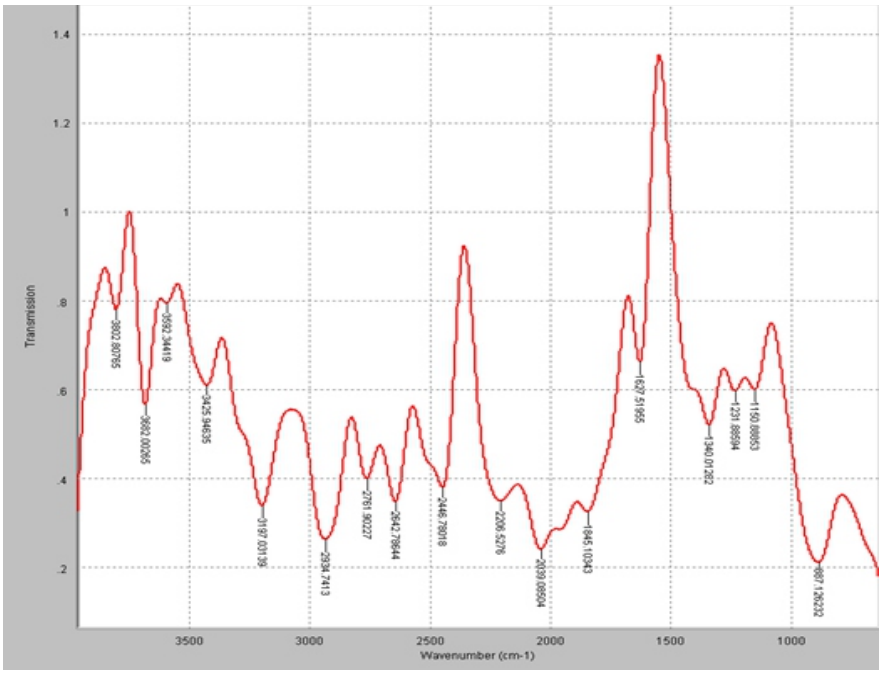

Figure 4: FTIR spectra of Metakaolin **(MK_{650})**

Table 3: Important IR bands of the produced geopolymer (B_{28})

Wavenumber (cm^{-1})	Geopolymer B_{28}	Assignment
1692	+	OH bending Vibrations
1240	+	Asymmetric Si-O-Al stretch
1089	+	Asymmetric stretch of Si-O
1005	+	Al-O, & Si-O Asymmetric stretching vibration.
756	+	Symmetric Si-O-Si or Si-O-Al stretch vibration.

Where B_{28} = geopolymer product cured at 28 days.

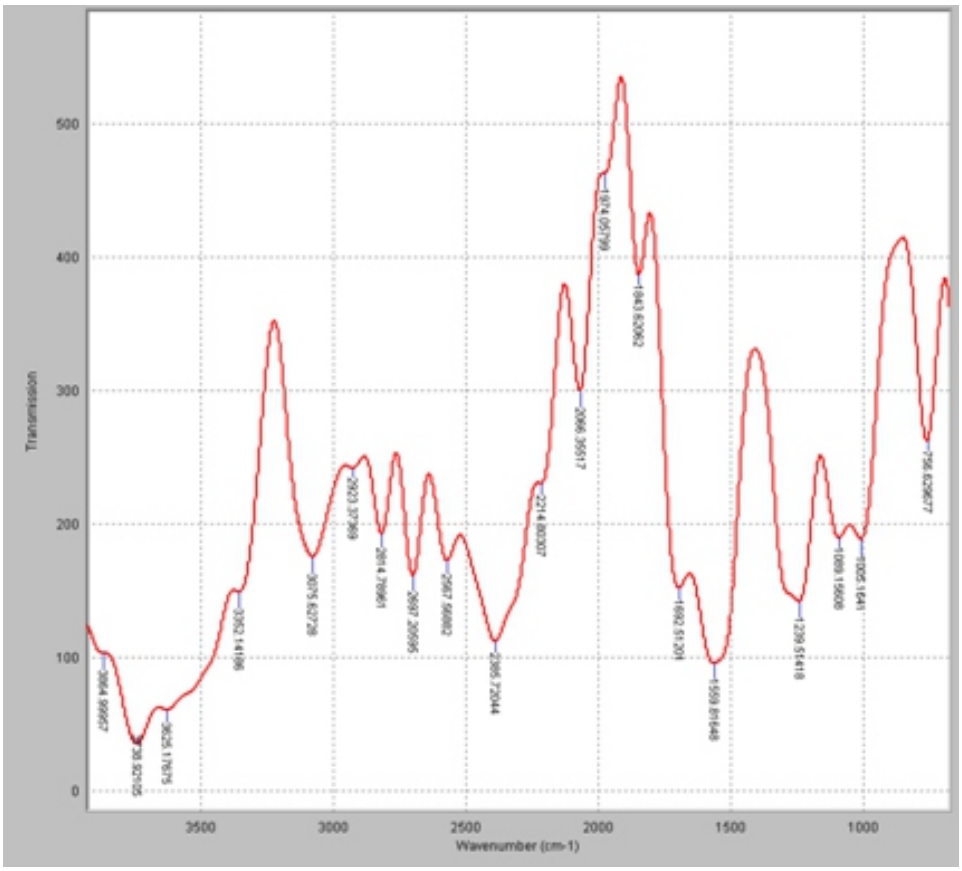

Figure 5**:** FTIR spectra of produced geopolymer (B_{28})

3.2 Discussion

FTIR study of Kaolin (raw clay), metakaolin (MK_{650}), and the produced Geopolymer

The IR study was done to give a detailed analysis of the structure of the raw, starting material and produced geopolymer. Table 1 lists the assignment of bands in the range of 4000 – 650 cm^{-1} present in the spectra of Kaolin (RK). The band at 3682 cm^{-1} for Kaolin (raw Auchi clay) is the main peak and is assigned to inner OH stretch. This agrees closely with 3655cm^{-1} reported by Davarcioglu & Ciftci (2009). The peaks at 3546 -3285 cm^{-1} in the raw Kaolin (RK) are indicative of Si – OH and Al-OH stretch (Aroke et al., 2013). Strong peaks at 2783 – 2106 cm^{-1} shows the presence of organic impurities in the raw Kaolin (RK) (Aroke et al., 2013). The band at 1268 cm-1 infers Si – O normal to the plane stretching while peaks at 1084, 856 and 769.9 cm-1 in Kaolin (raw Auchi clay) shows Si–O–Si and Si-O–Al asymmetric stretch Al–Fe–OH deformation and Al – O – Si inner surface vibration (Aroke et al., 2013; Alehyen et al., 2017).

The FTIR spectrum for Metakaolin (MK_{650}) is shown in Figure 4 while Table 2 highlights the assignment of bands for the material. The bands at 3682 cm^{-1} observed in the raw Kaolin (RK) spectra is indicative of inner OH stretch but present as Al–OH stretching vibration and a weak OH vibration at 3592 cm^{-1} in MK_{650} (Aroke et al., 2013). This suggests a loss of some water from the Kaolin (raw clay) during calcination process at 650 ºC, a C-H stretching vibration was observed at 2934.7 cm^{-1}. OH, stretch of absorbed water was observed at 3425 and 1845 cm^{-1}, indicating the H–O–H bending of water. Si–O stretching vibrations of the metakaolin was observed at 1151 cm^{-1} while Al–OH deformation was observed at 1340 cm^{-1}. The main peak in the functional group region is observed at 2039 while 887 cm^{-1} is the peak observed at fingerprint region. This is attributed to Si O and Al O asymmetric stretching vibration (Morrison & Boyd, 2008; Aroke et al., 2013).

The produced geopolymers showed new bands at 1692, 1089,1005 and 756 cm^{-1} (Table 3). These bands signify that the alkalization process resulted to a decreased intensity of the bands in the reacted materials. The band at 756 cm^{-1} is the main band in the fingerprint region and it is attributed to stretch vibration of Si-O-Si or Si-O-Al bridges. This band (756 cm^{-1}) is sharp because of the high degree of Al substitution in the Si-rich matrix ascribed to Na_2O/SiO_2 ratio (1:2.1) used (Trochez, Mejía de Gutiérrez, Rivera, & Bernal, 2015). Also, when the band of the produced geopolymer is compared to the main fingerprint values of the raw Kaolin (RK) and metakaolin (MK_{650}), it is the lowest. This shift is suggestive of a change in the structure of the starting materials when dissolved in the alkaline medium which formed an aluminosilicate framework. An Alkali environment leads to separation of the MK_{650} by fracture of Al–O bonds which have lower energy (60kcal/mol) than the Si-O bond of 80kcal/mol (Provis, Duxson, Lukey, Separovic, Kriven, & Van Deventer, 2005). Thus, higher alkaline conditions related with the $Na_2O:SiO_2$ favours the aluminosilicate starting material (MK650) initial dissolution which then reacts to form a geopolymer as T-O-T (T may be Si or Al) bands shifts to lower wave numbers.

The band at 1692 cm^{-1} infers bending vibrations of H-O-H. The result is similar to those previously reported by several authors such as Mitra, Mandal, Maitra, & Basumajumdar, 2001; Arioz, Arioz, & Mete 2012 and Trochez et al., 2015. This band show the presence of water (H_2O) in the geopolymer. The strong asymmetric stretching vibration peak of Si-O bond observed at 1089 cm^{-1} shifts to a low wave number (1005 cm^{-1}), infers -OH deformation which is suggestive of the solidification process, a chemical change generating a new substance (Trochez et al.,

2015; Liang, Zaiqin, Yuanyi, & Jing, 2016). The decrease in wavenumber observed during the geopolymerization process may be attributed to partial substitution of SiO_4 species by AlO_4 which leads to an increased Si-O-Al bond. A large shift usually indicates higher -Al inclusions (Alehyen et al., 2017).

Conclusion

The product obtained from the reaction of Metakaolin with the reaction solvent has closed spherical pores formed on the surface, either as a result of the dissolution of metakaolin or by entrained air during preparation. The differences between the Kaolin (RK), metakaolin (MK_{650}) and the product which is the geopolymer are revealed by FTIR spectra results. The main bands of the product which corresponds to a Si-O and Al-O vibration were shifted to a lower value. The geopolymer produced from of metakaolin by the calcinations of Kaolin (RK) is cost effective. The properties of metakaolin-based geopolymer can be productively utilized in the manufacture of fire resistant/fireproof materials, cement, refractories, ceramics, decorative pieces, and thermal insulators.

Acknowledgments

The authors are sincerely grateful to the staff of Somak Industries Limited, Auchi Edo State, Nigeria and Geomine Techno Nigeria Limited, Port Harcourt, Rivers State, for the provision of samples and equipment used for this Research. We also appreciate the efforts of Energy and Research Centre, the University of Nigeria Nsukka for granting us permission to use their laboratory for analyses of the materials.

References

Alehyen, S., El Achouri, M. and Taibi, M. (2017). Characterization, Microstructure and Properties of fly ash-based geopolymer. *Journal of Materials and Environmental Sciences*, 8(5): 1783-1796.

Aleksandar N., Ivan R. and Henk, N. (2017). Geopolymer Materials Based on Natural Zeolite. *Case Studies in Construction Materials,* 6:198–205.

Arioz, E., Arioz, O. and Mete, K. (2012). An experimental study on the mechanical and Microstructural properties of geopolymers. *Procedia Engineering,* 42: 100-105

Aroke, U.O., Abdulkarim, A. and Ogubunka, R.O. (2013). Fourier- transform InfraredCharacterization of Kaolin, Granite, Bentonite and Barite. Abubakar Tafawa Balewa *University Journal of Environmental Technology*, 6(1):43-51.

ASTM Designation C 618-05 (2005). Standard Specification for Coal Fly Ash and Raw or Calcined Natural Pozzolan for Use in Concrete. *Annual Book of ASTM Standards, American Society for Testing and Materials.*

Bell, J., Gordon, M. and Kriven, W. M. (2005). Use of Geopolymeric Cements as a Refractory Adhesive for Metal and Ceramic Joins. *Ceramic Engineering and Science Proceedings,* 26: 407-413.

Brindley, G.W and Nakahira, M. (1959). The kaolinite-mullite reaction series: II, Metakaolin.*Journal of American Ceramic Society,* 42(7): 314–318.

Cadena, A. and Amigó-Borrás, V. (2011). The Effect of Temperature on The Geopolymerization Process of a Metakaolin-Based Geopolymer. *Materials Letters,* 65, 995–998.

Chao, L., Henghu S. and Longtu L. (2010). The Comparison Between Alkali-activated Slag(Si+Ca) and Metakaolin (Si+Al) *Cements: A review. Cement and Concrete Research,* 40:1341–1349

Davarcioglu, B. and Ciftci, E (2009).

Investigation of central Anatolian Clays by FTIRSpectroscopy (Arapli-Yesilhisar-Kayseri, Turkey), *International Journal of Natural and Engineering Sciences,* 3 (3): 154-161.

Davidovits J. (2015). GEOPOLYMER *Chemistry and Applications*, 4th Edition, Institute Geopolymer

Davidovits, J. (1999). Chemistry of geopolymeric systems, terminology, *In Proceedings Second International Conference, Geopolymer* '99.

Egbai, J. C. (2013).Kaolin Quantification in Ukwu-nzu And Ubulu-uku Using Electrical Resistivity Method. *International Journal of Research and Reviews in Applied Sciences*, 14 (3): 692.

Fernandez-Jimenez (2014). A review on alkaline activation: new analytical perspectives, *Construction Material*, 6: 315

Huang, Y., and Han, M. (2011). The influence of α-Al2O3 addition on microstructure, mechanical and formaldehyde adsorption properties of fly ash-based geopolymer products. *Journal of hazardous materials*, 193: 90-94.

Janes, M. and Peter, K. (2001). Clays. Infrared Methods. *Baseline Studies of the Clay MineralSociety Source Journal,* 49 (5): 410-413.

Liang, C., Zaiqin, W., Yuanyi, W. and Jing F. (2016).Preparation and Properties of Alkali Activated Metakaolin-Based Geopolymer. *Materials*, 9(767): 1 – 12

MacKenzie, K.J.D (1978). Feats of clay, or mineral chemistry revisited. Chemistry in New Zealand, 3: 8–12.

Madejova, D. (2003). The Characteristics of Clay. *Journal of Ground Water and Environmental Engineering,*3248: 1-12.

Mitra, N.K., Mandal, A., Maitra, S. and Basumajumdar, A. (2001). Effect of TiO2 on the interaction of dehydroxylated Kaolinite with Al(OH)3 gel in relation to Mullitilisation. *Ceramics International*, 28: 235-243.

Morrison, R.T. and Boyd, R.N. (2008). Organic Chemistry. 6th edition. 590-596.

Ogundiran M.B., Kumar S. (2015). Synthesis and characterization of geopolymer from Nigerian Clay. *Applied Clay Science*,108:173-181.

Onyeobi, T.U.S., Imeokparia, E.G., Ilegiuno, O.A., and Egbuniwe, I.G. (2013). Compositional, Geotechnical and industrial characteristics of Some Clay Bodies in Southern Nigeria. *Journal of Geography and Geology,* 5(2): 73-84.

Pittiglio, S. and Doner, H.E. (2003). The Use of Micro FTIR to Characterize Soil Minerals and Boron Adsorption. *University of California, Berkeley, USA*. Pp 4-8

Provis, J. L., Duxson, P., Lukey, G. C., Separovic, F., Kriven, W. M., and Van Deventer, J. S.(2005). Modeling speciation in highly concentrated alkaline silicate solutions. *Industrial & engineering chemistry research,* 44(23): 8899-8908.

Richard W.D.A., Riessen A.V. and Vickers, L. (2015).). Fire–resistant geopolymers, Springer.

Riessen, A.V., Rickard, W.D.A., Williams, R.P. and Riessen, G.A. (2017). Methods for Geopolymer Formulation Development and Microstructural Analysis. *Journal of Ceramic Science and Technology,* 8(3): 421-432.

Romisuhani, A. Mustafa Al Bakri, A. M. and Nur Ain, J. (2015). Review on Development ofClay-based Geopolymer Ceramic Composites. Trans Tech Publications, Switzerland. *Materials Science Forum,* 803: 37-43.

Štubňa, I., Varga, G. and Trník, A. (2006). Investigation of kaolinite dehydroxylation is still interesting. *Építőanyag,* 58(1): 6–9

Trochez, J.J., Mejía de Gutiérrez, R., Rivera, J.

and Bernal, S.A. (2015). Synthesis of Geopolymer From Spent FCC: Effect of SiO2/Al2O3 and Na2O/SiO2 molar ratios. *Materiales De Construccion*, 65 (317), 1-8

Varga, G (2007).The structure of kaolinite and metakaolinite. *epitoanyag,* 2

Valeria F. F. B. and Kenneth J. D. M., (2003). *Materials Letters.* 57: 1477.

Yip Christina K, Provis John L, Lukey Grant C, van Deventer Jannie S.J., (2008). Carbonatemineral addition to metakaolin-based geopolymers. *Cement and Concrete Composite*, 30: 979–85.

Nigerian Journal of Polymer Science and Technology, 2020, Vol. 15, pp12-28

Received: 05/05/2020 Accepted: 24/08/2020

Reinforcing Effect of Kevlar 49 Fibre on the Mechanical Properties of Polypropylene

E. Danladi[1], P.A.P. Mamza[2], S.A. Yaro[3], M.T. Isa[4], E.R. Sadiku[5] and S.S. Ray[6,]

[1] *Department of Chemistry, Federal University, Gashua, Nigeria*
[2] *Department of Chemistry, Ahmadu Bello University, Zaria, Nigeria*
[3] *Department of Metallurgical and Materials Engineering, Ahmadu Bello University, Zaria, Nigeria*
[4] *Department of Chemical Engineering, Ahmadu Bello University, Zaria, Nigeria*
[5] *Institute of Nano Engineering Research (INER), Department of Chemical, Metallurgical, Materials Engineering, Tswane University of Technology, Pretoria, South Africa*
[6] *National Centre for Nano – Structured and Advanced Materials, Council for Scientific and Industrial Research, Pretoria, South Africa.*

Corresponding Author: danladielijah@yahoo.com

Abstract

It is common knowledge that Polypropylene can be reinforcedby using fillers, e.g. glassfibre, jutefibre, wood pulp, kenafand Kevlarfibresfor applications in the defence, automobile and engineering industries. Kevlar fibre has high strength to weight ratio, isthermally stable and highly resistant. Kevlar fibrecan be used as reinforcementto prepare advanced polymer compositeswith superior properties. In this study,the composites were fabricated by first melting the polymer pellets into films of 1 mm thick in a 100 mm x 100 mm mold, before stacking the polymer films and the woven Kevlar fabric and the whole arrangement preheated for 8 min before being pressed under 500 psi pressure at 190 ^{o}C for 4 min using compression molding technique, followed by cooling for 4 min under pressure followed by removal from the mold. The effect of Kevlar fibre loading (12% - 23%) onthe mechanicalproperties (flexural, impact and tensile strength as well as modulus) and morphology (interfacial bond)of polypropylene laminates fabricated by compression molding technique is reported. The reinforcementfibre increases the tensile, flexural and impact strength of the composite as well as the tensile and flexural moduli, as the percentage Kevlar fibre loading increases. More so, Kevlar fibre inclusion did not significantly affect the density of the composite. The percentage Kevlar fibre incorporated into the polypropylene composites resulted in different morphologies as evident from the microscopic examination.

Keywords: Polypropylene, Kevlar, Composite, Mechanical properties, SEM.

1.0 Introduction

The need for light weight body armor has necessitated the need for high performance fibre reinforced composites. A lot of investigations have been carried out with regard to ballistic impact response of thermoset composite laminates. The use of thermoset matrix material is limited due to a few shortcomings, namely, the need for low temperature storage and long curing process

(Bandaru*et al*., 2016).Thermoplastic on the other hand, are suitable alternative to the thermoset- based composite. This is due to the following attributes, viz: their long shelf life, short processing time, sufficiently tough, chemical resistant, melt processablilty and an ability to be recycled (Bandaru*et al.*, 2016).

Thermoplastics have relatively low brittleness transition temperatures, which allow potential improvement in terms of greater ballistic resistance high mechanical toughness and faster processing time (Bandaru*et al*., 2016; Ghoshal*et al*., 2016). Humanity has used textiles and compliant laminates, not only for clothing and protection against the elements, but for bodily protection. **From** the use of leather on Grecian shields, layered silk in ancient Japan, to chain mail and suits of armor in the middle Ages, personnel protection has sought to protect its wearer from the advances of armaments (Cheeseman and Bogetti, 2003).

However, the advent of firearms has relegated and rendered these forms of protection obsolete until the development of high – strength, high – modulus fibres in the 1960s. These materials ushered in a new era of body armor that offered a protection against small arms munitions (Cheeseman and Bogetti, 2003; Gopinath*et al*., 2012).

Kevlar 49 has a tensile strength comparable with that of carbon fibre and a modulus in between that of glass and carbon but a lower density than both (Isa *et al*., 2013; Yeung and Rao, 2012).

Aramid/ Polypropylene structures have not been studied extensively, despite the relatively cheap cost of polypropylene and the poor fibre adhesion exhibited for good ballistic protection (Carrillo *et al.,* 2012).Debonding and delamination are energy absorbing phenomena that are facilitated by the matrix material(Naik and Shirao, 2004; Zee and Hseih, 1993). Thermoplastics (in particular, PP) have not been studied in details despite the low adhesion of polypropylene to aramids (Zee and Hseih, 1993).

The safety and security of citizens are the primary responsibility of a responsible government. A national military security implies that the government should be able to defend itself in the face of any foreign aggression (Sadiku*et al*, 2019). The fibre type, nature of the fibre and type of matrix are said to determine the properties of a resulting composite material (Nuruzzaman*et al*., 2018). The specific gravity of polypropylene is low as such when Polypropylene is used as matrix; weight reduction can be achieved (Katogi and Takemura, 2014).

Body armors made of woven fabric composites are widely used by military and law enforcement agencies to protect personnel (Uzay*et al*., 2016; Gopinath*et al*., 2012).

When aramid fibres break, they do not fail by brittle cracking, as do glass or carbon fibres. Instead, the aramid fibres fail by a series of small fibril failures, where the fibrils are molecular strands that make up each aramid fibre and are oriented in the same direction as the fibre itself. These many small failures absorb considerable amount of energy, and therefore, resulting in very high toughness (Reis *et al*., 2012).

2.0 Experiment

2.1 Materials

Polypropylene homopolymer with a density of 0.905g/cm^3, melt mass flow rate of

5.3g/10min, was sourced from SASOL, South Africa.

Kevlar 49 woven fabric, 2/2 Twill weave, with a linear density of 42texand areal density of 110g.m^{-2} was sourced from AMT Composites, Kempton Park, Johannesburg, South Africa.The melting point of the polymer was determined as well as the degradation temperature of the polymer in order to ensure stability during processing.

The work was carried out at National Centre for Nano – Structured and Advanced Materials, Council for Scientific and Industrial Research, Pretoria, South Africa.

2.2 Fabrication of composite

The composite was fabricated by first melting 9.1g of the polymer into thin films of 1mm thickness on a Carver Press Model using a mold measuring 100mm x 100mm. This was followed by stacking of the polymer and fabric and placed in a mold in between two Teflon sheets of 2mm thickness at the top and bottom of the mold in order to avoid sticking of the polymer to the mold, before being placed into the Carver Press. The arrangement was preheated for 8min in order to ensure adequate flow of the polymer to enable wetting of the fabric and to remove the moisture content present in the material at190^{o}C, before a pressure of 500psi was applied for 4min. This was followed by cooling for another 4min using the tap cooling system, beforethe removalof the sample from the mold. Table 1 shows the different compositions of the composites and the respective number of plies. (Danladi*et al*., 2020)

Table 1: Fabrication compositions

S/NO	PP (%)	KF (%)	NO OF PLIES
0	100	0	0
1	88	12	3
2	82	18	5
3	77	23	7

2.3 Standards for Characterisations, including samples dimensions and conditions

2.3.1 Powder X – ray diffraction (PXRD) determinations were executed on X –ray diffractometer (XPERT PRO PAnlytical, Netherland) for phase identification. The patterns were run with CuKα radiation with a secondary, monochromator (λ=0.1545 nm) at 45 kV and 40 mA. The diffraction measurements were conducted at room temperature in a Bragg – Brenton geometry with a scan range of 2θ = 5 – 90 using continuous scanning rate of 0.02^{o}/s (Danladi*et al*., 2020)

2.3.2 Tensile properties were determine according to ASTM 638 – 14 types V by using the Instron 5966 model, computer equipped with Bluehill software, a crosshead speed of 5mm/min and applied load of 10kN.

2.3.3 Flexural strength was determined using a specimen of 80mm x 13mm x 3.2mm according ASTM D790 – 03 using the Instron 5966 model, computer equipped with Blue hill software, a crosshead speed of 1.4mm/min and applied load of 10kN.

2.3.4 Impact strength of the composite was determined using a specimen dimension of 85mm x 10mm x 3.2mm according to ISO

179 -01 using a speed of 3.681m/s and Hammer Potential Energy of 7.5J at room temperature.

2.3.5 Dynamic mechanical analysis was determine using a specimen dimension of 40mm x 10mm x 3.2mm according to ASTM 1640 – 04 at a single frequency and using double cantilever.

2.3.6SEM (JEOL JSM -7500F, Japan) operated with an accelerating voltage of 2kV and an emission current of 10μA was used to determine the morphology of the composites.

2.3.7 Water absorption of the composite was determined according to ASTM D570 – 98 for 24hour immersion at room temperature using a specimen dimension of 30mm x 30mm x 3.2mm

2.3.8 Density was determined according to ASTM D792 – 08 using a specimen dimension of 40mm x 10mm x 3.2mm, at 22^{o}C using 99% ethanol.

3.0 Results and Discussion

3.1 XRD result

Fig 1 shows the XRD diffraction pattern of the polymer, polypropylene and the composites. The Kevlar inclusion increased the crystallinity of the composites based on increased in intensity of the composites compare to the neat polymer, this complies with Weidinger - Hermann's equation (Terinte*et al*. 2011).

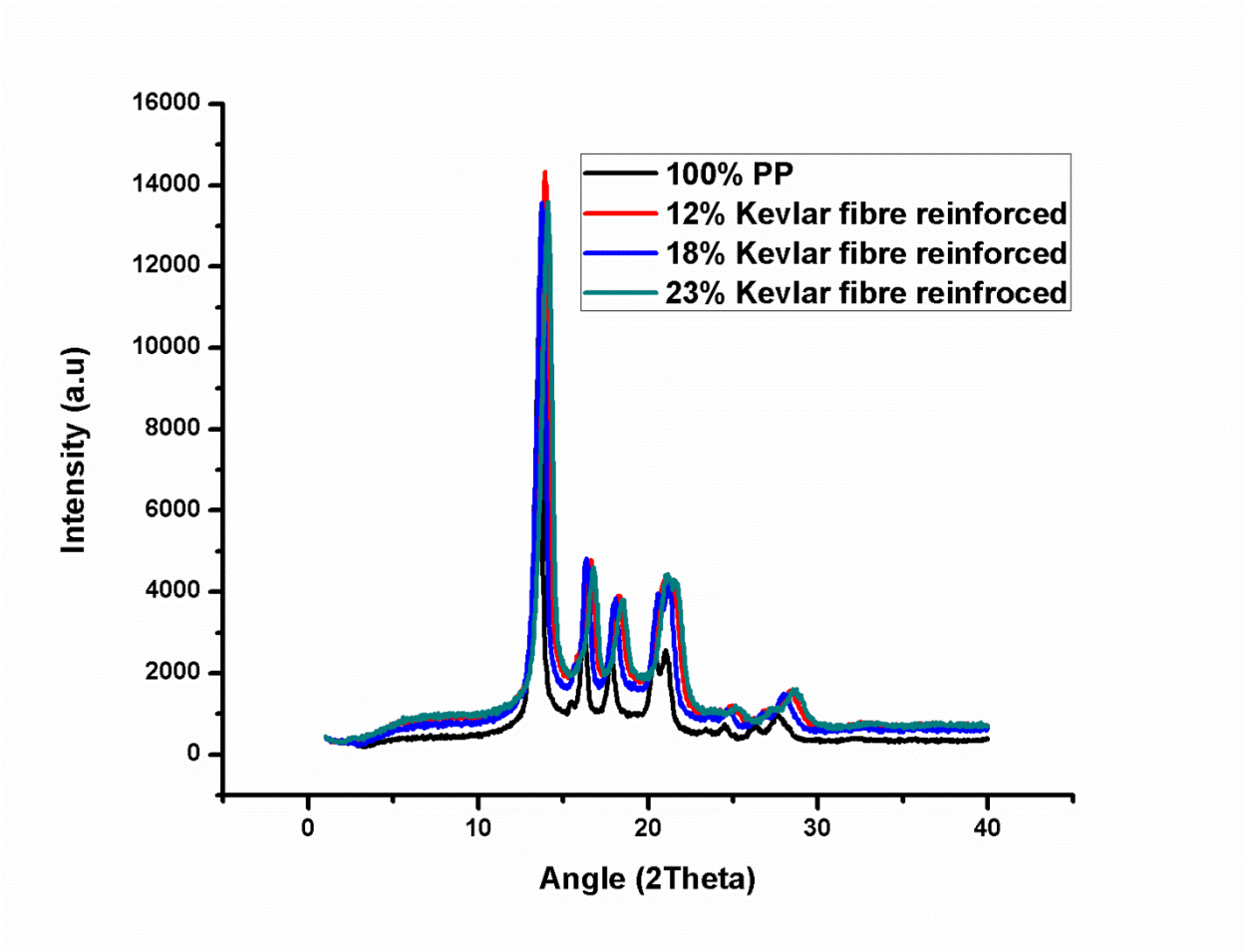

Fig 1: XRD pattern of the polypropylene

3.2 Tensile strength results

Figure 2 shows the effect of fibre loading on tensile strength, as the fibre loading increases. There is a near linear increasing relationship between the tensile strength of the composites and the extent of loading. A maximum tensile strength of 180.8 MPa was obtained at a fibre loading of 23 %, this compared to the tensile strength of the 100 % polymer matrix (41.1 MPa), had an increase on tensile strength of 336.7 %, this could be attributed to the excellent mechanical properties of the Kevlar fibre. Isa *et al*., 2013, reported a tensile strength of 375 MPa at a fibre loading of 40.8 % using unsaturated polyester resin as matrix.

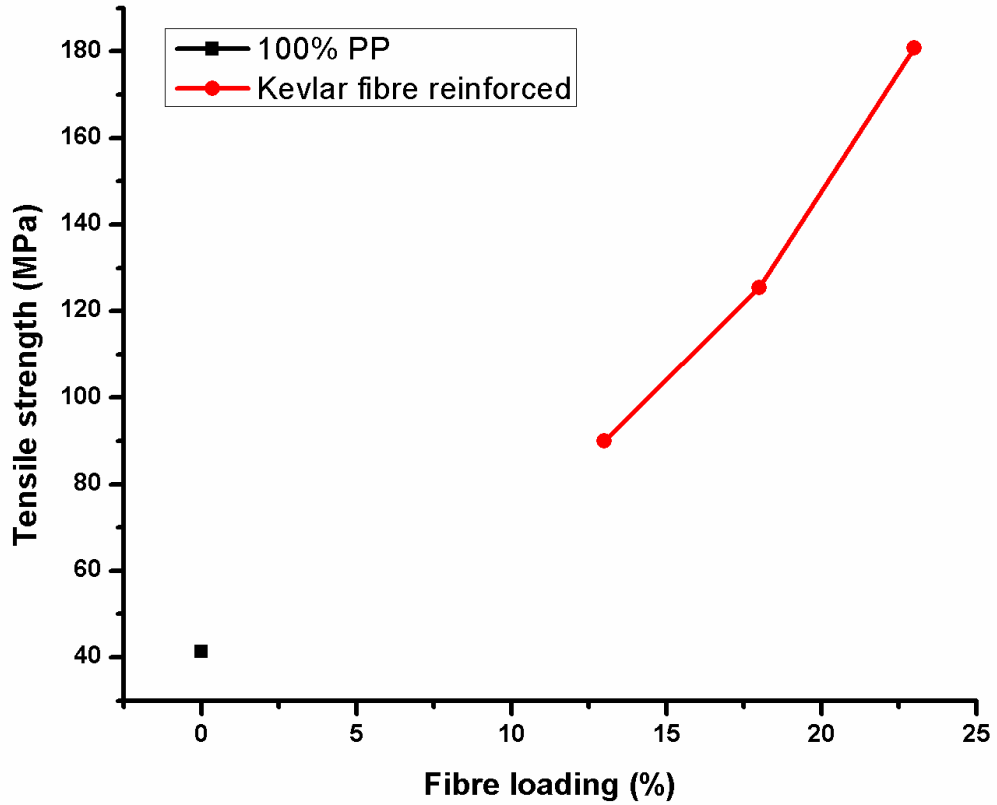

Fig 2: Effect of fibre loading on tensile strength of the composites

The difference could be attributed to the matrix material, unsaturated polyester and the fibre loading. Rajesh *et al*., 2018 reported a tensile strength of 163N/mm^2 using epoxy resin as matrix. Zhao *et al*., 2012 reported a tensile strength of 37.56 MPa at fibre loading of 5%. Valença *et al*. 2015 reported a tensile strength of 291.1MPa at fibre loading of 38.98% using epoxy resin as the matrix.

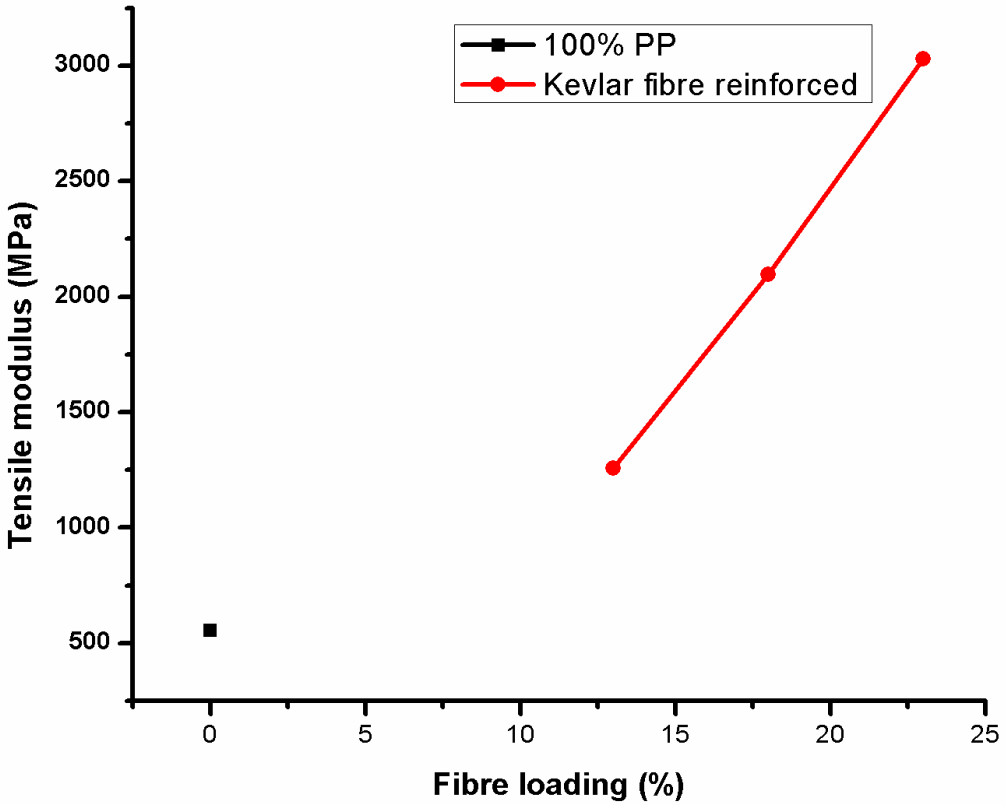

Fig 3: Effect of fibre loading on tensile modulus of composite

Fig 3 shows the effect of fibre loading on the tensile modulus of the composite. There was a sharp increase in the tensile modulus as the fibre loading increased from 12% to 23%. This also indicates that the toughness of the composite is quite high, 3030.8MPa at fibre loading of 23%.From Figure 3, the tensile modulus of the 100% polymer matrix was 555.2MPa. The inclusion of the Kevlar fibre had an increase on the tensile modulus of the composite of 445.9%. Isa *et al*., 2013 reported a tensile modulus of 12GPa using fibre loading of 40.8%. Valença *et al*., 2015 reported a tensile modulus of 12.75GPa at fibre loading of 38.98%.

3.3 Flexural strength results

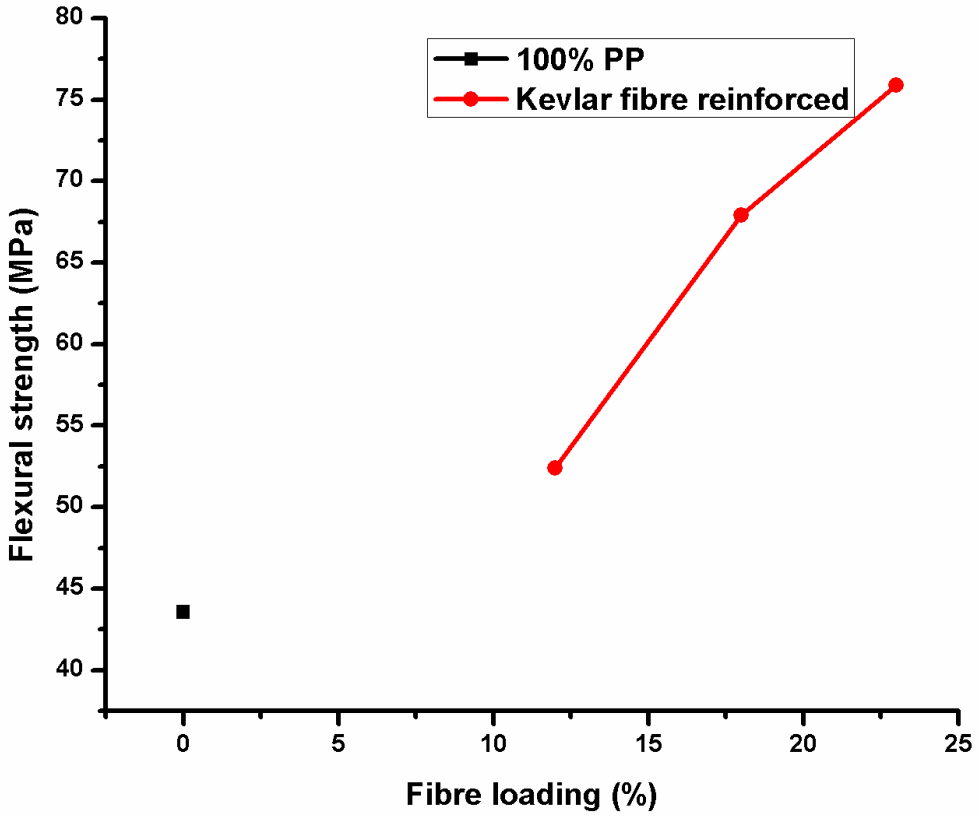

Fig 4: Effect of fibre loading on flexural strength

Figure 4 shows the effect of fibre loading on the flexural strength of the composite. As the fibre loading increases, there is a linear increase in flexural strength. The maximum flexural strength of 75.9MPa was obtained at a fibre loading of 23%.The flexural strength of the 100% polymer matrix was 43.55MPa. The results obtained showed an increase in flexural strength of 74.3%. Isa *et al*., 2013 reported a flexural strength of 200 MPa. Zhao *et al*., 2012 reported a flexural strength of 36.11 MPa.Valença*et al*., 2015 reported a flexural strength of 61.59MPa.

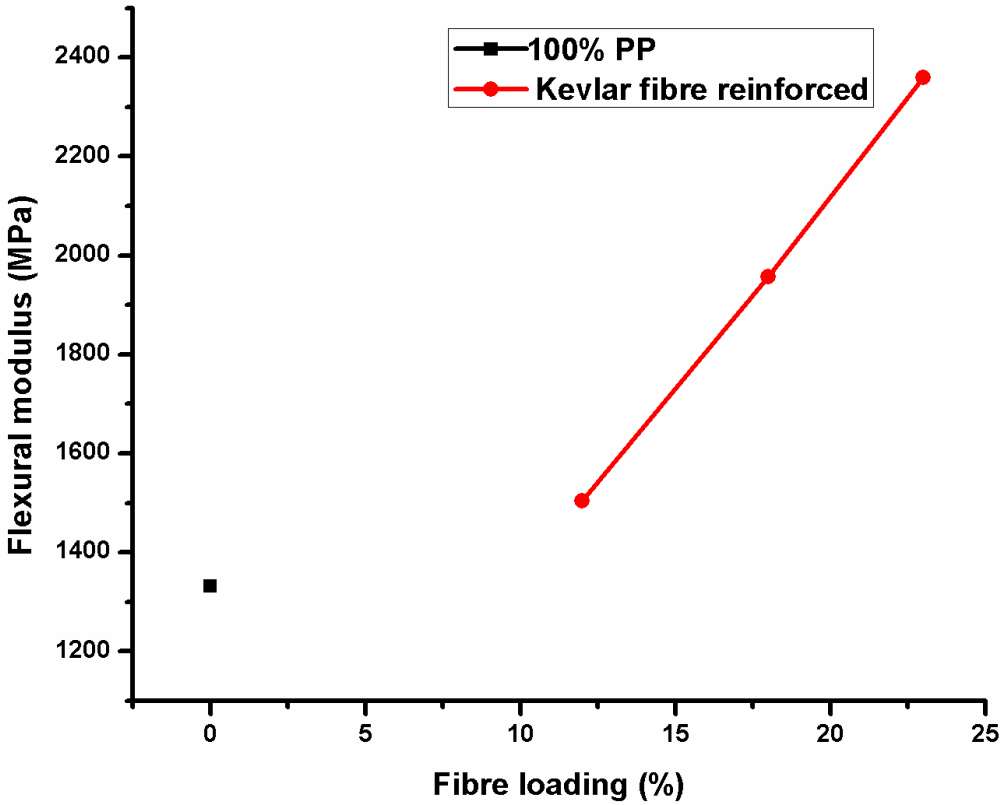

Fig 5: Effect of fibre loading on flexural modulus

Figure 5 shows the effect of the fibre loading on the flexural modulus of the composite, as the fibre loading increases, there is a linear increase in the flexural modulus, which indicates increasing toughness of the composites with increasing fibre loading. The maximum flexural modulus recorded is 2360.07MPa at fibre loading of 23%.The flexural modulus of the polymer matrix was 1331.98MPa. The inclusion of Kevlar fibre had an increasing effect on the flexural modulus of the composite, 77.2%.Valença *et al*., 2015, reported a flexural modulus of 5.68GPa.

3.4 Impact strength result

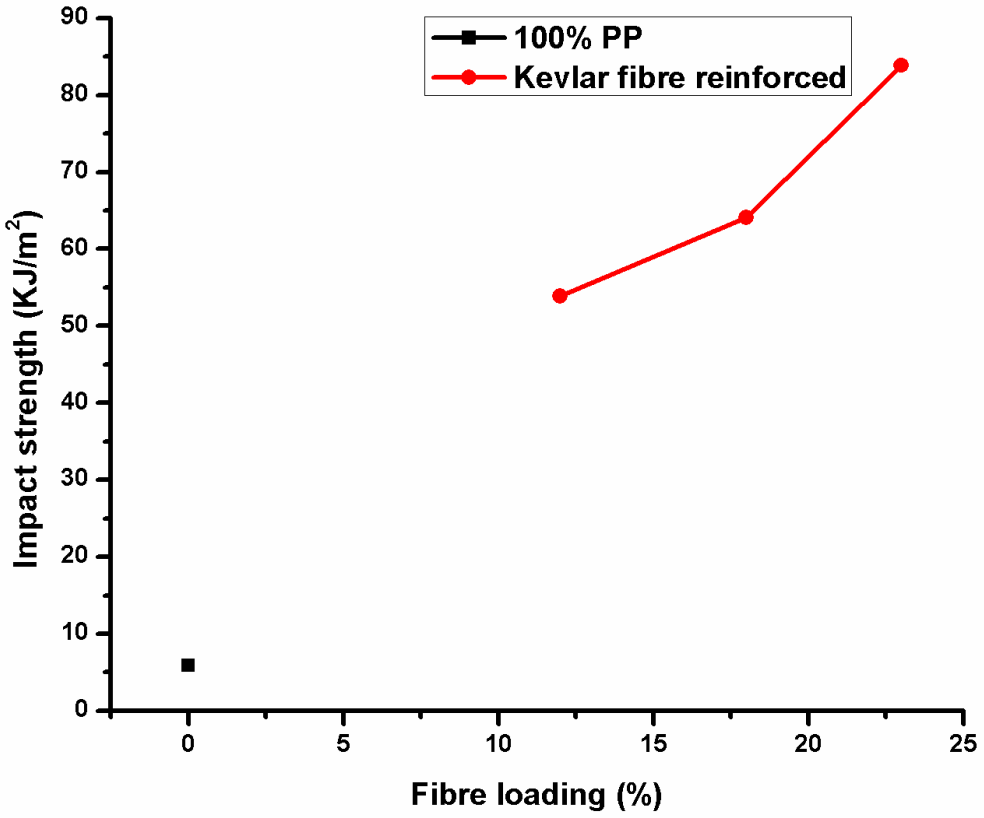

Fig 6: Effect of fibre loading on impact strength

The impact strength of the composites is shown in Fig 6. As the fibre loading increased, the impact strength of the composites increased. Maximum impact strength of 83.856KJ/m^2 was obtained at a fibre loading of 23%.The impact strength of 100% Polymer matrix was 5.93KJ/m^2. The inclusion of Kevlar fibre led to an increase on impact strength of 1314.2%. Zhao *et al*., 2012 reported impact strength of 17.03 KJ/m^2. Yahaya *et al*., 2016 reported a charpy impact strength of 175 KJ/m^2 using epoxy as matrix, Valença *et al*., reported an impact strength of 91.97KJ/m^2.

3.5 Dynamic mechanical analysis result

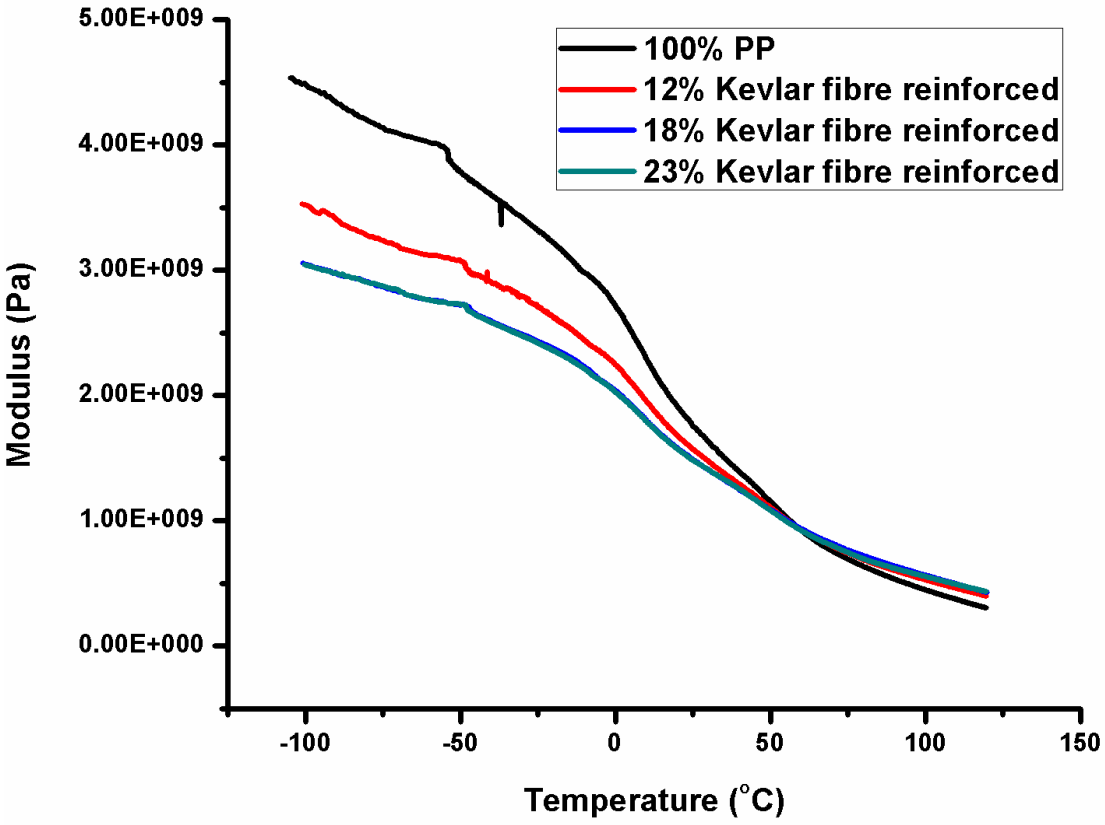

Fig 7: Effect of temperature on storage modulus

Fig 7 shows the effect of temperature on storage modulus of the composite. The results show that there was an increase in the storage modulus as the temperature decreases and decreases as the temperature increase. It also showed that that as the temperature increase; fibre loading does not have significant effect on the storage modulus. The 18% and 23% Kevlar fibre-loaded composites displayed virtually same storage modulus values throughout the temperature range of scan, while all 3 composites displayed same values between 40-125°C. This may be as a result of the available free molecular motion in the constituents of the composites (Jesuarockiam*et al*., 2019; Etaati*et al*., 2014).

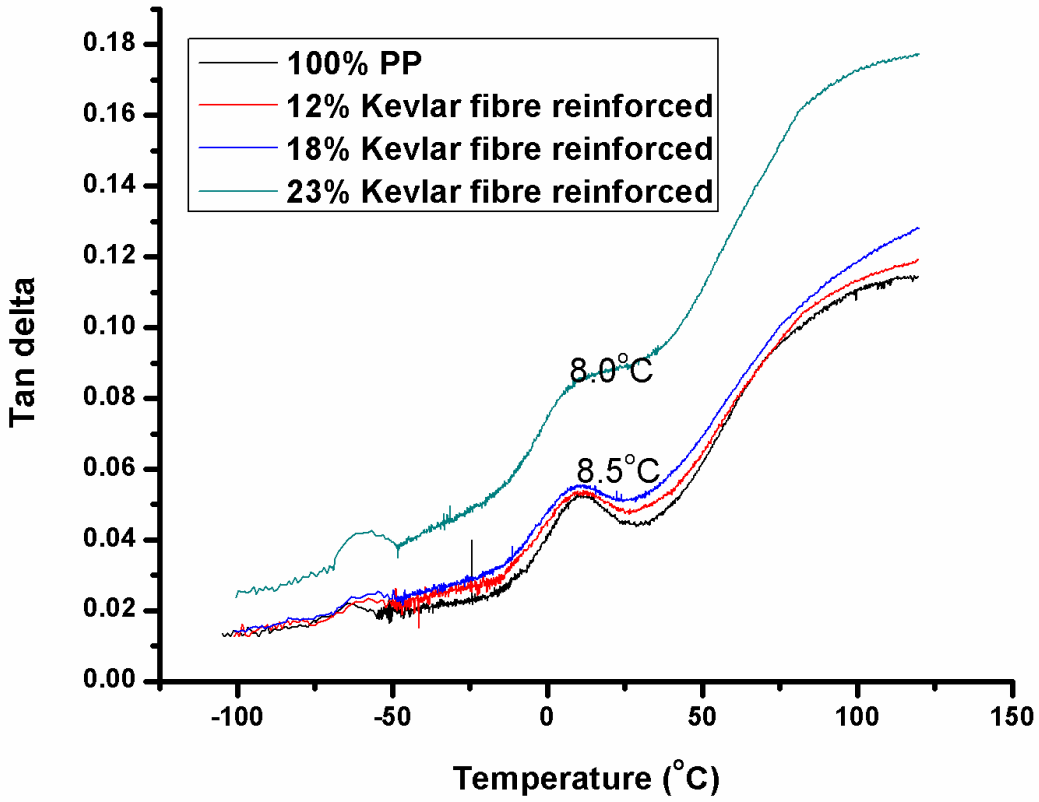

Fig 8: Effect of fibre loading on glass transition temperature

Fig 8 shows the effect of fibre loading on the loss tangent(damping), representative of glass transition temperature. From the results, it shows that glass transition temperature was affected by the fibre loading of 23% more than the 12% and 18%, this could be due to higher rigidity of the composite as a result of the Kevlar fibreloadingof 23%. Fig 8 shows the glass transition of 8.5°C for the polymer matrix, 12% Kevlar fibre and 18% Kevlar fibre respectively. 23% Kevlar fibrehad a higher damping above 50°C, this could be attributed to the stiffness of the composite due to higher percentage of the filler(23%) and molecular motion (Etaati*et al*., 2014).

3.6 Morphology of the composites after impact test.

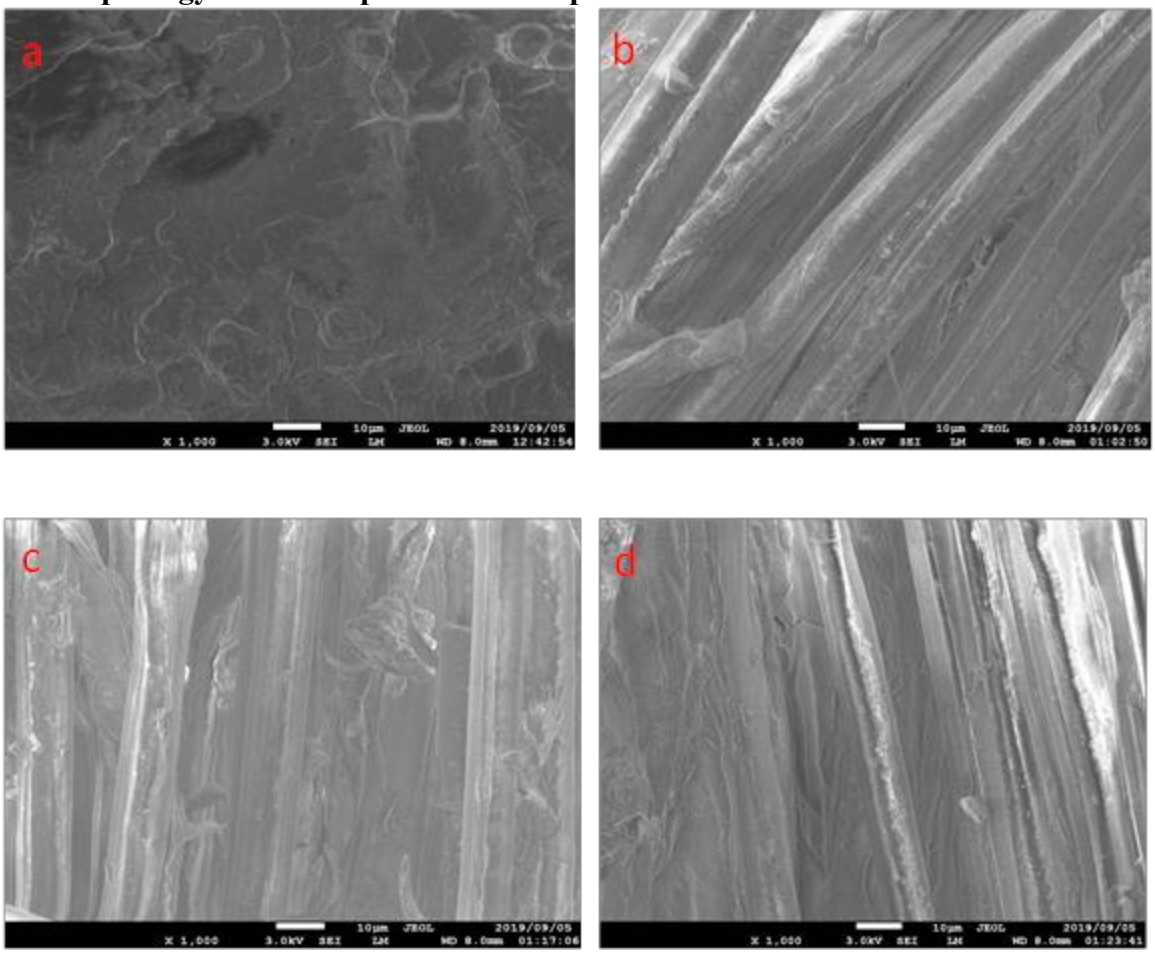

Fig 9: SEM micrographs of (a) Polypropylene (b) 12% Kevlar reinforced (c) 18% Kevlar reinforced (d) 23% Kevlar reinforced

Fig 9 shows the morphology of the composites after impact. From the images, it can be observed that there was a poor interfacial bonding between the fibre and the polymer; this leads to delamination, hence good energy absorption on debonding. For ballistic applications, the weaker the bonding between the polymer and the fibre, the better the energy absorbing capacity of the composite (Carrillo *et al*., 2012).Weak fibre – matrix interaction is required for composites meant for light weight ballistic application to in order to enable the maximum deformation of the fibres on impact (Cheeseman and Bogetti, 2003).

3.7 Density results

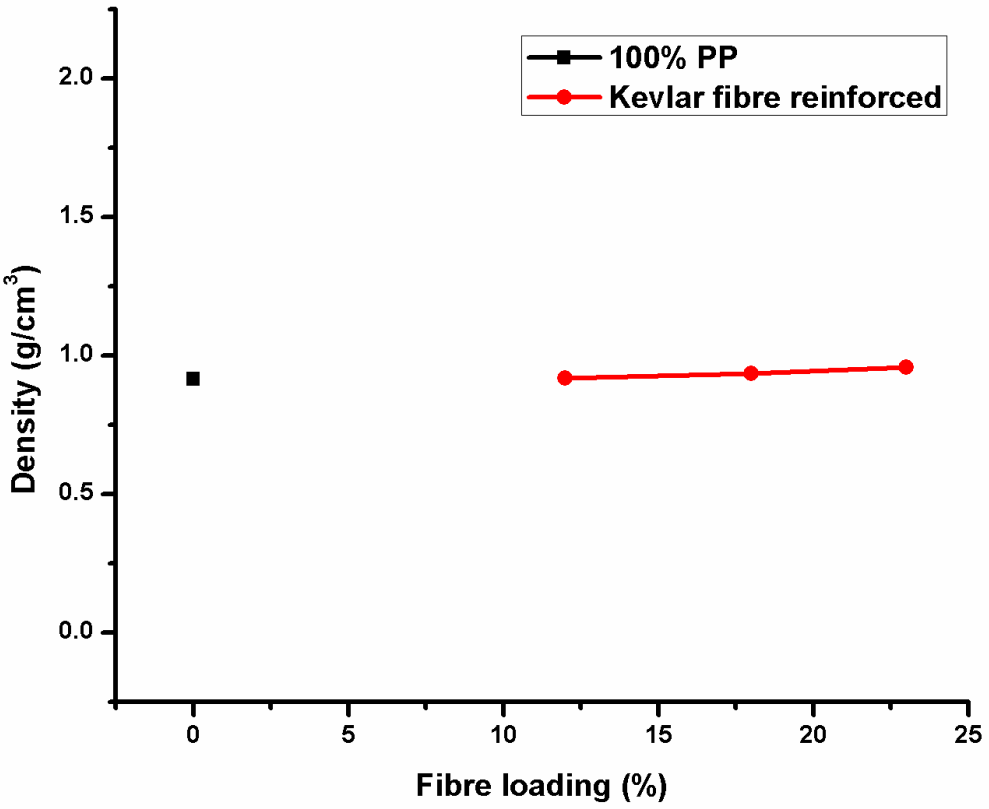

Fig 10: Effect of fibre loading on density of composite

Fig 10 shows the effect of fibre loading on the density of the composite. The density increased with increasing fibreloading. The maximum density observed was0.957gcm^{-3} at a fibre loading of 23%. This is not quite significant when compared to the density of the matrix polymer, 0.905gcm^{-3} as reported by the manufacturer. The density of the polymer matrix was recorded to be 0.916gcm^{-3}, this when compare with that of the composite, shows that the inclusion of the Kevlar fibre had an increase on the density of 4.5%. Isa *et al*., 2013 reported a density of 1.146g/cm^{3}.

3.8 Water absorption results

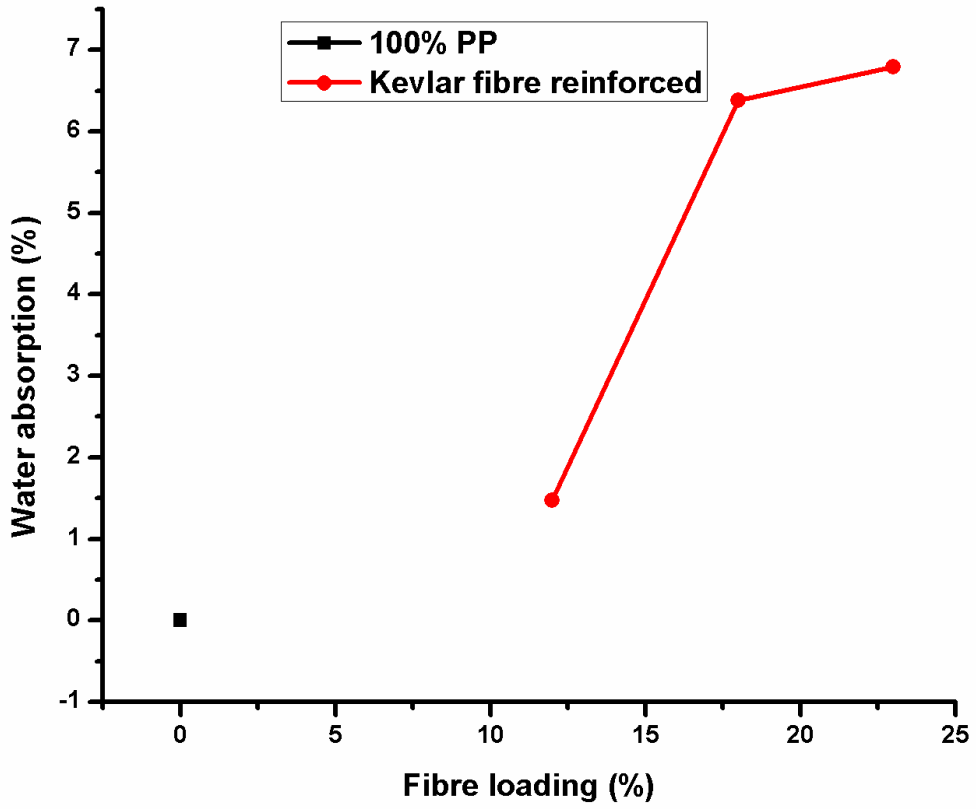

Fig 11: Effect of fibre loading on water absorption of composite

Fig 11 shows the effect of fibre content on the water absorption capacities of the composites. The water absorption increase significantly from 1 from ~1.5% water absorption for the 12% Kevlar fibre-loaded composite to ~6.5% water absorption for the 18% Kevlar fibre-loaded composite and attained maximum water absorption of 6.8% at a fibre loading of 23%. The water absorption of the polymer matrix was recorded as 0.001%. The inclusion of Kevlar matrix led to an increase in water absorption of 6,799.000%. Isa *et al*., 2013 reported water absorption of 2.0030%. Yahaya *et al.,* 2016 reported water absorption of 7.83%.

Conclusions

The fabrication of Kevlar fibre reinforced polypropylene was successfully carried out. From the results of the characterization, the following conclusions can be made;

a. Fabrication of Kevlar fibre reinforced polypropylene composite was carried out successfully;
b. The Kevlar fibre loading had a positive effect on the tensile, flexural and impact strength on the resulting composites;
c. The morphological analysis showed that there was weak polymer matrix – Kevlar fibre interaction, which is necessary for adequate ballistic

resistance due to delamination and debonding of the composites;

d. The fibre loading of the polymer matrix (polypropylene) had little effect on the density of the resulting composites; and
e. The water absorbing capacity of the composites were evaluated successfully and were seen not to be extremely high as to create concern during usage.

References

Bandaru, A.K., Chawan, V.V., Ahmad, S. and Alagirusamy, R. (2016). Ballistic Impact Response of Kevlar® Reinforced Thermoplastic Composite Armors. International journal ofimpact Engineering, 89, 1 -13

Carrillo, J.G., Gamboa, E.A., Flores – Johnson, E.A. and Gonzalez – Chi, P.I. (2012). Ballistic performance of thermoplastic composite laminates made from aramid woven fabric and polypropylene matrix. *Polymer Testing 31(4), 512 -519.*

Cheeseman, B.A. and Bogetti, T.A. (2003).Ballistic impact into fabric and compliant structures. *Composite structures, 61. 161 – 173.*

Danladi, E., Mamza, P.A.P., Yaro, S.A., Isa, M.T., Sadiku, E.R. and Ray, S.S. (2020). The effect of Glass – Kevlar 49 fibre loading on the mechanical,thermal and physical properties of polypropylene hybrid composites. Communication in physical sciences, 5(2), 99 - 105

Etaati, A., Pather, S., Fang, Z. and Wang, H. (2014). The study of fibre/matrix bond strength in short hemp polypropylene composites from dynamic mechanical analysis. *Composites: Part B*, 62, 19 - 28

Acknowledgement

The authors would like to thank Tertiary Education Trust Fund, Nigeria; Federal University, Gashua; National Centre for Nano Structured and Advanced Materials, Council for Scientific and Industrial Research, Pretoria, South Africa. Appreciation also goes to Tswane University of Technology, Pretoria, South Africa for inviting E.Danladi for the bench work.

Ghoshal, S., Wang, P., Gulgunje, P. and Verghese, N. (2016). High impact strength polypropylene containing carbon nanotubes. Polymers, 100, 259 – 274.

Gopinath, G., Zheng, J.Q. and Batra, R.C. (2012). Effect of matrix on ballistic performance of soft body armor. *Composite structures, 94, 2690 – 2696.*

Isa, M.T., Ahemd, A.S., Aderemi, B.O., Taib,R.M. and Mohammed – Dabo, I.A. (2013). Effect of fibre type and combinations on the mechanical, physical and thermal stability of polyester hybrid composites. *Composite Part B,52, 217 – 223.*

Jesuarockiam, N.,Jawaid, M., Zainudin, E.S., Sultan, M.T.H. and Yahaya, R. (2019). Ehnanced thermal and dynamic mechanical properties of synthetic/natural hybrid composites with grapheme nanoplateletes. *Polymers*, 11, 1 – 18

Katogi, H. and Takemura (2014). The effect of crystallinity on the mechanical properties of plain woven carbon reinforced composites using polypropylene. WIT Transactions on the Built Environment, Vol 137, 301 – 309

Naik, N.K. and Shrirao, P. (2004). Composite structures under ballistic

impact. *Composite structures, 66(1-4), 579 – 590*

Nuruzzaman, D.M., Kuaseh, N.M., Chowdhury, M.A., Rahman, N.A.N.A., Oumer, A.N., Fatchurrohman, N., Iqbal, A.K.M.A and Ismail, N.M.(2018). Experimental investigation on flexure and impact properties of injection molded polypropylene-nylon 6-glass fiber polymer composites. *IOP conference series:Material Science and Ebgineering, 342(1), 1 – 7*

Rajesh, S., Ramnath, B.V., Elanchezhian, C., Abhijith, M., Riju, R.D. and Kishan, K.K. (2018). Investigation of tensile behaviour of Kevlar composite. *Materials today: Proceedings* 5, pp. 1156 – 1161

Reis. P.N.B., Fereira, J.A.M., Santos, P., Richardson, P.O.W. and Samntos, J.B. (2012). Impact response of Kevlar composites with filled epoxy matrix. composite structures, 94, 3520 – 3528

Sadiku, E.R., Agboola, O.,Mochane, M. J., Fasiku,V.O., Owonubi,S. J., Ibrahim,I.D., Abbravaram, B. R., Kupolati, W.K.., Jayaramudu, T., Uwa, C. A., Dramola,O. O..,Iheaturu, Nkuna, C., Sanni, S.E.,Biotidara, O.F.,Eze, A. A.,Varaprasad, K., AdeyeyeO. A., Selatile, K. M. and Ndamase, A.S. (2019). The use of polymer nanocomposites in the aerospace and military/defence industry in *Polymer Nanocomposites for Advanced Engineering and Military Applications. Chapter 11, 316 – 348*

Terinte, N., Ibbett, R. and Schuster, K.C. (2011). Overview of native cellulose and micro crystalline cellulose I structure studied by X – ray diffraction (WAXD): comparison between measurement techniques. *Lenzigerberichte 89,, 118 – 131.*

Uzay, C., Boztepe, M.H. and Geren, N. (2016). Impact energy absorption capacity of fibre reinforced polymer matrix (FRP) composites.*Conference of the International Journal of Arts & Sciences,9 (1), 211 – 220*

Valença, S.L., Griza, S., de Oliveira, V.G., Sussuchi, E.M. and de Cunha, F.G.C. (2015). Evaluation of mechanical behaviour of epoxy composite reinforced with Kevlar plain fabric and glass/Kevlar hybrid fabric. Composites: Part B, 70, 1 – 8.

Yahaya, R., Sapuan, S.M., Jawaid, M., Leman, Z. and Zainudin, E.S. (2016). Water absorption behaviour and impact strength Kenaf – Kevlar reinforced epoxy hybrid composites. Advanced composite letters, 25(4), 98 – 101

Yeung, H.K.K and Rao, K.P. (2012). Mechanical properties of Kevlar – 49 Fibre reinforced thermoplastic composites. *Polymers and polymer composites, 20(5). 411 – 423*

Zee, R.H. and Hseih, C.Y. (1993). Energy loss parititoning during ballistic impact of polymer composites. *Polymer composites, 14(3), 265*

Zhao, S., Cheng, L., Guo, Y., Zheng, Y. and Li, B. (2012). PA6 and Kevlar fibre reinforced isotactic polypropylene; structure, mechanical properties and crystallization and melting behaviour. *Materials and Design*, 35, 749 – 753

Nigerian Journal of Polymer Science and Technology, 2020, Vol. 15, pp29-42

Received: 16/06/2020 Accepted: 28/08/2020

Characterization of Mango Seed Starch grafted with methacrylic acid and the determination of some physical properties of its plastic films

Michael Ifeanyichukwu Ugbaja[1], Wilson Uzochukwu Eze[1*], EuchariaNgozi Oparah[2], Maryann Ifeoma Uzochukwu[1] and Euphemia Chinwe Egwu[2]

[1]*Department of Polymer Technology, Nigerian Institute of Leather and Science Technology Zaria*
[2]*Department of Science Laboratory Technology, Nigerian Institute of Leather and Science Technology Zaria*

Corresponding Author: Wilson UzochukwuEze; wilstyrene@yahoo.ca; https://orcid.org/0000-0003-3106-9759

ABSTRACT

This study is focused on the graft copolymerisation of mango seed starch with methacrylic acid and its characterisation. The starch was isolated from mango seed embryo and characterised in terms of its pH, moisture and ash contents, and gelatinisation temperature. Varying concentrations (i.e. 0.4; 0.6; 0.8 and 1.0 mol/dm^3) of methacrylic acid was grafted onto the isolated starch using ceric ammonium nitrate (CAN) and N, N' methylenebisacrylamide and the resulting grafted products were characterized to determine grafting parameters such as graft yield and graft efficiency. Evidence of grafting was confirmed by Fourier Transform Infra-Red (FTIR) spectroscopy. Film samples were produced by casting the ungrafted and grafted starch products on a glass slide and the corresponding hardness, solubilty of the cast films were measured. The isolated starch has a pH of 5.06; moisture and ash contents of 6.5 % and 0.12 % respectively, and a gelatinization temperature range of 70 – 80 ˚ C. The graft yield of the grafted products increased slightly with increasing monomer concentration while the graft efficiency decreased with increasing monomer concentration. The FTIR spectra of the grafted and ungrafted mango seed starch film confirmed that grafting took place. The hardness of the produced films was found to decrease from 76.33 shore A value for the ungrafted starch to 46.33 shore A value at monomer concentration of 1.0 mol/dm^3. Starch based grafted products may serve as alternative material for production of single-use plastic articles for packaging and have been recommended for industrial applications such as in agricultural mulching, oilfield applications, etc.

Keywords: Graft copolymerization; mango seed starch; methacrylic acid; plastic films.

INTRODUCTION

Starch is a naturally occurring, abundantly available, biodegradable polysaccharide polymer. It can be found in the roots, stems, leaves, fruits and seeds of green leafed plants such as corn, potatoes, cassava, wheat, rice, etc. The two polymers of glucose present in native starch include amylase (15-30 %), and amylopectin (70-85 %) while other constituents such as proteins,

and lipids, can also be present (Meimoun *et al*., 2018). Amylose is predominantly the linear form even though some studies have shown a branched structure, composed of 100-10000 glucose units, with a molecular weight ranging between 10^5 and 10^6 g/mol (depending on its botanical source), while amylopectin is a highly branched form of starch with a molecular weight ranging from 10^6 to 10^9 g/mol, depending on the botanical source. Both forms of the starch differ in the biodegradability, elongation and strength (Irshad *et al*., 2018; Meimoun *et al*., 2018).

Althoughstudies on the isolation of starch from variety of food sources such as potato, maize, corn, and rice and their applications have been reported in some details, but very few literatures are available on isolation of starch from non-conventional sources like the seeds of fruits, for example, mango. Depending on their variety, the proximate composition of mango seed kernels, have been reported to be on the average 6.0 – 10.00 % protein; 9.84 – 13.08 % fat; 1.78 – 2.87% ash; 2.0 – 3.71% crude fibre; and 70 – 77% carbohydrates contents on dry weight (Mutua *et al*., 2017; Fowomola, 2010; Abdalla*et al*., 2007).Native starch, however, suffer from high tendency to retrograde, thermal instability, high water sensitivity and low shear resistance irrespective of its source. To overcome these limitations, the native starch can be modified by altering its structure through physical, chemical, or enzymatic modifications including notably blending (Meimoun *et al*., 2018; Vargha and Truter, 2005; Yu and Dean 2006), chemical functionalisation (Meimoun *et al*., 2018; Fang *et al*., 2004), and graft copolymerization to obtain thermoplastic starch (Meimoun *et al*., 2018, Irshad *et al*., 2018; Apopei *et al*., 2012).

Among the various methods available for modification of starch, graft copolymerization is one of the approaches where monomers are covalently bonded onto a starch (Irshad *et al*., 2018; Bhattacharya and Misra, 2004), and most versatile way of functionalisation allowing access to materials with a combination of the properties of the polymers involved (Meimoun*et al*., 2018; Jyothi, 2010). Grafting of methacrylic acid (MA) on starch gives the possibility to perform numerous further chemical reactions and to synthesize new materials having highly-added value for various applications such as sizing agents, waste water treatment for removal of dyes, and as hydrogels for drug delivery systems (Nikolic *et al*., 2013).

Starch is gaining more relevance in recent years due to its abundance, low cost and biodegradability. Moreover, the increase in environmental pollution caused by wastes from synthetic polymers has motivated more research and renewed efforts in the development and synthesis of biodegradable plastics from naturally occurring polymers such as starch for end use materials (Clasen and Kulicke*et*, 2001).However, the hydrophilicity and brittleness of these materials is a major drawback to their use in most application (Athanasios and Georgios, 2001; Maharana and Singh, 2006). In this study, attempts have been made to solve these problems through graft copolymerisation of methacrylic acid onto starch isolated from mango seed embryo. The success of this study will add value to huge volume of seeds from most fruits like mango that are considered as waste in Nigeria and several other African countries were they are grown in commercial quantities. Furthermore, global call for ban on single-use plastic items suggests that the time is now for suitable degradable plastics to emerge.

EXPERIMENTAL

Materials

Mango seed starch (MSS) was isolated from mango seed embryo obtained from mango fruit from local market in Samaru, Sabon Gari, Zaria, Nigeria. The mango variety selected is the *DuricZubethinusmurr* (peter) variety. Methacrylic acid (MAA), 97 % purity, manufactured by Central Drug House, India was used as received.Ceric ammonium nitrate (CAN), 98 %, and N,N' methylenebisacrylamide (MBA), were both manufactured by Sigma-Aldrich while Sodium hydrogen sulphite, is reagent grade and was used as received.Glycerol used as a plasticizer with composition purity of 98% supplied by Orient Global Manufacturing Nigeria Ltd.

Isolation of starch

Mango seed obtained from mango fruits were sun dried for 72 hours, the outer hard shell of the seed was removed manually and the recovered embryo was washed, cut into smaller pieces of about 4-12mm size and then soaked in 0.16 % aqueous solution of sodium hydrogen sulphite for 24 hrs at 50 ˚C. The solution was decanted afterwards, and the sample was ground into slurry with a laboratory blender. The ground slurry was sievedusing a muslin cloth. After 1 hr the supernatant was decanted and the settled starch was re-suspended in distilled water. This was repeated until a white layer was obtained, collected and dried at a temperature of 50 ˚C for 8 hrs to obtain the brownish-white starch Figure 1(a)-(d).

Fig. 1: (a) Mango fruit (b) Dried mango seed (c) Dried mango seed embryo (d) Isolated mango seed starch

Characterisation of the isolated starch

Confirmation Test of Starch

Starch test: A solution of iodine and potassium iodide in water known as lugol solution was used to confirm the presence of starch in the sample. Sample of the extracted mango seed starch was added to the solution, an intense blue-black colour indicating the presence of starch was observed. If no starch is present, the colour of the solution remains the same.

Moisture content

A sample of known weight was placed in the humidity chamber maintained at a definite humidity level for 2 hours. The sample was then taken out and final weight was noted immediately. Percent moisture absorbance was calculated as follows:

$$\%Water\ absorption = \frac{Wf-Wi}{Wi} x100 \quad (1)$$

Where, Wf and Wi are the final and initial weight of the sample respectively.

pH test

The pH of the sample was determined according to a procedure reported by International Starch Institute, ISI 26-5e. 5g of the MSS was mixed with 25.0 ml distilled water and stirred thoroughly for 60s. The starch was allowed to settle for 15 min. with the aid of pH meter, average of three trials was takenand recorded.

Ash content

Ash content was carried out according to AOAC (1990) method Thiex *et al*., (2012). In apre-weighed empty crucible (W1), 5g of starch was taken and isagain weighed (W2). The crucible is then kept in a mufflefurnace for 5hours at 900˚C. The crucible was then allowed to cool and weighed (W3). The ash content was determined usingthe following equation

$$\%Ash\ content = \frac{W3-W1}{W2-W1}x100 \qquad (2)$$

Biodegradability Test

The starch specimens both grafted and ungrafted were cut into pieces of 3.0 $cm^2$by measuring square sides of approximately 1.73 cm each using a vernier caliper and buried in 400 g of soil collected from farm land having slight moisture content and stored in a container. One sample was buried inside the soil at a depth of 4 cm and another buried at a depth of 6 cm for 42 days at room temperature. The weight of the specimen was measured before and after the testing. The biodegradability test was determined using Equation (3):

$$\text{Weight Loss } (\%) = \left[\frac{Wo - W}{Wo}\right] \times 100 \qquad (3)$$

Where,W_o and W are the weights of samples before and after the test.

Gelatinization temperature

Gelatinization temperature was determined by heating 1g of the starch in 5 ml of water at different temperature ranges from 40 - 90 ˚C at 10 ˚C intervals, and the sample was viewed under microscope to observe swelling, bursting and gel formation.

Grafting of methacrylic acid onto mango seed starch

Grafted starch products were prepared according to method reported by Chayapa and Jutarat (2018). 5 g of dried starch with 50 ml of distilled water at 75 ˚C were constantly stirred. The slurry was cooled to 30 ˚C, treated with 30 mmol/L of ceric ammonium nitrate (CAN) solution for 10 minutes. Afterwards, varying concentration (0.4, 0.6, 0.8, and 1.0 mol) of methacrylic acid was added and the volume of the reaction mixture was made up using distilled water. Five (5) ml of 0.01M of N, N' methylenebisacrylamide (MBA) crosslinker was added. The polymerization was continued with constant stirring under nitrogen atmosphere.The reaction mixture was allowed to warm up to 60 ˚C and thereafter was neutralized by dropwise addition of 5 % NaOH with stirring until it assumed a reddish-brown colour. After cooling the slurry to room temperature, its pH was adjusted using glacial acetic acid and it was then precipitated in excess of acetone. The precipitate was washed with ethanol to neutrality and dried under vacuum at 70 ˚C. The dried product was ground to powder and stored.

Film production

Films of the samples were obtained by dispersing 4g of the samples in distilled water. The solution was heated with a

heating mantle at 85 ˚C for 90 minutes under constant stirring until a gel was formed. The heating was stopped and the blend of the gel and plasticizer was cooled to room temperature and then was cast on a 10 x 4 cm glass slide cover with mould release agent. The cast film was allowed to dry at temperature of 30 ˚C fig. 2(a) and (b).

Figure 2(a)**: Un-grafted MSS film**

Figure 2(b)**: Grafted MSS film**

Characterization of the grafted Starch films

Grafting parameters

Grafting parameters such as graft yield, and graft efficiency of the grafted starch products were calculated as follows:

$$Graft\ yield\ (\%) = \frac{W_g - W_o}{W_o} \times 100 \quad (4)$$

Where W_g is the weight (g) of the grafted starch, W_o is the weight (g) of the ungrafted starch.

$$Graft\ efficiency\ (\%) = \frac{weight\ of\ starch}{weight\ of\ grafted\ polymer} \times 100$$

(5)

Density Measurement

The density of bioplastic was investigated according to ASTM D 729 standard on50 mm length, 20 mm width samples. The bioplastic mass was measured using analytical balanceand density was calculated as follows:

$$Density(\rho) = \frac{Mass\ (g)}{Volume\ (cm^3)} \quad (6)$$

Hardness

Samples were cut to size 10 mm x 10 mm and 6mm thickness with the test standard following ASTM D 2240. For every sample, three test measurements were taken and average value recorded.

Solubility in water

Solubility in water was determined as reported by Gontard *et al*. (1992) for grafted and ungrafted MSS film. Initially, 2 cm diameter film samples were incubated in a drying and sterilization oven at 100 °C, for 24 h. Then, the samples were weighed (w i) and incubated in 50.0 mL of distilled water at 175 rpm in a rotary shaker, at 25 °C, for 24 h. The samples were removed from the water and then their dry mass (w f) was determined under the same described conditions to obtain the initial dry mass. The solubility in water was expressed as a percentage of dissolved material, calculated from Eq. (7).

$$S = \frac{Wi - Wf}{Wi} x\ 100 \quad (7)$$

Where, w_i is initial mass and w_f is final mass, all in grams

Fourier Transform* Infrared *Spectroscopy analysis of the films

The FTIR spectra of the film samples were examined using the FTIR thermo Nicolet Model No. Nexus 870. The wavelength was 4000 – 650 cm^{-1} at 8 cm^{-1}resolution.

RESULTS AND DISCUSSION

Result of confirmatory Test for Starch

The change in colour from white to blue-black was as a result of the formation of linear triiodide ion complex of starch and iodide solution. The confirmation test of isolated starch is shown in Figure 3.

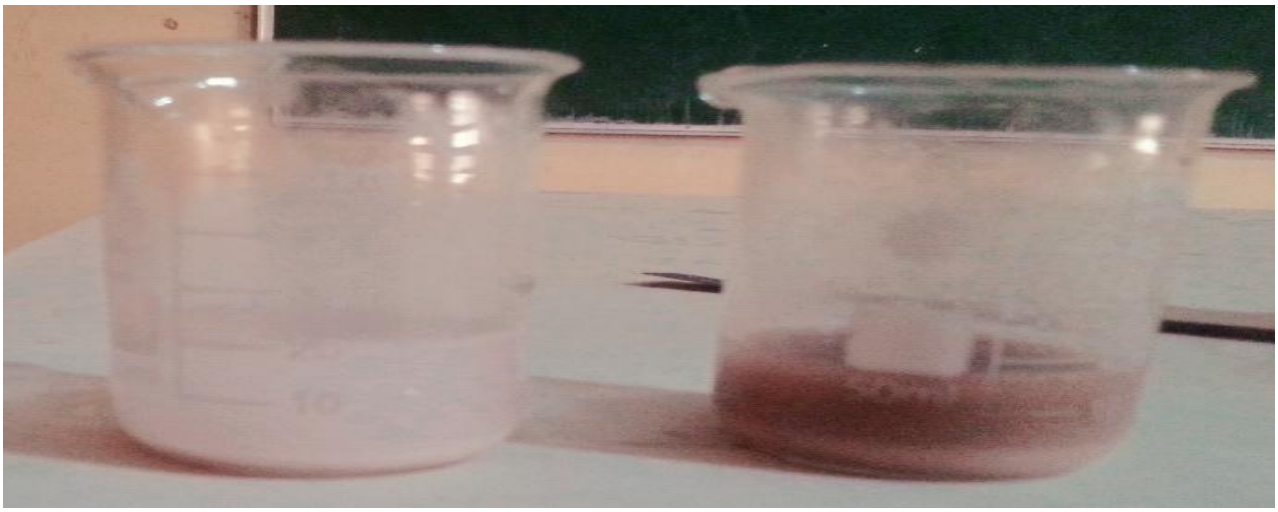

Fig 3: Starch Test (white) without lugol solution and Positive (Blue Black) for Starch with lugol solution

Moisture content

From table 1, it can be seen that the moisture content at dry weightof the isolated mango seed starch was 6.50 % at room temperature (25˚C). The relatively low moisture content of the starch makes it easy to be stored at room temperature and less prone to colonization by organism degradation as it is in root, tuber and cereal starches (Nielsen, 1998), making them suitable for use in making most single use plastic articles in packaging and alsoamiable for use in the pharmaceutical industry that requires low moisture content starch (Linus, 1995; Nuwamanya *et al*., 2011). This result is close to that reported for some commercially available biodegradable plastics like; Mater - Bi® with moisture content of 7.06 % at room temperature. It is a biodegradable thermoplastic material made of natural components (corn starch and vegetable oil derivatives) and of biodegradable synthetic polyesters. The material is certified as biodegradable and compostable in accordance with European Norm EN 13432 and with the national regulations UNI 10785 and DIN 54900 (Novamont, 2008). Other biodegradable material reported to have close moisture content is chitosan with moisture content of 6.25 % at room temperature and is currently used as a

commercial bioplastic material (Yadavand Bhise, 2004 and Radhakumary*et al*., 2005).

Table 1: Summary of some physical properties of MSS

S/N	Parameters	Values
1	Moisture content (%)	6.5
2.	pH	5.06
3.	Ash content (%)	0.12
4.	Gelatinization temperature range (˚C)	70 – 80

pH of MSS solution

The pH of the isolated starch solution was observed to be 5.06 (table 1). The pH of starch solution is very significant in its film forming ability (Valeria *et al,* 2018). In this study, the pH was not adjusted because it was observed to be stable for the production of film.

A***sh content of MSS***

The value of the ash content was also low at 0.12 %. The ash content is a measure of the total amount of minerals present within the starch, whereas the mineral content is a measure of the amount of specific inorganic components present within a satrch, such as Ca, Na, K and Cl. This is an indication of the good quality of the starch because high mineral content are sometimes used to retard the growth of certain microorganisms (Nielsen, 1998). Therefore, low ash content is an indication of low mineral contents and higher organic matter which in turn promotes biodegradation of the MSS film.

Biodegradability test

Biodegradability test conducted on the MSS shows a good biodegradability of the material after 14 days. The weight loss of the sample indicated the process of biodegradation of the specimen by the micro-organisms in the soil sample used. Both buried samples at the different depths showed the same degradation rate. The samples buried had the initial and final weights values of 0.512g and 0.322g respectively, corresponding to 59% degradation. The result suggests that MSS can effectively replace non-biodegradable synthetic plastic materials for making single-use plastic articles.

Gelatinisation temperature of MSS

Starch gelatinization is a process of breaking down the intermolecular bonds of starch molecules in the presence of water and heat, allowing the hydrogen bonding sites (the hydroxyl hydrogen and oxygen) to engage more water. This irreversibly dissolves the starch granule in water. Water acts as a plasticizer.

The gelatinisation temperature range was obtained at 70 – 80 ˚C, where the swelling, bursting and gel formation was observed on the starch. The gelatinisation temperature of the MSS is close to that of starch obtained from cassava (70˚C) (Bergo *et al.* 2008), but lower than starch from potato, maize and banana (98˚C) (Hernández *et al.* 2008). The gelatinization process is represented by transition temperatures and gelatinization enthalpies in the paste, and these measures are characteristic for each species of starch. High transition temperatures correspond to a high degree of crystallinity, high stability and resistance of the granule structure to gelatinisation (Tester *et al*., 2004). The lower gelatinisation temperature of the MSS compared to starch sourced from potato, maize and banana shows that the former will retrograde faster than the later.

Graft yield and graft efficiency of MSS

The effect of monomer concentration on the graft yield and graft efficiency of the grafted starch is shown in table 2. It can be seen that the graft yield increases significantly from 13.4 % at 0.4 mol/dm^3 of the methacrylic acid to 22.2 % at 0.6 mol/dm^3 and thereafter no significant increase was observed at higher monomer concentration. While the graft efficiency was observed to decrease as the concentration of the methacrylic acid monomer was increased.

Table 2: Grafting parameters of grafted starch products

S/N	Monomer conc. (Mol/dm^3)	Graft yield (%)	Graft efficiency (%)
1.	0.4	13.4	90
2.	0.6	22.2	48
3.	0.8	22.4	27
4.	1.0	22.8	9

Density and Shore (A) hardness of the produced films

The density is the ratio of weight to volume; density is a physical property of materials. Table 3 shows that addition of acrylic group into the MSS caused significant decrease in the density of the MSS films;1.321, 1.186, 1.172, 1.161 and 1.154g/cm3, for ungrafted, grafted with 0.4, 0.6, 0.8 and 1.0 mol/dm^{3}of methacrylic acid respectively. The observed trend could possiblybe due to improve orderliness and regularity in the arrangement of molecules, making the crystalline structure more compact. The extent of crystallinity and molecular rearrangement affects their volume with consequential effect on the density.

Table 3 shows the effect of monomer concentration on the shore A hardness of the produced films. The hardness was observed to decrease continuously from maximum shore A value of 76.33 for ungrafted starch to minimum value of 46.33 at 1.0 mol/dm^3 monomer concentration. This could be attributed toconcentration of MMA available for grafting which led to disruption in crystalline phase of starch as a result of increase in acrylic group introduced to the polymer chain for copolymerization, which promotes mobility of the starch chains and caused the resulting polymer to be more flexible. Similar observation was reported by Chayapa and Jutarat (2018) in their study on characterization and properties of biodegradable thermoplastic grafted starch films by different contents of methacrylic acid. They concluded that higher degree of grafting participated in increasing mobility of the starch molecules and flexibility of side chain.

Table 3: Densities and Shore (A) hardness of the produced films

S/N	Sample	Density (g/cm^3)	Shore (A) Hardness
1.	Ungrafted starch	1.321	76.33
2.	Grafted (0.4 Mol/dm^3)	1.186	63.33
3.	Grafted (0.6 Mol/dm^3)	1.172	57.67
4.	Grafted (0.8 Mol/dm^3)	1.161	56.67
5.	Grafted (1.0 Mol/dm^3)	1.154	46.33

Solubility

Table 4 shows the result for solubility of the ungrafted and grafted films at 1.0 mol/dm^{3}to

be33.26% and 15.62 %respectively. There was adecrease in solubility with the grafting of the MSS.With increasing concentration MMA from (0 to1.0 Mol/dm^3), solubility was found to decrease. This was because high degree of grafting of MAA monomer not only reduced hydroxyl groups of starch backbone significantly but also generated hydrogen bonding between two methacrylic groups, which lead to the decrease in affinity for water absorption (Mostafa, 1995).The observation can beattributed to the high hydrophilic characteristics of MAA monomer (Chayapa and Jutarat, 2018). Furthermore, water absorption of bioplastic is one of important properties for evaluating their suitability for most packaging application. Starch contains hydroxyl (OH), carbonyl (CO), and ester (COOH), causing improved hydrophilicity, which can accelerate the decomposition process in the soil. However, grafting of MSS has shown a marked improvement in the water absorption resistance of MSS film.

Table 4: Solubility of the produced films at different monomer concentrat ions

S/N	Sample	% Solubility
1.	Ungrafted starch	33.26
2.	Grafted (0.4 Mol/dm^3)	30.61
3.	Grafted (0.6 Mol/dm^3)	17.92
4.	Grafted (0.8 Mol/dm^3)	16.03
5.	Grafted (1.0 Mol/dm^3)	15.62

Function group analysis

Free radical – addition occurs between the methacrylic acid (MAA) and the starch macromolecules (St-O*) to form a new covalent bond, thereby, initiating a chain. More MAA molecules added to the initiated chain promotes grafting onto starch molecules to form poly (MAA)-starch radicals (PMAA-St) (Eq. 8) (Zahran*et al*., 2016).

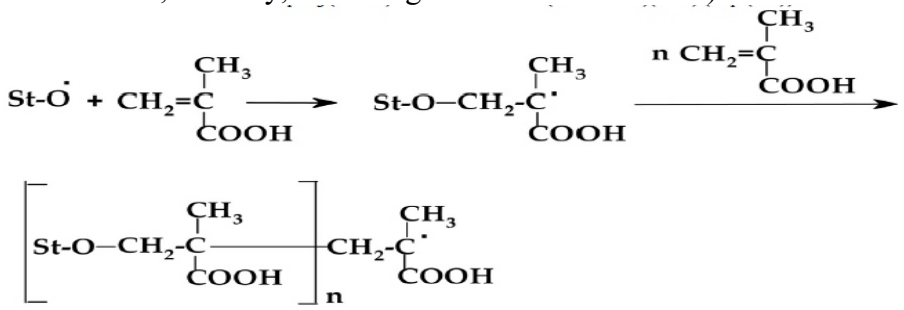

(8)

Macromolecules of polymethacrylic acid (PMAA*) can also react with the starch macromolecule to form graft copolymer (Eq. 9) (Zahran *et al*., 2016; Salisu *et al*., 2013).

$$PMAA^* + {}^*O\text{-}St \longrightarrow PMAA\text{-}O\text{-}St \quad (9)$$

The undesired reaction for grafting (i.e. homopolymerisation reaction) may also be initiated since the grafting reactions indicated above are conducted in an aqueous medium.

The analysis of starch films with the help of Fourier-transform Infra-red spectroscopy shows that similar characteristic peaks appeared in both spectra for the grafted and ungrafted film Figure 4 and 5. A hump is present in between 3000-3500 cm^{-1}

representing the stretching of O-H bond appeared in both film samples. Peak appearing at 2926 cm^{-1} represent the stretching of C-H bond. Peak at 1077 cm^{-1} in both film samples indicate the presence of glycosidic bond and a ring structure of glucose in the starch (Irshad *et al*., 2018). However, the only difference in the spectra of the grafted and ungrafted film is an absorption band at 1703 cm^{-1}which appeared only on the grafted film spectra Figure 5. This could be attributed to the C=O stretch of methacrylic group in the copolymer (Chayapa and Jutarat, 2018) this peak is very significant because it confirm the success of the graft copolymerization with MAA monomer onto MSS chain structure.

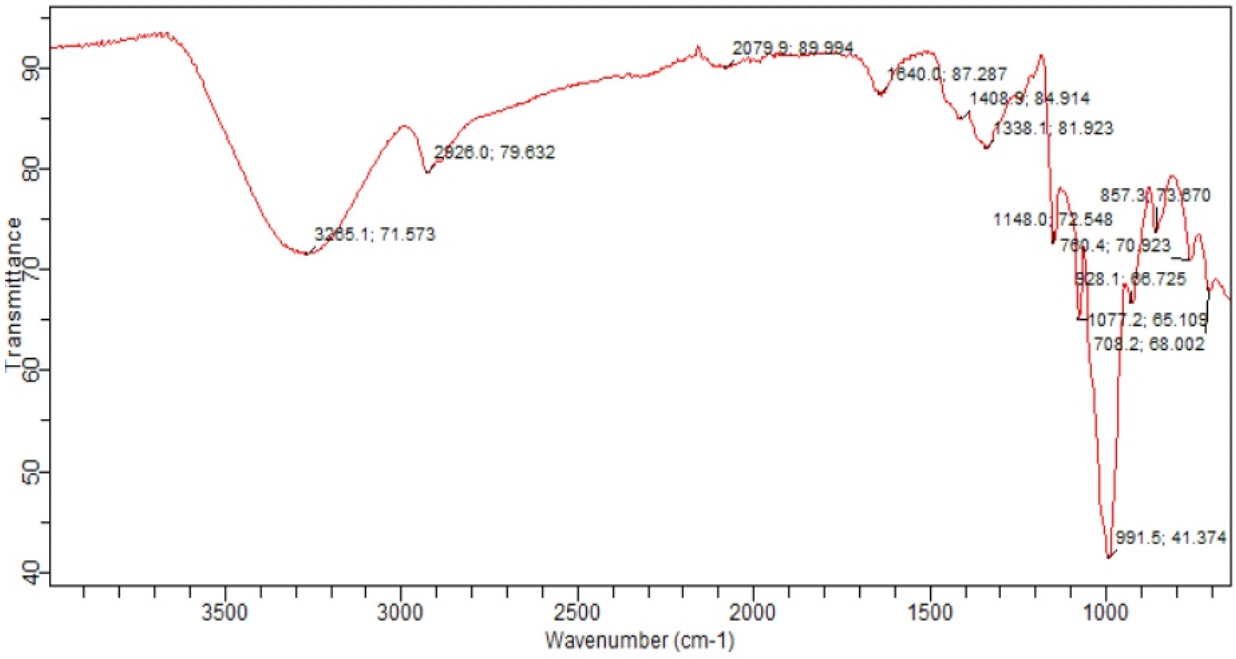

Figure 4: FT-IR spectrum of ungrafted mango seed starch film

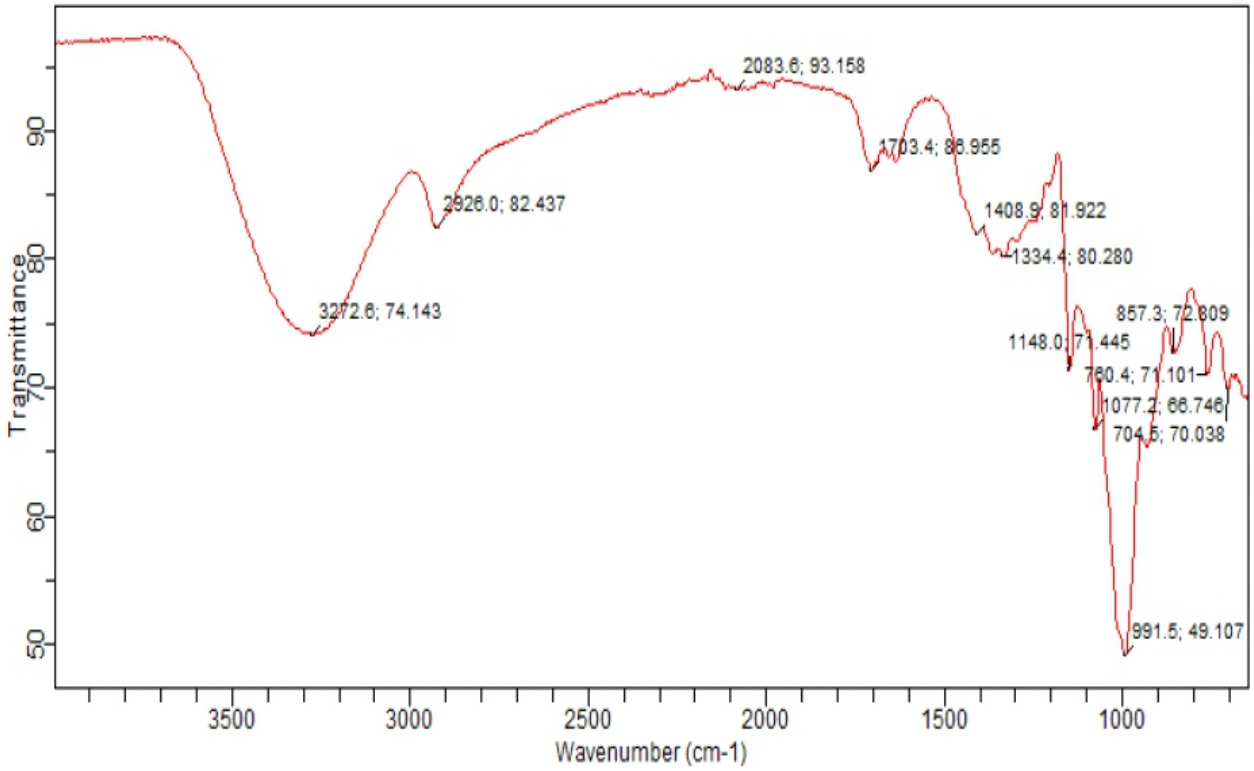

Figure 5: FTIR spectrum of grafted mango seed starch film at 1.0 monomer concentration

CONCLUSION

Graft copolymerisation of methacrylic acid onto mango seed starch has been studied. The isolated starch was found to have low moisture and ash contents and a pH of 5.06 and gelatinisation temperature in the range 70-80 ˚C. Graft parameters such as the graft yield and graft efficiency was found to vary with monomer concentration. Increase in the monomer concentration decreased the shore a hardness of the produced films. The results further showed that different MSS films grafted by MAA also demonstrated biodegradability by soil burial test. In addition,, MSS films grafted with 1.0 Mol/dm^3 of MAA exhibited improved flexibility, lighter and more soluble in water when compared with ungrafted MSS film and MSS films grafted with low concentration of MMA. From the above results, it can be concluded that the bioplastics can be used as packing materials and can be used as an alternative to synthetic non-biodegradable plastic bags. However, the use of the MSS in pharmaceuticals will require investigation of its purity and/or toxicity if any.

ACKNOWLEDGMENTS

The authors would like to express their gratitude and sincere appreciation to the Nigerian Institute of Leather and Science Technology (NILEST), Zariawhose laboratory and facilities was used for this study.

CONFLICT OF INTEREST

The authors declare no conflict of interest

REFERENCES

Abdalla, A. E. M. Darwish, S. M., Ayad, E.H. E. El-Hamahmy R. M. (2007): Egyptian Mango By-Product 1. Compositional Quality of Mango Seed Kernel, *Food Chemistry*, 103: 1134 – 1140.

AOAC (1990): Association of Official Analytical Methods of Analysis, 12th Ed. Washington DC.

Apopei, D.F, Dinu, M.V, Dragan, E.S (2012): Graft Copolymerisation of Acrylonitrile onto Potatoes Starch by Ceric Ion, *Digest Journal of Nanomaterials and Biostructures*, 7 (2): 707-716.

ASTM D 2240, "Standard test method for rubber property durometer hardness, United States: ASTM International, 2004.

ASTM D 729, "Standard test methods for density and specific gravity (relative density) of plastics by displacement, United States: ASTM International, 2004.

Athanasios H. G., Georgios A. N. (2001).The potential use of Ricinuscommunis L. (Castor) Stalks as a Lignocellulosic resource for particleboards, Industrial Crops and Products, 13, 209-218. DOI:10.1016/S0926-6690(00)00078-9

Bergo PVA, Carvalho RA, Sobral PJA, dos Santos RMC, da Silva FBR, Prison JM, Solorza- Feria J, Habitante AMQB (2008) Physical properties of edible films based on cassava starch as affected by the plasticizer concentration. Packaging Technol Sci 21(2):85–89

Bhattacharya A, Misra B. (2004): Grafting: A Versatile means to Modify Polymers: Techniques, Factors and Applications, *Progress in Polymer Science,* 29: 767-814.

Chayapa W., Jutarat P., (2018), Characterization and properties of biodegradable thermoplastic grafted starch films by different contents of methacrylic acid, Biomac, https://doi.org/10.1016/ j.ijbiomac.2018.11.083

Clasen, C., Kulicke, W. M. (2001) Determination of Viscoelastic and Rheo-optical properties of Materials, Progress Polym. Sci., 26, 1839. DOI:10.1016/S0079-6700(01)00024-7

CRA Standard Analytical Methods B-44, C-44, E-48Joint FAO/WHO Expert Committee on Food Additives (JECFA) Monographs and Evaluations the European Pharmacopoia 4

Fang, J.M., Fowler, P.A., Sayers, C., Williams, P.A. (2004): The Chemical Modification of a Range of Starches under Aqueous Reaction Conditions, *Carbohydrate Polymers*, 55: 283-289.

Fowomola, M. A (2010): Some Nutrients and Antinutrients Contents of Mango (Mangiferaindica) Seed, *African Journal of Food Science*, 4 (8): 472 – 476.

Gontard N, Guilbert S, Cuq J-L. (1992) Edible wheat gluten films: influence of the main process variables on film properties using response surface methodology. J Food Sci. 57:190–195. doi: 10.1111/j.1365-2621.1992.tb05453.x.

Hernández O, Emaldi U, Tovar J (2008) In vitro digestibility of edible films from various starch
sources. Carbohydr Polym 71:648–655

Irshad, H. Khalid, N. Rubab, Z. Ullia, M. Amjad, A. Saeed, F. Dastgir, G. Ahmad B and Anwar
P (2018): Study of Biodegradability by Graft Copolymerisation of Starch backbone with Acrylic Acid, Methacrylate, Acrylonitrile with the Advancement of Ni-Doped Nanoparticles, *Advances in Applied Science Research,* 9(1): 47-55.

Jyothi, A. (2010): Starch Graft Copolymers: Novel Applications in Industry, *Compos Interface*, 17: 165-174.

Linus, A.J. (1995): TablatingBehaviour of some Depolymerised Local Starches, An M.Sc. (Pharmaceutics) Dissertation, Ahmadu Bello University, Zaria, Nigeria, Pp. 42-45.

Maharana, T.: Singh, B. C. (2006) Synthesis and characterization of biodegradable polyethylene
by graft copolymerization of starch using glucose–Ce(IV) redox system, J. Appl. Polym. Sci.,2006, 100, 3229. DOI: 10.1002/app.22928

Meimoun, J., Wiatz, V., Saint-Loup, R. Parcq, J., Favrelle, A., Bonnet F and Zinck P (2018): Modification of Starch by Graft Copolymerisation, *Starch/Staerke*, 70, 1600351: 1-23.

Mostafa, Kh. M. (1995) Graft polymerization of methacrylic acid on starch and hydrolyzed starches, Polym. Degrad. Stab. 50, 189-194. https://doi.org/10.1016/0141-3910(95)00147-6.

Mutua, J. K. Imathiu S and Owino W (2017): Evaluation of the Proximate Composition, Antioxidant Potential, and Antimicrobial Activity of Mango Seed Kernel Extracts, *Food Science & Nutrition*, 5 (2): 349 – 357.

Nielsen, S.S. (1998), Food Analysis, 2nd Edition Aspon Publication, Gaithersberge, Maryland, Pp. 40-250.

Nikolic, V., Velickovic, S., Antonovic D and Popovic, A (2013): Biodegradation of Starch-Graft-Polystyrene and Starch-Graft-Poly(Methacrylic acid) Copolymers in Model River Water, *Journal of the Serbian Chemical Society*, 78(9): 1425-1441.

Novamont company, 2008. http://www.materbi.com/ing/html/PDF/EPD_PE_ 180202.pdf
Oerlemansplastics company, 2008. www.oerlemansplastics.nl and www.azenos.com_navinfo_biopl_php

Nuwamanya, E., Baguna, Y., Wembabazi, E., and Rubaihayo, P. (2011), A Comparative study of the Physicochemical Properties of Starches from Root, Tuber and Cereal Crops, *African Journal of Biotechnology*, 10 (56): 12018-12030.

Radhakumary C., Prabha D. Nair1, Suresh Mathew and C.P. Reghunadhan Nair (2005). Biopolymer Composite of Chitosan and Methyl Methacrylate for Medical Applications, *Trends Biomaterials and Artificial Organs*, 18 (2): 7-24.

Salisu A., Naim, A.A. Sanagi, M.M (2013). In Magdy K. Zahran, Enas M. Ahmed, Mohamed H.
El-Rafie (2016): Synthesis and Characterisation of Hydrolysed Starch-g-Poly(methacrylic acid) Composite, *International Journal of Biological Macromolecules*, 87: 473-480.

Tester, R. F., Karkalas, J., & Qi, X. (2004). Starch - Composition, fine structure and architecture.

Journal of Cereal Science, 39(2), 151-165. http://dx.doi.org/10.1016/j.jcs.2003.12.001.

Thiex, N., Novotny L and Crawford A (2012) Determination of Ash in Animal Feed: AOAC *Official Method* 942.05 Revisited *Journal of AOAC INTERNATIONAL*, 95, 5, 1:1392–1397, https://doi.org/10.5740/jaoacint.12-129

Valeria C., Giosafatto L., Al-Asmar Asmaa, D'Angelo Antonio, Roviello Valentina, Esposito Marilena and Mariniello Loredana (2018) Preparation and Characterization of Bioplastics from Grass Pea Flour Cast in the Presence of Microbial, Coatings, 8, 435; doi:10.3390/coatings8120435.

Vargha, V., Truter, P. (2005): Biodegradable Polymers by Reactive Blending Trans-Esterification of Thermoplastic Starch with Poly(Vinyl acetate) and Poly(Vinyl acetate-co-butylacrylate), *European Polymer Journal*, 41: 715-726.

Yadav, A. V. and S. B. Bhise, (2004). Chitosan: A potential biomaterial effective against typhoid, Current Science, 87(9).

Yu, L., Dean, K., Li, L. (2006): Polymer Blends and Composites from Renewable Resources, *Progress in Polymer Science*, 31: 502-576.

Zahran, M. K., Ahmed, E. M., El-Rafie M. H. (2016): Synthesis and Characterisation of Hydrolysed Starch-g-Poly(methacrylic acid) Composite, *International Journal of Biological Macromolecules*, 87: 473-480.

Nigerian Journal of Polymer Science and Technology, 2020, Vol. 15, pp43-48
Received: 05/07/2020 Accepted: 24/09/2020

Mechanical and Morphological Properties of Leather Fatliquored Using Modified *Lophiralanceolata* Seed Oil

Habila, B[*1].,Mamza, P.A.P[2]., Gimba, C.E[3].

[1]*Directorate of Research and Development, Nigerian Institute of Leather and Science Technology; P.M.B. 1034, Zaria.*
[2,3]*Department of Chemistry, Faculty of Physical Sciences, Ahmadu Bello University, Zaria.*
bitrushabila@yahoo.com

Abstract:
In leather processing, fatliquor is one of the most important chemicals used by the Tanneries. This research showed the potential use of locally available raw material Lophiralanceolata (Namijinkade) seed oil for fatliquor production and potentially substitute for the imported vegetable oil sulphatedfatliquor. The fatliquors were prepared by sulphation reaction. The degree of sulphation were varied as, 2%, 4%, 6%, 8% and 10% concentrations of the sulphuric acid. Also, the leather treated with fatliquors were characterised for their mechanical properties and morphological arrangement and these properties were compared to a leather fatliquored with a commercially available fatliquor. Mechanical properties such as tensile strength, percentage elongation and ball-burst of the fatliquored leathers increased with increase in the degree of sulphation. An optimum tensile strength of 23.20 MPa at 10% degree of sulphation (4% fatliquor offer), percentage of elongation of 97.04% at 4% fatliquor offer and 6% degree of sulphation and a distension of 12.13 mm, respectively. The morphological properties of the fatliquored leather at 300x magnification indicated penetration of the fatliquor into the leather collagen fibres which caused the flexibility observed on the fatliquored leather compared to the non-fatliquored leather. The optimum tensile strength of 23.20 MPa at 10% degree of sulphation compared to the United Nation Development Programme (UNDP) (10.10MPa) standard for fatliquored leather, proved that the prepared fatliquor can substitute the imported fatliquor. Therefore, as a result of the high tensile strength of 20.45 MPa and 23.20 MPa at 8% and 10% degree of sulphation respectively (4% fatliquor offer). The fatliquored leather can be used as clothing leather, wallet and Automated Teller Machine (ATM) card packs. Also, the distension properties of the leather at 12.13 mm, indicated the use of the fatliquored leather for shoe upper leather.

Keywords: Ball-burst, Fatliquor, *Lophiralanceolata* seeds oil, Namijinkade, UNDP.

1.0 INTRODUCTION

Special mechanical performance properties of leather depends on the fields of use (especially shoes) and specific performance characteristics of the leathers (Urbanija*et al*., 2004). This is in relation to the body weight, comfort and health. In a process of choosing a quality leather product, people most are times pay close attention to its handle character, although its physical-mechanical properties contribute to capability of withstanding wear and tear (Xiao-Lei *et al*., 2006). It is also observed that, the shoe upper leathers are affected by foot movements and must protect foot from outer mechanical impacts. Leather production involves the conversion of hide and skin into leather which requires several chemical and mechanical processes to remove non-collagenous matter in pre-tanning operation (Chen *et al.,* 2012). After the tanning operation, to produce a good leather of desirable quality, the tanned leather is lubricated in a fatliquoring processes (Cuq*et al*., 1998). The physical properties of leather change depending on

the animal type, apparent density, breed, sex and age. Furthermore these properties exhibit variations in different parts over the leather area (Mutlu*et al*., 2014). Fatliquoris the largest amount of leather-chemistry material in leather industry and has extremely important impact on the performance of leather (Senait, 2014). It can penetrate to the collagen fibres, making the leather plastic and lubricant. The fatliquor can make the molecular chain segment easily move by separating the leather fibres from each other, giving the leather flexibility, water proof, moisture and softness (Hassan *et al.,* 2017). In leather chemistry, there are different technologies for production of anionic fatliquor which are mostly used in chrome tanning, this includes: Saponification using strong alkali, sulphation using sulphuric acid, sulphur trioxide or chlorosulfonic acid and sulphitation using a strong solution of sodium bisulphite.

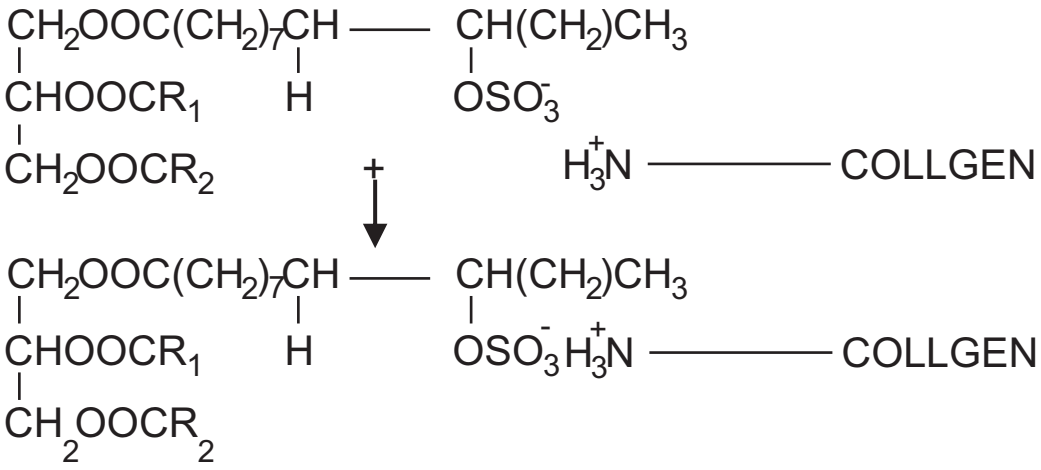

Scheme 1: Reaction of Fatliquor with the Collagen Protein

2.0 MATERIALS AND METHODS

2.1 Material

The modified *Lophiralanceolata*oil was sourced from the Department of Chemistry, Ahmadu Bello University, Zaria and the goat skins from Samaru Market, Sabon-Gari Local Government Area of Kaduna State. BAFS fatliquor, was the imported fatliquor used as the control in the experiment.

2.2 Tensile Strength

To determine the tensile strength of the leather, the test samples were cut according to a total length of 100 mm and gage length of 47 mm. The testing of the samples was done at Engineering Materials Development Institute, Akure, Ondo State, Nigeria in accordance with ASTM D638 (2014) standard. The samples were machined to dumb bell shape and then placed in Instron universal tensile testing machine 3369 model and the tensile strength and modulus were evaluated.

2.3 Lastometer (Bursting Ball Test)

To determine the grain crack distension and load when a circular leather test specimen is secured in between two circular rings of 25 mm diameter and stretched with the help of a spherical head. Unto grain crack appears on the grain surface of leather (IULTCS, 2002).

2.4 Scanning Electron Microscopy of Leather

Scanning electron microscopy (SEM): Scanning Electron Microscope Pro X: Phenonm World 800-073 in the Department of Physics, Umaru Musa Yaradua University, Katsina-Nigeria was used to study the surface morphology of the fatliquored and unfatliquored leather. Samples imaging was done at accelerating

voltage of 15kV at 350, 500, 1000, 1500 and 2000 magnifications respectively.

3.0 RESULT AND DISCUSSION

3.1 Result of Tensile Strength (4% Offer)

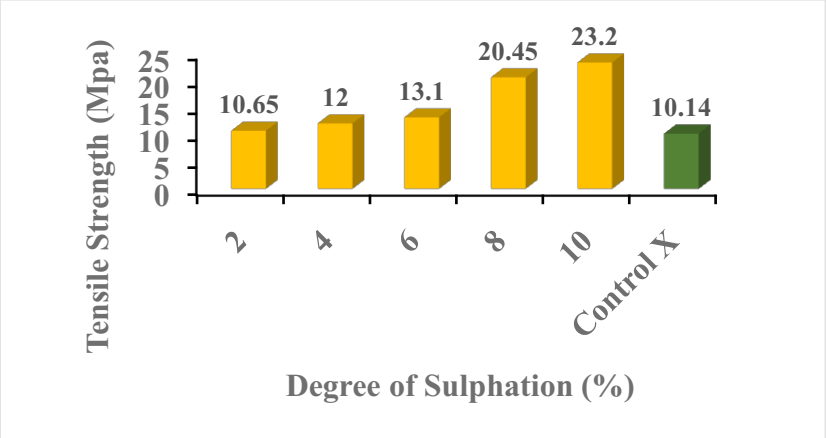

Figure 3.1: Tensile strength of leathers fatliquored with sulphated*Lophira* seed oil (4% Offer)

A high tensile strength is required in all types of leather, it is a characteristic property of a good quality leather (Venkatachalam, 1962). The tensile strength of the manufactured leather with the synthesized fatliquor increases with increase in the degree of sulphation. Figure 3.1 illustrated the variation of tensile strength with increase in degree of sulphation, due to the fact that more of the emulsifying group (SO_3) is been added to the liquor. The result 4% fatliquor offer of 2%, 4%, 6%, 8% and 10% degree of sulphation produced results that are higher than that of the control fatliquor (commercial fatliquor). The optimum tensile strength of the fatliquored leather was observed at 8 and 10% degree of sulphation with ultimate tensile strength values of 20.45 MPa and 23.20 MPa, respectively. This is in agreement with the biennial report of CLRI, (2015), stated that; fatliquored leather complying with the minimum tensile strength requirements of 15 N/mm^2 for articles are to be use in the manufacturing of footwear and in the leather goods industry.

3.2 Ball-burst Distension Properties of the Fatliquored Leather

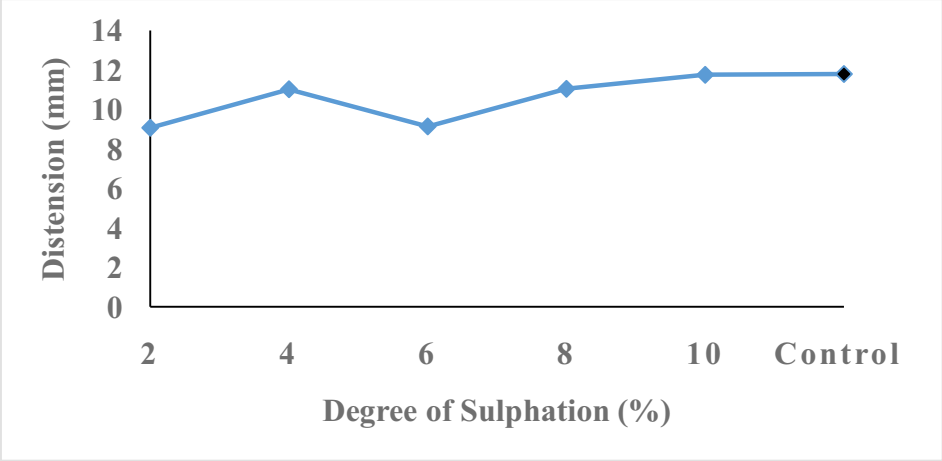

Figure 3.2: Distension of Leather fatliquored with sulphated*Lophira* oil (4% offer)

The reason for this test is to determine the grain crack force (load) and distension of leather when used for shoe upper. Shoe upper leather often shows little crack in the toe area at the time of lasting operation despite the fact that, the leather has good tensile strength. It could be observed from figure 3.2that the highest distension of the fatliquored leather at various degree of sulphationwas at 10% degree of sulphationwith a distension value of 12.13 mm.At 6% degree of sulphation, the distension properties of the leather tend to decrease due to the variation in the toughness of the animal skin before processing and also the varieties of conditions such as the age and breed of the animal, the weave of the collagen fibre bundles, the apparent density of the skin and glycosaminoglycan contents of the skin (Wang and Attenburrow, 1993).

Table 3.1: Percentage Elongation in relation to Percentage Degree of Sulphation/Percentage Offer of the Fatliquor

Degree of Sulphation (%)	Offer (%)	Elongation (%)
2	4	64.20
4	4	45.43
6	4	97.04
8	4	54.71
10	4	40.58
Control X	4	52.63

The elongation at break of leathers is a useful index on the elastic properties of the leathers. The elongation is measured simultaneously with the measurement of tensile strength. Table 3.1 is the result of percentage elongation at 4% offer for 2, 4, 6, 8 and 10% degree of sulphation. In the study, leathers fatliquored with the produced fatliquor gave the highest value 97.04% elongation at break at 4% offer and 6% Degree of sulphation, whereas, the leather obtained with commercial fatliquor gave highest value of 52.53%. Sharphouse, (1989), reported that, the minimum level of elongation required for the manufacture of footwear and other leather goods is 40%, this being extensively completed by each of the fatliquored leathers and this is a prove that, the leather fatliquored with *Lophira*fatliquor has a high percentage elongation as compared to the standard.

3.3 Result of the morphology of the leather fibre

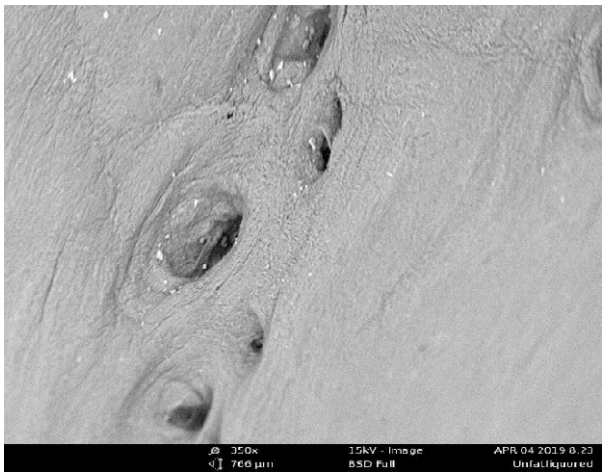

Plate 3.3 (a): Un-fatliquored leather

SEM looks deeply into the leather fibre structure and shows the effect of fatliquor on fibre and grain surface. SEM of the grain surface (x 350) of the fatliquored leather exhibits a soft grain as indicated in plate 3.3 (b) by the squeezing of the collagen fibre as compared to un-fatliquored leather in plate 3.3 (a) with a smooth and well-arranged fibres. The pores on the fatliquored leather was also an indication that the fatliquor has penetrated the leather grain surface as compared to the un-fatliquored leather with the pores widely opened. The SEM Micrograph of the leather fatliquored with the manufactured fatliquor, agrees with the reports of El-shahat and Mohammed, (2010), stating that, the improvement in the mechanical properties of the treated leather is due to good lubrication of the fibres because of the interaction between the active centers in the collagen molecules of the leather fibre and the emulsifying group penetrating into the leather fibre.

Plate 3.3 (b): Fatliquored leather

4.0CONCLUSION

The outcome of the experiment conducted were analysedaccording to the application of the leather based on the physical, mechanical and morphological characterization of the fatliquored leather.Based on the analysis of experimental results, it can be stated that this study on the manufactured fatliquored leather proved that:

i. The leather processed by the manufactured fatliquor and conventional fatliquor are closer in respective of their mechanical strength properties with a tensile strength of 20.66 MPa for the synthesisedfatliquor and 21.59 MPa for the conventional fatliquor.
ii. The optimum tensile strength was achieved at 8 and 10% degree of sulphation (4% fatliquor offer) with a tensile strength of 20.45 MPa and 23.20 MPa as compared to 10.14 MPa of the conventional fatliquor. This indicated that the leather can be used as a clothing leather, wallet and Automated Teller Machine (ATM) card packs.

Finally it can be concluded that *Lophiralanceolata*seed oil sulphatedfatliquor has a greatpotential to substitute the imported vegetable oil sulphatedfatliquor in Nigeria Leather ProcessingIndustry.

ACKNOWLEDGEMENTS

We sincerely acknowledge the laboratory facilities provided by the Directorate of Research and Development, Nigerian Institute of Leather and Science Technology (NILEST), Zaria; Nigeria, Department of Chemistry, Ahmadu Bello University (ABU), Zaria, Department of Physics, Umaru Musa Yaradua University (UMYU), Katsina-Nigeriaand also Engineering Materials Development Institute (EMDI), Akure; OndoState, Nigeria, for the analysis of the oil sample.

REFERENCE

ASTM D638. (2014). Standard Test Method for Tensile properties of polymer matrix composite matter. ASTM International, West Conshohocken, PA.

Chen, W.T. and Li, S.F. (2012). Synthesis of fatliquor from palm oil and hydroxyl-terminated organosilicon. *Asian Journal of Chemistry,* 24(1): 63-67.

CLRI (2015). Bureau of Indian standards: Leather Specification of CLRI Guideline, Biennial Report, Central Leather Research, New Delhi, pp. 3-6.

Cuq, M.H., Benjelloun-Mlayah, B., and Delmas, M. (1998). Oil extracted from seal hides:

characterization and use as leather fatliquor. *Journal of the American Oil Chemists' Society*, 75(8): 1015-1019.

El-Shahat, H.A.N. and Mohamed, G.M. (2010). Ester phosphate of discarded palm oil from potato chip factories as fatliquoring agent. *Journal of American Science*, 12(6): 617-626

Hassan, M. T., Gurashi. A. G. and Faki, E.F.M. (2017). Application of fatliquor prepared from sudanese castor oil in leather fatliquoring process. *International Journal of Engineering Sciences and Research Technology*, 6(10): 248-253.

International Organization for Standardization (IOS) (2002). 3379 (IULTC/UP 9) Determination and strength of grain-- Ball burst test.

Mutlu, M.M., Ork, N., Yegin, O. and Bas, S. (2014). "Mapping the Variations of Tensile Strength over the Area of Sheepskin Leather", Annals of the *Universıty of Oradea*, 15, 157-162.

Senait, G. N. (2014). Fatliquor Product Development from *Vernoniagalamensis* Seed Oil via Modified Sulphitation Process. M.Sc. Thesis, Addis Ababa Institute of Technology, Ethiopia.

Sharphouse, J.H., (1989). Leather Technician's Handbook, Leather Producers Association Northampton, pp. 575-589.

Urbanija, V. and Gersak, J. (2004). "Impact of the Mechanical Properties of Nappa Clothing Leather on the Characteristics of Its Use", Journal of the Society of Leather Technologists and Chemists, 88, 181-190.

Venkatachalam, P.S., (1962). Lectures Notes on Leather, APO, Central Leather Research Institute (CLRI), Madras, India.

Wang, Y.L and Attenburrow, G.E. (1993). Strength of Brazilian Goatskin Leathers in Relation to Skin and Animal Characteristics. *Journal of Society of Leather Technologists and Chemists,* 78(1): 55-68.

Xiao-Lei, Z., Qing-Lan, L. and Wei-Ping, Z. (2006). "Evaluation of Leather Handle Character by Discriminatory Two Class Analysis", Journal of the Society of Leather Technologists and Chemists, 91, 201-207.

Nigerian Journal of Polymer Science and Technology, 2020, Vol. 15, pp49-57
Received: 05/06/2020 Accepted: 25/09/2020

Design of Sand/Palm Kernel Shell Particles as Binder for Block Making Applications

Ichetaonye, S.I.[a*], Igwe, N.C.[a], Adekoya, J.G. [a]and Amoke, A.[b]

[a] Department of Polymer and Textile Technology, Yaba College of Technology, Lagos, Nigeria.*
[b] Department of Polymer Technology, Auchi Polytechnic, Auchi, Nigeria.

***Corresponding Author:*ik4simon@yahoo.com**

Abstract
This paper discusses the study of sand / Palm Kernel Shell (PKS) particles for suitability in block production using cement and hardener as binder. The mix proportion of the blocks was based on 16g with filler ratios (20/80, 40/60, 60/40 and 80/20) % represented as samples A, B, C and D respectively, and then cured for 30 days before testing. Tests conducted on the blocks were dry shrinkage, compressive strength, apparent porosity, bulk density, water absorption, hardness and SEM. Preliminary analysisof the results revealed that the physico-mechanical properties of the cement blocks were slightly better of than the hardener blocks across the various ratios. But sample D (80/20) amongst the other samples proved to be the best ofboth cement and hardener blocks. Clearly, the dry shrinkage of the hardener blocks was 0%,the compressive strength, apparent porosity, water absorption, hardness and also bulk density of the hardener blocks were in the range of 403 – 1050 KN/M^2, 25 – 40 %, 18 – 41%, 47.6 – 74.7 Hv, 0.84 – 1.48 g/cm^3 respectively. Thus, we can conclude that sand/PKS exhibit the better mechanical effect among other represented samples; as a result of its better tight network structure and stronger bond within the particles. This presents sand / PKS as a suitable substitute to cement in block making applications.

Keywords:Agricultural waste, binder, block, cement, hardener, sand

1.0 Introduction

In any built environment, block remains the most versatile and commonest composite construction materials for infrastructural development of any nation. It is composed of cement, fine or coarse aggregate and water in a specified proportion. Though, sand and cement have been used in the construction of buildings as well as roads but the demands for these materials continue to grow [1]. Many sand mining sites have been closed because of the damage they cause to the environmental degradation such as the popular sand mining site within the campus of the Federal University of Technology, Owerri, Imo state of Nigeria. Problem of sand scarcity is of great concern that some equipment manufacturers have developed rock crushing equipment that produce ‘‘manufactured sand’’ which resemble that of natural river sand [2]. Attempts have been made to either completely or partially replace sand with the use of alternative cheaper local materials which will greatly enhance the production of block with the desired properties at lower cost [3].

In developing countries like Nigeria, proper utilization of agricultural waste such as rice husk, groundnut shell, Palm kernel Shell etc had not been given due

attention thereby constitutes an environmental nuisance as they form refuse heaps in the areas where they are disposed [4]. Palm kernel Shell (PKS) as an agricultural product has been regarded as waste from palm oil processing. They are obtained after extraction of the palm oil, the nuts are broken and the kernels are removed with the shells mostly left as waste. The PKS are hard stony endocarps that surround the kernel and the shells come in different shapes / sizes with good mechanical properties for light weight structures [5].

In Nigeria, cement is averagely the most expensive ingredient in the production of block.Due to the negative impact resulting to environmental pollution, degradation of natural resources such as limestone and high cost of Portland cement, there is, therefore, need for available substitute for cement in block production [6]. One of the practical solution is the use of an alternate binder such as ‘‘hardener’’. Hardener is a component of certain types of mixtures that can be used in a majority of bonding situations at lower temperatures, and to produce a rapid cure that develops its physical properties quickly at room temperature. Also, it can be a reactant in the chemical reaction during mixture once it set or used as a curing component [7].

Therefore, the purpose of the research is to explore the potential of using PKS as a combination with sand and hardener as binder for sustainable economic development in block production and also as a replacement for cement.

2.0 Experimental

2.1 Materials Preparation

The PKS obtained from Umuodom village, Isiala Mbano, Imo – state, Nigeria, was agitated in 5 Litres of water and soaked for 72 Hrs to remove both live and dead organic matters that could have affected the physico – mechanical properties of the PKS after which the clarified water was sieved off. The shell (Fig. 1(a)) was sun dried for about 3 days, ground and sieved through 80µm sieve to obtain fine particles. These sieving processes were repeated for the Silica sand obtained from Badagry Beach Badagry, Lagos, South West, Nigeria at the sea shore. 88 Universal mold release wax (Meguiar’s Mirror Giaze)was used as a mould releasing agent while Ordinary Portland cement (OPC) manufactured by Dangote cement, Nigeria and hardener (West System 205) were used as binder.The chemical composition of OPC is listed in Table 1.

Fig. 1: (a) Dried PKS (b) Ground PKS (c) Ordinary Portland cement (d) Silica sand (SS) (e) Hardener (f) 88 Universal mold release wax (g) Stainless steel mould with detachable base

Table 1. Chemical analysis of OPC

Parameter	OPC (%)
SiO_2	21.7
Al_2O_2	5.61
Fe_2O_2	3.83
CaO	64.47
MgO	2.01
Na_2O	0.13
K_2O	0.17
SO_3^2	1.69

2.2 Preparation of BlocksSamples

Caution was taken in the preparation of large number of samples at all production stages. The mixture of SS / PKS with cement and SS / PKS with hardener was based on 16 g. The mixture was done properly to obtain mouldable test samples in different filler ratios of (20/80, 40/60, 60/40 and 80/20) represented as samples A, B, C and D respectively. They were sun-dried for 30 days preparatory to the various tests of linear shrinkge, bulk density, apparent porosity, compressive strenght, water absorption and scanning electro microscope.

Fig. 2: (a) Hardener samples at various ratios and (b) OPC samples at various ratios

3.0 Test Procedures

3.1 Dry Shrinkage

The dry shrinkage (DS) was determined by measuring the length of the dried sample as (L_d) and later as (L_o) after oven drying at 120^0 C for 60 minutes. The DS was then calculated using Equation (1) [8].

$$\%DS \quad \frac{L_d \quad L_o}{L_d} \quad 100 \qquad (1)$$

3.2 Compressive Strength

The compressive strength (CS) of the samples was determined by placing the samples in a compressive testing machine andload applied axially by turning the hand wheel at a uniform rate till failure occurs using a well calibrated scale. The tensometer readings were recorded and compressive strength calculated using Equation (2).

$$CS \quad \frac{Maximum \quad Load \quad to \quad Failure}{Cross \quad Sectional \quad Area} \quad \frac{KN}{M^2} \tag{2}$$

3.3 Apparent Porosity and Bulk Density

Apparent porosity (AP) and Bulk density (BD) of the samples were determined by drying freshly compacted samples in the oven at 120^0 C for 2 Hrs to obtain specific constant weight (W_d). Thereafter, each of the samples was soaked in water for seven (7) hours and the wet weight of the samples taken as (W_w). The AP was calculated using Equation (3) while the BD was determined with Equation (4) where ρw is the density of water [9].

$$\%AP \quad \frac{W_w \quad W_d}{W_w \quad W_s} \quad 100 \tag{3}$$

$$\%BD \quad \frac{W_d \quad w}{W_w \quad W_s} \left| g \Big/ cm^3 \right| \tag{4}$$

3.4 Water Absorption

The water absorption (WA) was determined by totally immersing the dried weighed sample (W_d) in 250 ml beaker of water for 24 Hrs. After which they were taken out, wiped with a clean cloth, weighed (W_w) and recorded according to ASTM D 570 standard. The WA was calculated using Equation (5).

$$\%WA \quad \frac{W_w \quad W_d}{W_d} \quad 100 \tag{5}$$

3.5 Micro- Hardness

The micro – hardness (MH)was determined by placing a sample in a Leitz Hardnes (OS-2H) tester. This tester had a diamond indenter, in the form of a right pyramid with a square base and an angle 136^0 between opposite faces under a load of 3 N in accordance with ASTM E384.

3.6 Scanning Electron Microscope

The scanning electron microscope (SEM) was determined by placing a small piece of the dried compacted samples in a PHENOM G2 Pro SEM machine to access the morphology of the sample on the monitor screen using 15.0 KV.

4.0 Results and Discussion

4.1 Dry Shrinkage

Fig. 3 revealed the dry shrinkage of hardener and cement blocks at various filler ratios. Cement blocks presents the maximum shrinkage value of 2.6 % across every filler ratios maybe this was due to the presence of impurity within the particles while that of the hardener blocks showed no shrinkage effect. This may also be as a result of no contraction within the individual particle [10].

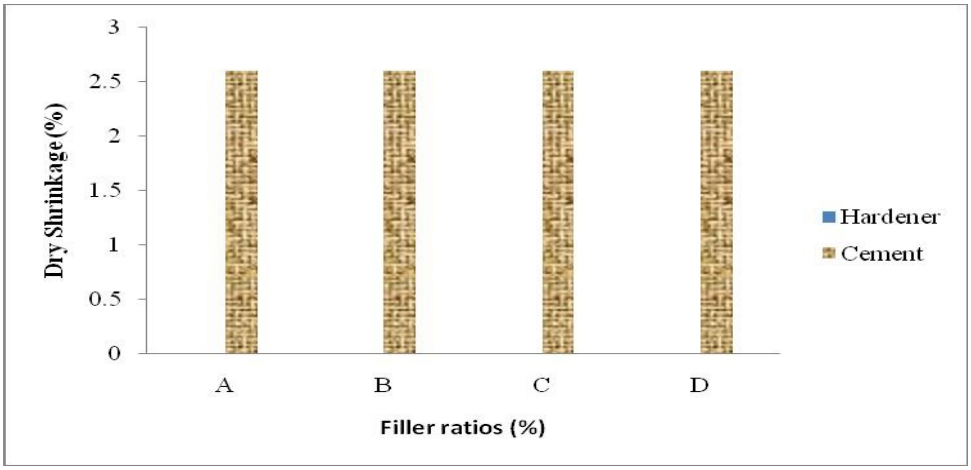

Fig. 3: Dry shrinkage of hardener blocks and cement blocks at various filler ratios

4.2 Compressive Strength

The CS for both the hardener blocks and cement blocks at different filler ratios is shown in Fig. 4. Though the figure shows that the compressive strength increases across the various samples but sample D presents a greater strength with 1050 KN/M^2 and 1200 KN/M^2 for both hardener and cement blocks respectively compared to other samples. This could be attributed to increase in cohesive bond / interfacial bonding between individual grains [11][12].

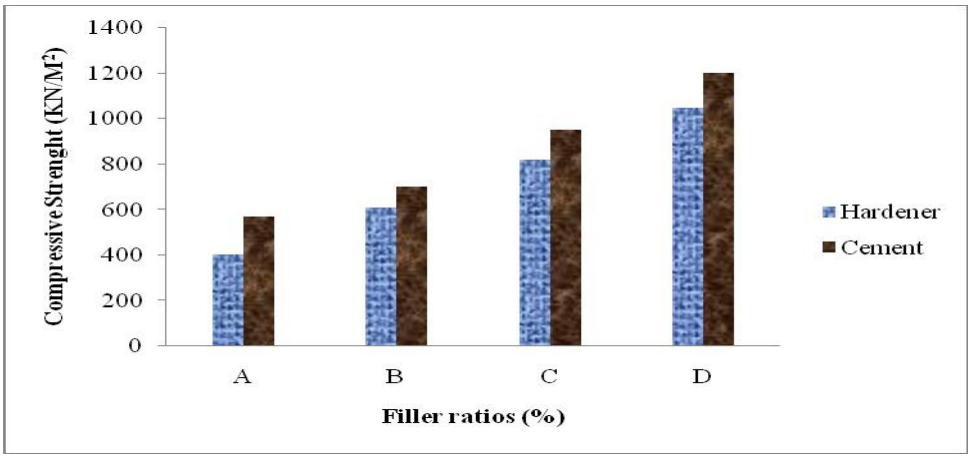

Fig. 4: Compressive strength of hardener blocks and cement blocks at various filler ratios

4.2 Bulk Density

In Fig. 5, there was gradual increase in BD across the various ratios. With the increase in BD of the samples, where the hardener blocks ranges between 0.84 g/cm^3 – 1.47 g/cm^3 and the cement blocks was between 0.9 g/cm^3 – 1.64 g/cm^3, sample D still exhibits the maximum BD of 1.47 g/cm^3 for hardener blocks and 1.84 g/cm^3 for cement blocks. This was due to increase in closure of internal pores while other samples possess lesser closure of internal pores between the binder and the particles [11][12].

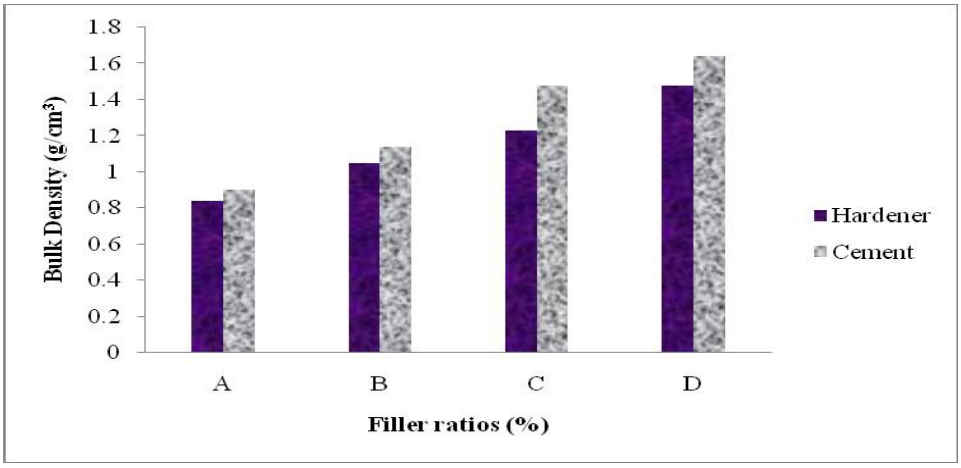

Fig. 5: Bulk density of hardener blocks and cement blocks at various filler ratios

4.3 Water Absorption and Apparent porosity

Fig. 6 presents the WA of hardener and cement blocks at different ratios. Across the various ratios, sample D reveals the least absorption rate of 19 % for hardener blocks and 13 % for cement blocks. This was as a result of strong interfacial bonding as well as high closure of internal pores between the binder and particles compared to other ratios with poor bonding and increase in macro-cracks were WA rate is based on fluid penetration resistance. This WA trend can be related to AP rate as shown in Fig. 7 were sample D shows the least porosity rate of 25 % and 21 % for hardener and cement blocks respectively. This was due to better cohesive bonding between the binder and the particles which can also lead to improve in strength higher than that of other ratios [13].

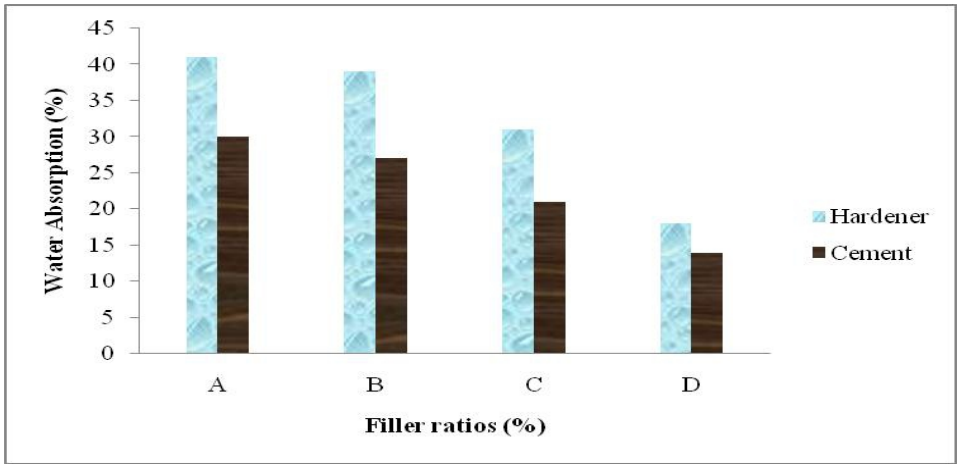

Fig. 6: Water absorption of hardener blocks and cement blocks at various filler ratios

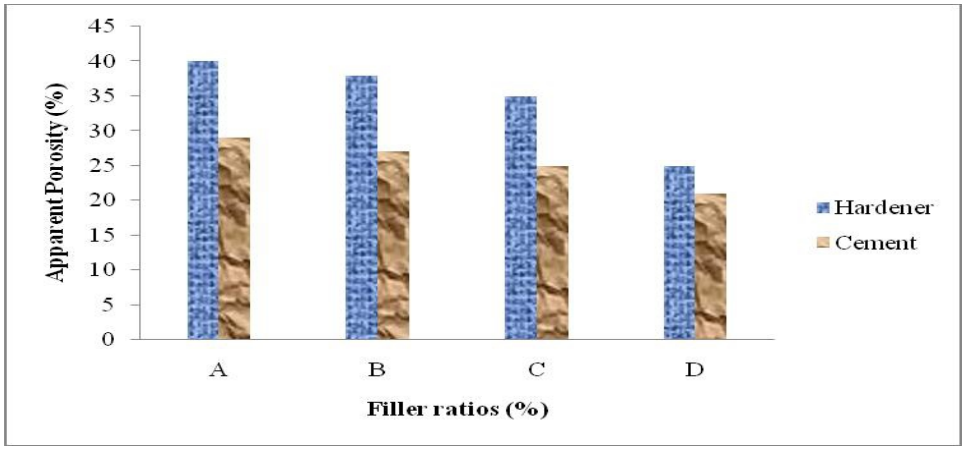

Fig. 7: Apparent porosity of hardener blocks and cement blocks at various filler ratios

4.4 Micro-Hardness

Fig. 8 showed that the MH increase began from the initial filler ratios (Sample A). The maximum MH value was shown at sample D with 74.7 Hv and 80 Hv for hardener and cement blocks respectively. This was due to increase in compactness and better interlocking within the individual particles than other filler ratios which ranges between 47.6 Hv - 67.8 Hv for hardener blocks and 58.2 Hv – 75.1 Hv for cement blocks [14].

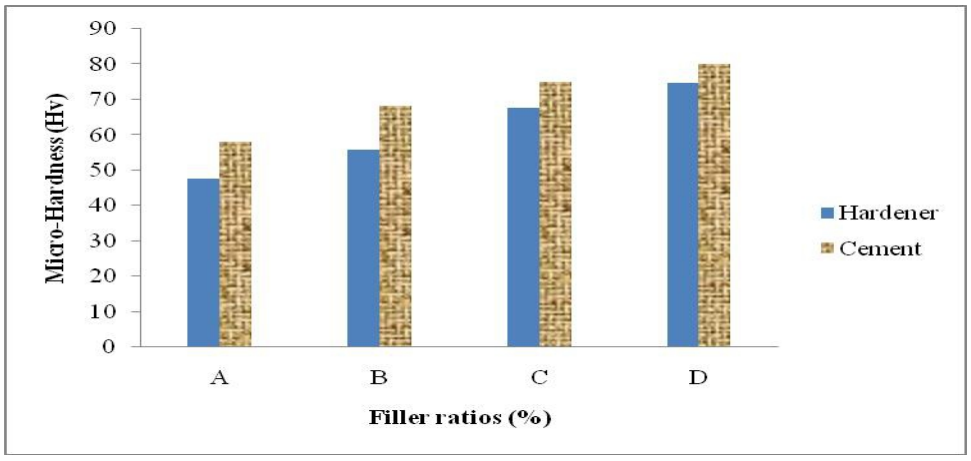

Fig. 8: Micro hardness of hardener blocks and cement blocks at various filler ratios

4.5 Scanning Electron Microscope Analysis (SEM)

The morphological texture of samples A presented in Fig. 9 (a) and (b) for hardener and cement samples show increased disaggregation in the texture; and this accounts for the increase in porosity due to the opening up of internal pores in the block samples as well as poor bonding of the binder with the individual particles. Fig. 9 (c) and (d) for samples C show the existence of aggregated individual particles which indicates fairly tight bond and present increased closed network of structures; which could combat dispersive behaviour [10].

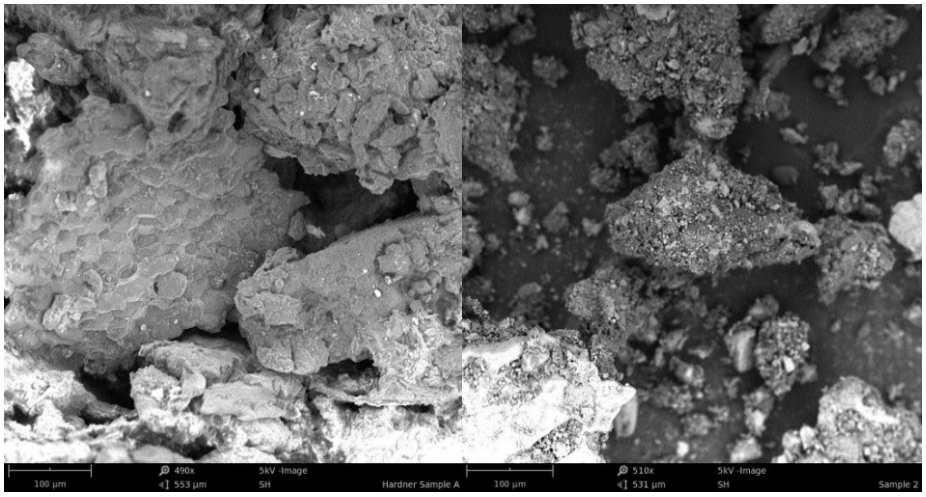

(a) **(b)**

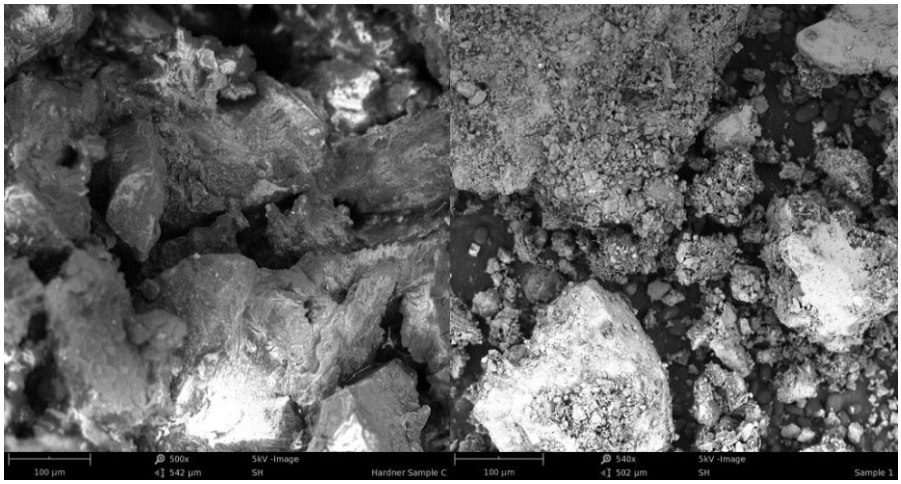

(c) **(d)**

Fig. 9: Morphological texture of the block samples at different filler loadings: (a) Hardener samplefor A (b) Cement sample for A (c) Hardener sample for C (d) Cement sample for C

5.0 Conclusions

In general, the 80/20 ratio represented by sample D for both hardener and cement samples exhibit the better mechanical effect among other represented samples; as a result of its better tight network structure and stronger bond within the particles. Also, the hardener blocks present comparable values to that of the cement samples at same ratio and its combination with sand / PKS could be explored as binder for block production.

References

1. Anosike, B. and Oyebade, H. (2012). Sandcrete blocks and quality management in Nigeria building industry. Journal of Engineering, Project and Production Management, 2 (1): 37 – 46.
2. Nanda, R.P., Das, A.K. and Moharana, N.C. (2010). Stone crusher dust as a fine aggregate in concrete for paving blocks. International Journal of Civil and Structural Engineering, 1(3): 613 – 620.
3. Oluremi, A.A. (1990). Input of local materials in buildings as a means of reducing cost of construction. Journal

of the Nigerian Institute of Quantity surveyors, 12 – 14.

4. Al-khalaf, M.N. and Yousif, H.A. (1984). Use of rice husk ash in concrete. The International Journal of Cement Composites and Light Weight Concrete, 6 (4): 241 – 248.
5. Alangaram, U.J., Jumaat, M.Z. and Mahmud, H. (2008). Some physical and mechanical properties of palm kernel shell (PKS). Botswana Journal of Technology, 17.
6. Yusuf, M.O.(2001).Partial replacement of ordinary Portland cement with groundnut shell ash in concrete production. Postgraduate Diploma Research Project, Department of Agricultural Engineering, Federal University of Technology, Minna, Nigeria.
7. Forbes, A. (1996). Fibre glass and composite materials: An enthusiast's guide to high performance non – metallic materials. Penguin Books Limited, 138.
8. Amuda, M.O.H., Lawal, G.I. and Majolagbe, F.O. (2005): Characterization and Evaluation of Refractory Properties of Clays from South-West Deposit. Nigeria Society of Engineering Technical Transaction, 40 (4): 13 – 23.
9. Ichetaonye, S.I. (2014). Physico-chemical and morphological properties of alumina-silica refractory blend. PGD dissertation, Department of Metallurgical and Materials Engineering, University of Lagos, Nigeria.
10. Amuda, M.O.H., Ichetaonye, S.I. and Lawal, F.T. (2019). Refractory Properties of Alumina/Silica Blend. The West Indian Journal of Engineering,22-32.
11. Ichetaonye, S.I. and Amuda, M.O.H. (2018). Comparative Study of Sandcrete Cement and Carbonized Balanite Shell Blocks for construction. 17thNigerian International Materials Congress (Nimacon 2018) at Raw Materials Research and Development Council Abuja.
12. Oyejobi, D.O, Abdulkadir, T.S., Yusuf, I.T and Badiru, M. J. (2012). Effect of Palm Kernel Shells Sizes and Mix Ratios on Lightweight Concrete. Journal of Research Information in Civil Engineering, 9 (2): 217 -226.
13. Donald K.D. and Jonas, E.Y. (2015). Palm Kernel Shells as A Partial Replacement for Sand in Sandcrete block Production. Chemistry and Materials Research, 7 (10): 61 – 72.
14. Alewo, O. A., Mohammed, T. I. and Ibrahim, S. (2015). Effect of Particle Size and Concentration on the Mechanical Properties of Polyester / Date Palm Seed Particulate Composite. Leonardo Electronics and Technologies, 65 – 78.
15. ASTM D570 (2018). Standard Test Method for Water Absorption of Plastics. Vol. 08.01.
16. ASTM E 384 (2017). Standard Test Method for Micro-indentation Hardness of Materials. Vol. 3.01

Nigerian Journal of Polymer Science and Technology, 2020, Vol. 15, pp58-65
Received: 27/07/2020 Accepted: 30/09/2020

Utilization of Carbonized Cashew Nut Shell Powder (CNSP)Particles for the Reinforcement of Natural Rubber Filled Composite

[1]Okele, A.I., [2]Gimba C.E., [2]Mamza, P.A.P., and [2]Abba, H.

[1] Department of Polymer Technology, Nigerian Institute of Leather and Science Technology, Samaru-Zaria
[2] Department of Chemistry, Ahmadu Bello University, Zaria.

Corresponding Author: walislove4real@yahoo.com

Abstract
Natural rubber was reinforced with particles of cashew nut shell powder (CNSP) as filler. The filler was loaded in the compound from 0-50pphr of natural rubber. The cashew nut shell powder was carbonized and characterized for pH, moisture content, particle size, bulk density and ash content. The characterization results revealed 8.13 pH value, 0.58% moisture content, 276.4 d.nm at 69.2% and 404 d. nm at 30.8% particle size, 0.4032g/ml bulk density and 15.99% ash content. The mechanical analyses carried out were tensile strength, compression strength, hardness and abrasion resistance. The obtained results showed that as filler loading was increased from 0-50pphr, the tensile strength also increased from 0.30Mpa to 5.60Mpa which is agood indication of reinforcement of the filler. The compound filled wit h 10pphr gave the best percentage compression strength of 11.1% while that of 50pphr revealed 22.2%. The hardness values were not left out in the trend as the filler also increased, the hardness resistance also increased from 25-44 IRHD. The abrasion resistance increased as the filler loading was increased from 0-40pphr with abrasion values of 6.78, 0.84, 0.57, 0.35 and 0.21% respectively before it increased at 50pphr to 1.73%.

Key words: Ash content, Fillers, Moisture content, Natural rubber and Tensile strength

1.0 Introduction

The need to develop industrial products from renewable, environmental friendly and sustainable raw materials and processes is attracting global attention. Natural rubber is a gummy substance isolated from the white fluid of certain tree species called HeveaBrasiliensis with major chemical constituent of natural hydrocarbon polymer (polyisoprene) of 2-methyl-1,3 butadiene. It is the major feed stock to the rubber industries, however, in its raw state, natural rubber is not suitable for use in any given application because of their viscoelasticity (tendency of both plastic and elastic behaviour)(Egwakhide et al; 2013).

Nanotechnology, technologies at nanoscale, is a new science that involves enhancing and engineering the material properties and technologies at the nanoscale. In comparison with the microtechnology, nanotechnology leads to extremely different phenomena and performances. The nanocomposite products contain reinforcing or fillers in nanoscale (less than 100 nm).Most of the mechanical properties can be improved using nanoscale fillers. Researchers have studied the current

and future prospective products within the nanoscience(Islam et al; 2013).

In natural rubber compounding, fillers are majoradditives. Incorporation of fillers into natural rubber matrix enhances properties such as tensile strength, modulus, tear strength, abrasion resistance, stiffness and processibility. Also significantly reduced by the addition of additives is the cost of the manufactured rubber products (oboh et al; 2008).

The mechanism of elastomeric reinforcement by fillers has been reviewed by several workers. One of the mechanisms by which particulate fillers reinforces elastomers is that reported by Bueche and Flemimert. They considered that the effect of filler is to increase the number of chains, which shared the load of a broken polymer chain. Fillers used in rubber industries may be classified on the basis of sources, properties and colour(Egwakhide et al; 2013).

Composites are multifunctional materials of two or more distinct components. Macroscopically, they have identifiable distinct interface that separate them. Polymer composites basically have discontinuous phase (fillers) embedded in a continuous phase (polymer). They are termed hybrid composites when two or more discontinuous phases are incorporated into a continuous phase. Hybrid fillers reinforced composites have been reported to enhance the mechanical, thermal, damping properties compared to single filler reinforced composites(Oboh et al; 2018b). Extensive works have been going on in the search for possible substitutes for some grades of carbon black as filler for rubber products. For instance, by-products from agricultural sources have been used – maize cobs, rubber seed shell, ground nut husk, cassava peeling, plantain peel, coconut fibre, rubber seed shell carbon (Aguele and Madufor, 2012)

2.0 Materials, Equipment and Methodology

Cashew nut shell was locally sourced from AuchiCommunity of Edo State. Natural rubber was obtained from Rubber Research Institute of Nigeria, Iyanomo, Benin city, Edo State. All other compounding additives used (zinc oxides, stearic acid, trimethylquinoline, Sulphur and mercaptobenzolthiazoledisulphide) are of analytical grades and products of British Drug House (BDH), England.

2.1 Equipment

The equipment used are Endocott test sieve shaker, by Endocott test sieve ltd., London, Ball Miller by Pascal Engineering Co. Ltd. Sussex, England, Furnace, soxhlet apparatus, beakers, stop watch and Two roll mill, Reliable Rubber and Plastics Machinery, model 5189, Advanced Material Testing Machine, Zwick/Roell, Hardness tester MuverFranscisco, Munoz Irles, Abrader, Santra test equipment, and Wallace compression set machine.

2.2 Methodology

2.2.1 Preparation and Characterization of Filler

Cashew nut shell powder was winnowed to remove sand particles and other adhering foreign bodies and then washed. The washed Cashew nut shell powderwas placed in the planetary mill with a spherical grinding media which consists of planetary balls (< 0.1mm diameter) made of hardened steel (0.24 to 0.95cm diameter). The Cashew nut shell powderand the grinding media were placed in a stationary tank followed by an agitation with an armed shaft rotating at 250rpm. The forces of shear and impact exerted by the grinding media on the Cashew nut shell powderreduced it to a

dispersion of fine powder. The resultant slurry formed was discharged, air-dried and further oven-dried. The cake was further extracted with N-hexane to discard off the oil in the Cashew nut shell powderand was carbonized at the temperature of 200^{o}C, the residue was ball milled using the top-down technique (i.e. critical speed grinding under a continuous process ofapproximately 48hrs) to a fine particle size. Standard tests method was used to characterize the powder for moisture content (ASTM 1509) at 105^{o}C, pH (ASTM 1512) and particle size [Ojinmah et al; 2017].

2.2.2 Compounding of the composites

The compounding of the rubber with other additives were done using a laboratory two roll mill in accordance with ASTM D3184-80 method at temperature of 70 ± 5^{o}C, followed by in-situ moulding and curing at 130^{o}C with a hydraulic press machine.

2.2.3 Tensile Strength

These tests were conducted in accordance to ASTM D412. Tensile tests were carried out at room temperature using an Advance Material Testing machine model 3366 with a load cell 1kN. Pre-moulded dumbbell shaped specimens with dimensions of 50 X 8 X 4 mm^3 were used to perform the experiment ata loading speed of 200 mm/min (Islam et al; 2013)

2.2.4 Hardness test

The hardness test of a rubber is the relative resistance of the surface to indentation by an indentor of specified dimension under a specified load. Hardness of the vulcanisates was determined by standard dead load method (BS903 part A 26) [Egwakhide et al; 2007].

2.2.5 Abrasion resistance

Wallace Akron tester was used in accordance with BS method Abrasive resistance index = (S) 1000/ T ……. (1) [Egwakhide et al; 2007].

2.2.6 Compression set

Wallace compression set machine (Mode/Ref No (2, H250) was used to determine the compression set of the vulcanizates. Compression set % = t0- tr/t0 X 100 …… (2) [Egwakhide et al; 2007].

Table 1: Formulation table

S/NO	Ingredients	PPhr
1	Natural rubber	100
2	Zinc oxide	5
3	Stearic acid	2
4	Trimethylquinoline (TMQ)	1.5
5	Mercaptobenzolthiazole	3
6	Cashew shell powder	0,10,20,30,40,50
7	Processing oil	2
8	Sulphur	3

3.1 Results and Discussions

Table 2: Characterisation Results

S/NO	Characterisation	Results
1	Moisture content (%)	0.58
2	Bulk density (g/ml)	0.4032

3	Ph	8.13
4	Ash content (%)	15.99
5	Oil absorption number (ml/100g)	64,7
6	Iodine absorption number (cm^3/100g)	109.94
7	Refractive index	1.586
8	% Loss on ignition at (950^{o}C)	11

also influenced by the presence of volatile substances, the porosity of the surface and the presence of extractable (ASTM-D1510).

The result Cashew nut shell powder (CNSP) was characterized in terms of moisture content, pH, bulk density, particle size, ash content; oil absorption number, refractive index and iodine absorption number see Table 2. The above parameters were necessary because they play an important role in determining the distribution and dispersion of the fillers in natural rubber (Egwakhide*et al.,* 2017).

The pH of the filler slurry shows that the filler is alkaline in nature with alkaline value of 8.13 which in turns accelerates vulcanisation, moisture content of 0.58%, bulk density of 0.4032 g/ml, ash content of 15.99%.

The bulk density result which reveals 0.4032 g/ml is an indication of the material being light weight filler and its alkaline nature will help to accelerate vulcanization.

The low moisture content of 0.58% was as a result of the filler being carbonized at 200^{o}C.

The iodine absorption number is the amount of iodine taken up by 100 g of the material. It is also a direct proportion to the surface area. The absorption number isinTable 2 shows that cashew nut shell powder has an iodine absorption number of 109.94cm^3/100g, this implies that the higher the iodine absorption number the higher the surface area and the better reinforcement the filler will be.

The oil absorption which is the amount of linseed oil required to exactly wet 100g of the pigment, depending on the surface, particle shape, surface type (morphology) of the pigment/extender will determine the quantity of oil to be absorbed (ASTM D281-95, 2007). The higher the oil absorption numbers of the pigment/extenders, the higher the materials surface area and the more binder it will require to bind it. The results obtained in Table 4.2 shows that CNSP has the lowest oil absorption number of 64.7ml, per 100g of the material. This in turn categorised CNSP as a medium oil absorption material materials.

The loss on ignition (LOI) is the mass loss from solid combustion residues upon heating in an air or oxygen atmosphere to a prescribed temperature. The mass loss can be due to loss of moisture, carbon, sulphur, and so forth from the decomposition or combustion of the residue (ASTM D7348-08).

The results obtain shows thatCNSP has a loss on ignition of 11% at 950^{o}C which signifies that the CNSP has higher volatile matters such as moisture, carbon and sulphur contents in it. The weight loss on ignition is a measure of carbon content lost during burning. The larger the non carbon element of the agricultural by-product, the lower reinforcing the fillers will be for elastomers (Ojinmah et al; 2017).

Refractive index is mostly used to identify a particular substance, confirm its purity or measures its concentration. It is used to measure the concentration of solutes in an aqueous solution.

The results obtained from Table 2 showed that the refractive indices of CNSP, JSSP and CB are 1.586 per 0.1g of the material dissolved in 50ml of methanol;these results were not far from that of Aguele et al; (2012) which reported R.I of carbonized coir to be 1.5191.

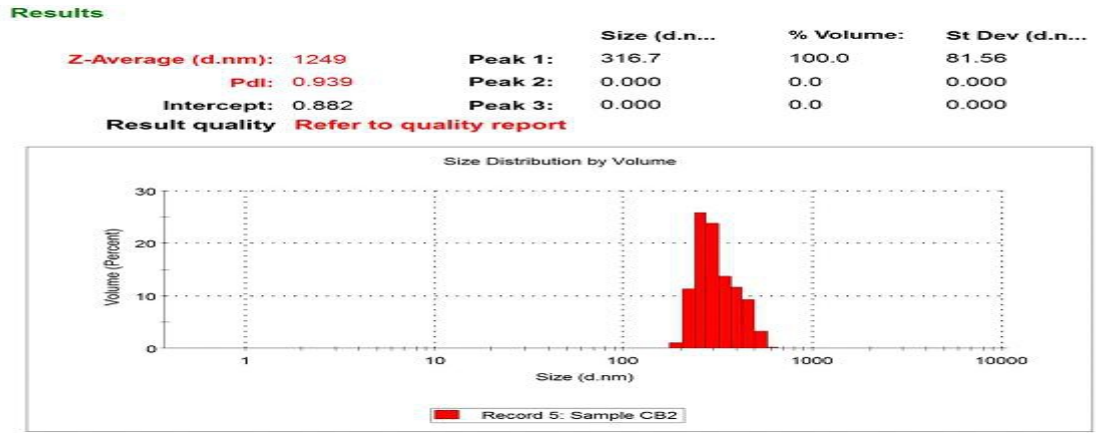

Figure 1: Dynamic light scattering of Cashew nut shell powder (CNSP)

The dynamic light scattering was use to analyse the particle size of the filler, the results obtained revealed that 100% of the particle size of the carbonized cashew nut shell powder falls in 316.7 d.nm, which falls above the 0 to 100 nm range to be classified as nano filler, rather can be categorized as semi-nano filler

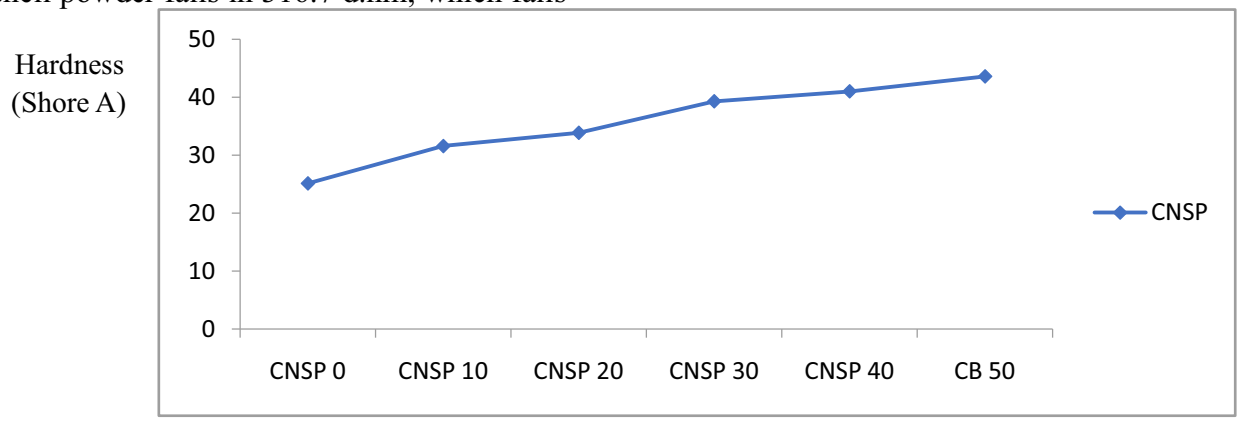

Figure 2: Effect of filler loading on Hardness

The mechanical properties of the compound showed that hardness values increased as the filler content increased from 0-50pphr. See Figure 2. With the blank compound showinghardness value of 25 IRHD and that of 10pphr of CNSP showed a hardness value of 32 IRHD. The result further increased to

that reinforced with 50pphr with a hardness value of 44 IRHD.

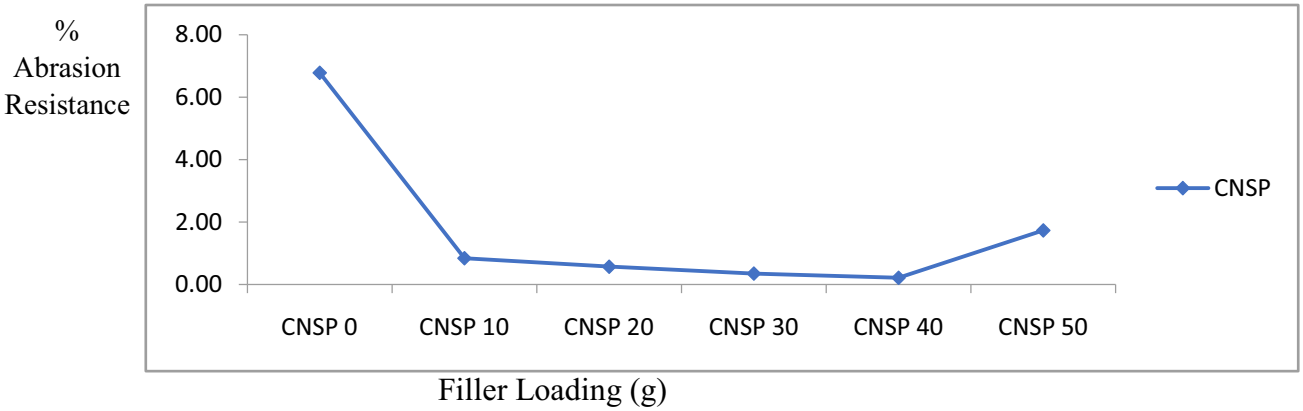

Figure 3: Effect of filler loading on Abrasion resistance

Figure 3 shows the results for percentage abrasion resistance which reveals reinforcement of filler with respect to the utilization was particulate nature. The compound without filler showed the poorest abrasion resistance percentage with value of 6.78% wear and the result became better as the filler loading increased from 10-40pphr with abrasion values of 0.84, 0.57, 0.35 and 0.21% respectively. And it later increased to 1.73% at 50pphr. This could be as a result of too much filler dosage and the NR matrix was no longer sufficient to wet the filler which can as well give rise to inhomogeneous compound mix.

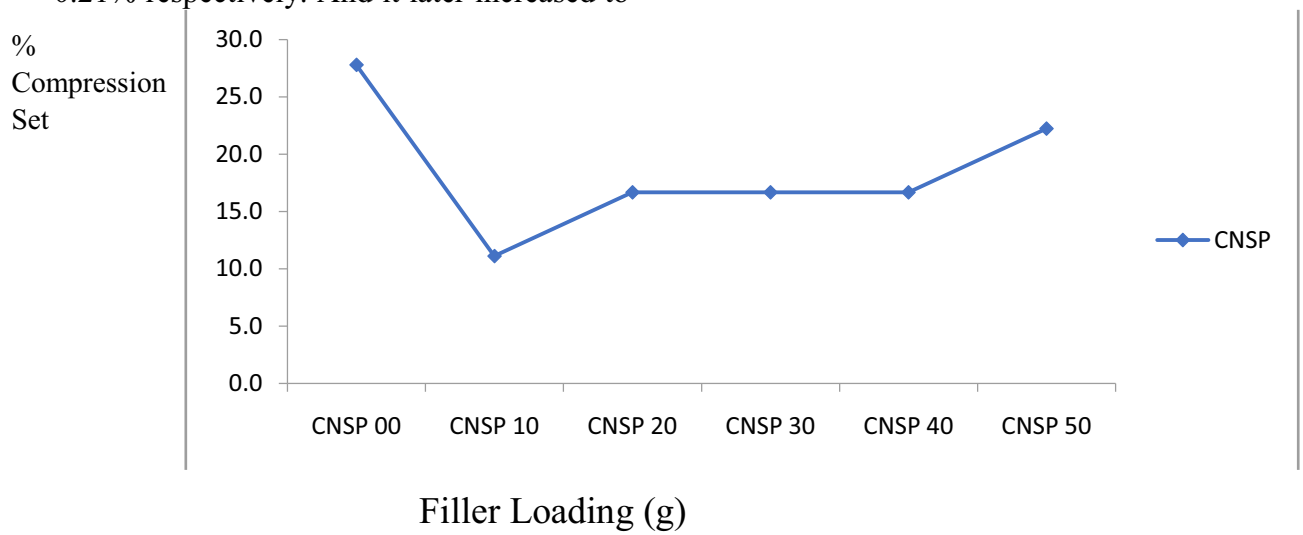

Figure 4: Effect of filler loading on Compression set

Figure 4 shows that the percentage compression set was not left out as it increased with increase in filler loading from 0-10pphr as 11.1% compression which revealed the best percentage compression set compound amongst all and there was a slight increased from 20-40pphr with percentage compression as 16.7% across board and further decreased to 22.2% at 50pphr.

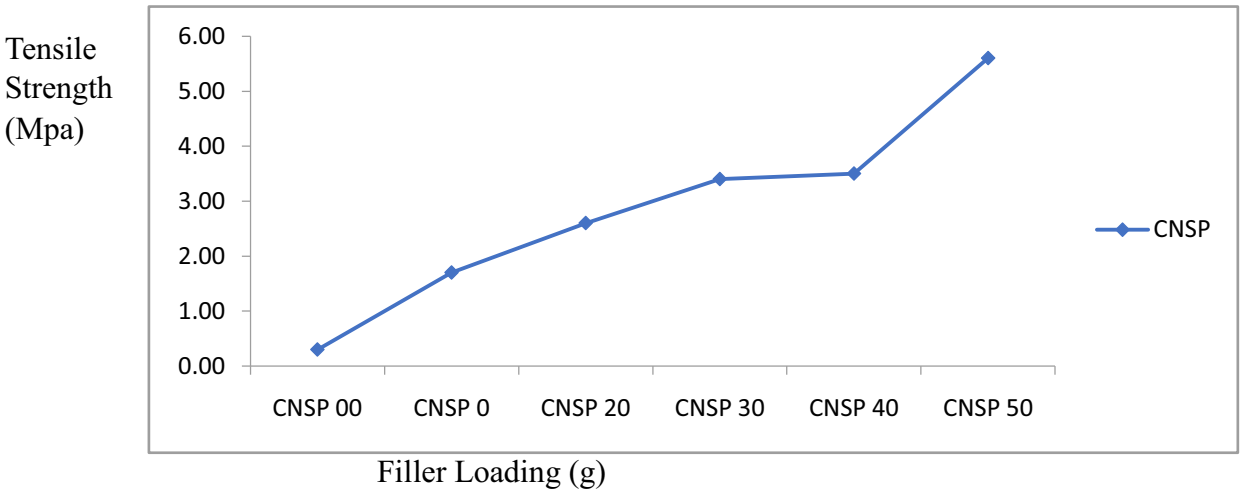

Figure 5: Effect of filler loading on Tensile strength

Figure 5 shows the result for tensile strength and it is an indication of filler reinforcement. The result of natural rubber filler cashew nut shell powder show a considerably increase in the tensile strength as the filler content was increased from 0-50pphr with the unreinforced compound having the least tensile strength result of 0.30 Mpa, and then a continual increase from 10-50 pphr with tensile strength values of 1.7, 2.6, 3.4, 3.5 and 5.60 Mpa respectively.

Conclusion

The utilization of cashew nut shell powder as filler was characterized for bulk density, moisture content, pH, ash content and particle size distribution. Also analised were the mechanical tests such as hardness, abrasion resistance, tensile strength and compression strength. The preliminary characterization revealed that the filler is a light weight material and it is alkaline in nature, hence can promote vulcanization.

The tensile strength and hardness resistance were increasing as the filler loading were increased from 0-50pphr. This has proved that carbonized cashew nut shell powder is a potential reinforcing agro waste filler to be utilized in rubber compounding in order to reduce the cost of production or rubber articles as increase in filler loadings tends to increase the mechanical properties of the rubber compounds.

References

Aguele, F.O and Madufor, C.I. (2012) "effects ofCarbonised Coir on physical of Natural Rubber Composites" *American Journal of Polymer Science, 2(3): 28-34.*

Egwaikhide, A. P., Okieimen, F. E. and Lawal, U. (2013). Rheological and Mechanical Properties of Natural Rubber Compounds Filled with Carbonized Palm Kernel Husk and Carbon Black (N330). *Science Journal of Chemistry*, *1*(5), 50. https://doi.org/10.11648/j.sjc.20130105.11

Islam, M. S., Masoodi, R., & Rostami, H. (2013). The Effect of Nanoparticles Percentage on Mechanical Behavior of Silica-Epoxy Nanocomposites. *Journal of Nanoscience*, *2013*, 1–10. https://doi.org/10.1155/2013/275037

Oboh, J. . O., Ibrahim, A. . M., Patrick, B. T., & Okele, I. . A. (2018). Reinforcement of Natural Rubber with Sisal / Sugarcane Hybrid Nanofiller. *Journal of Polymer & Composites*,

6(3), 35–42.

Oboh, J. O., Okafor, J. O., Kovo, A. S., Abdulrahman, A. S., & Okele, A. I. (2018). Isolation of Cellulosic Nanoparticles from Coir Fibre for the Preparation of Natural Rubber Composites. *Journal of Polymer & Composites*, *6*(1), 9–16. Retrieved from www.stmjournals.com

Ojinmah N, Uchechukwu T.O, Ezeh V.O and Ogbobe, O. (2017) "Studies on the Effect of Rice Husk SemiNano Filler on the Mechanical Properties of Epoxidized Natural Rubber Composite" *European Journal of Advances in Engineering and Technology, 2017, 4 (3): 164-171.*

Nigerian Journal of Polymer Science and Technology, 2020, Vol. 15, pp66-76
Received: 29/07/2020 Accepted: 04/10/2020

Mechanical, Biodegradation and Water Absorption Properties of Linear Low Density Polyethylene Composites: Effects of Eggshell and De-oiled Cashew nutshell.

Okey-Onochie, N.O., Otaigbe, J.O.E.,Oriji,O.G., Umeileka, C. C.,

Department of Pure and Industrial Chemistry, Faculty of Science, University of Portharcourt, Nigeria.

Corresponding author: onuoha.oriji@uniport.edu.ng

Abstract
The effects of de-oiled cashew nutshell powder (CNSP) and eggshell powder (ESP) on the physical,mechanical, water absorption and biodegradation properties of linear low density polyethylene (LLDPE) composites were studied. The LLDPE composites were prepared with 150μm particle sizes of 30%wt. ESP and varying amount of CNSP (10, 20, 30 wt.%) using injection molding machine at a hopper and nozzle temperatures of 200^{o}C and 220^{o}C respectively and at rotor speed of 60rpm. Results showed that the tensile, flexural and impact properties decreased with increasing CNSP filler. Whilst the mechanical properties of ESP-filled composites were lower than those of the non-ESP composites, there was a drastic drop in the composite with 20%wt. CNSP. The water absorption rates of the composites increased with duration and increasing CNSP amount for both the ESP and non-ESP composites. Similarly, the rates of biodegradation of the composites increased with duration and increasing CNSP for the composites.

Keywords: Biodegradation, Cashew Nutshell, Composites, Eggshell, Mechanical.

1.0 INTRODUCTION

Compositing in the plastic industry has stemmed from three main reasons, viz strength improvement, enhancement of biodegradability and reduction in production cost(Carraher,2014.1-232).Polymercomposites are composed of thermoplastics or thermosets which act as the matrix, with fillers (natural or synthetic fibers) as the reinforcement medium. These fillers can either enhance or decrease the properties of the composites depending on the even or uneven interaction between the polymer resin and the fillers during compounding and formulation processes. Many literatures have studied the effects of different materials on some polymer composites such as, low density polyethylene, high density polyethylene, polypropylene and linear low density polyethylene. These materials include sawdust(Najafi,Hamidinia& Tajvidi,2006,3641-3645), microcrystalline cellulose (Boran,2016.1741-1752),walnut shell flour (Nitin&Singh,2012.233-238),eggshell powder (Nwanonenyi&Chike-Onyegbula,2013,352-358;Shuhadah and Supri,2009,87-98;Farahana,Supri&Teh,2015,1-9),fish bone powder (Igwe and Onuegbu,2012,56-61),and cashew nutshell powder (Ilavbare,et al,2018,56-61 and Abubakar,2016).

Presently, composites are made for benefits beyond just improved strength and enhancement of other mechanical properties, they are also tailored towards enhancing other properties, such as, heat conductivity and insulation, electrical conductivity and insulation, biodegradability, water absorption, aesthetics, anti-corrosive, anti-static etc. The non-biodegradability of polyethylene (PE) has constituted environmental pollution due to little or non-existent methods of proper disposal. The need for an alternative which has both enhanced mechanical and biodegradable properties more than PE is pertinent to expand and not constrict its applications.Recent studies have been geared towards development of composite materials made from waste products, such as agricultural wastes (Elhaijar, LASaponara and

Mullana,2017,1-430 and Fazeli, Keley and Biazar,2018,272-280).This study is therefore aimed at developing and exploring new applications for de-oiled CNSPin the polymer field.

Cashew nut shell is a byproduct of cashew tree (*Anacardiumoccidentale, L*), which is grown in the tropical region of the world, notably the Ivory Coast, Vietnam, Indian, North and Southern America including the Caribbean Islands.They are also grown in Indonesia, Tanzania, Kenya, Mozambique, Benin, Guinea-Bissau, Nigeria and other countries with smaller production volumes.Cashew is made up of the cashew seed (commonly referred to as cashew nut) and the cashew shell (commonly referred to as cashew nutshell).The cashew nutshell is the residue or waste obtained after the extraction of the cashew nutshell liquid which consists of phenolic lipids, anacardio acid and cardanol (Ferri,2011,29-31).Recently de-oiled cashew nut shells are used as reinforcement in cement making due to their fibrous nature. They are also used as fillers in certain special proposed polymer composites.According to the study reported by Ilavbare*et al,2018,49-54,*titled "*Hybridisation of Carbon Black: Cashew Nutshell Powder as Fillers on the Mechanical Properties of Natural Rubber Composites*".Results of the study showed an increase in the tensile strength, micro-hardness, impact strength and abrasive resistance of the produced natural rubber composites.Abubakar,2016,also reported an increase in the micro-hardness and a decrease in the tensile strength, impact strength and abrasive resistance properties of the polypropylene composites.

Eggshell is also a waste generated in the processing of agricultural produce. It is mainly composed of calcium carbonate ($CaCO_3$) crystals usually stabilized by a protein matrix. It is estimated that about 80,000 tons of eggshell is generated in Nigeria annually, of which 26% is used in fertilizer production, 20% is used in animal feed production, 5% is used for other uses, leaving us with 49% (39,200 tons) which are thrown away annually (Daengprok, Garnjanagoochorn and Mine,2002,199-204; Matson and Hecht,1999,2487-2508).These eggshells are excess in the environment and thus pose challenges with disposal. Recent innovations in the eggshell industry have devised ways to separate the calcium rich eggshell from the protein rich inner membrane, thus expanding the applications of eggshell. Some applications of eggshell include: its use as abrasive agents, stabilizing agents to improve soil properties, coating pigment for ink-jet printing paper additive, calcium source for both human and animal nutrition. Many studies have reported some properties of eggshell filled polyethylene composites, but there is norecorded or existing literature on the combination of eggshell and de-oiled cashew nutshell in the production of LLDPE composites. The study is therefore aimed at determining the effects of eggshell and de-oiled cashew nut shell on the mechanical properties, water absorption and biodegradation behavior of LLDPE composites.

2.0 Experimental

Materials

The Linear low density polyethylene (LLDPE) of density range 0.915-0.925 g/cm^3 was supplied by Indorama Eleme Petrochemicals Limited, Port Harcourt, Rivers State, Nigeria. De-oiled Cashew nut shell (CNSP) was obtained after the extraction of its liquid with acetone and then carefully processed to obtain powdered cashew nut shell of mesh size 150µm. The cashew nutshell was sourced from Auchi, in Edo State, Nigeria.Eggshells were also sourced from Okpunor pastries, Rivers State, Nigeria and thenprocessed to obtain same mesh size as CNSP which was used for the study.

Method

Preparation of Cashew nut shell and eggshell filled composites

The filler materials were initially oven-dried in its powdered form and the moisture contents were determined. Compounding and production of the composites were done at Ceeplast Industry, Ltd., Aba, Nigeria. The ESP (30 wt.%), CNSP (10, 20, 30 wt%) and LLDPE were mixed in different ratios to produce the final composites as shown in Table 1. They were introduced into the injection moulding machine

(4.6KW, 10 H, Taiwan) through the hopper at 200°C. The mixing was done at a hopper and nozzle temperatures of 200°Cand 220°C respectively and at a rotor speed of 60rpm, while the average thickness of the composites produced was 3.5-4mm.

Table 1: Composition of CNSP and ESP filled polymer composites

Samples	Percentage weight Composition		
	LLDPE	CNSP	ESP
NEAT LLDPE	200	-	-
LLDPE/CNSP-10	190	10	-
LLDPE/CNSP-20	180	20	-
LLDPE/CNSP-30	170	30	-
LLDPE/CNSP-0/ESP-30	170	-	30
LLDPE/CNSP-10/ESP-30	160	10	30
LLDPE/CNSP-20/ESP-30	150	20	30
LLDPE/CNSP-30/ESP-30	140	30	30

LLDPE: Linear low density polyethylene; CNSP: Cashew nut shell powder; ESP: Eggshell powder

Mechanical properties

Tensile properties: The tensile strength and its complementing properties were tested using universal instron tester according to ASTM D638 procedure, which is the method used for testing materials of between 1-14mm thicknesses. The composite samples were preparedat 25^{0}C and a fixed crosshead speed of 1mm/min to obtain tensile strength, tensile modulus and elongation at break. The results presented are the meanvalue of three different runs for each of the samples.

Flexural properties: The flexural strength and its complementing properties were also determined using same universal instron tester in accordance with ASTM D790, at a cross head rate of 0.01 mm/min by using three-point bending geometry to evaluate the flexural strength and modulus. The test was carried out atroom temperature and the mean value obtained for three runs for each of the samples was recorded.

Impact test: The Impact strength of the composites was determined using NotchedIzod impact tester in accordance with ASTM D256 procedure. Different values arising from the three runs were obtained for each of the composites and the average value was computed.

Water absorption test: Each sample formulation was cut into 6 pieces of dimensions (25mm x 2.5mm), cleaned and then their initial thicknesses (L_i) were determined separately using the micrometer screw gauge. Theweight (W_i) of each sample was determined and then the samples were immersed in 150ml of water for 42days. After intervals of 7days, one sample for each formulation was removed, cleaned, and then weighed immediately as (W_f), with the final thickness (L_f) determined and recorded.The percent water absorption was computed using the equation below:

$$\textit{Weight gain } w_g \ (g) = \frac{w_f - w_i}{w_i} \ x \ 100\%$$

Where W_f = final wet weight

W_i = initial dry weight

Biodegradation test: Each sample formulation was cut into 4pieces of dimensions (25mm x 2.5mm), cleaned and then their initial thicknesses (L_i) weredetermined separately using the micrometer screw gauge. The weight (W_i) of each sample wasdetermined and then the samples were buried at a depth of 25cm below ground surface for 100days.After intervals of 25days, one sample for eachformulation was exhumed, thoroughly washed with water to remove sand particles, cleaned, sundried for 12 hrs to remove any absorbed moisture and weighed as (W_f) with the final thickness(L_f) determined and recorded.The percent rate of biodegradation was calculated using the equation below:

$$\text{Weight loss \%} = \frac{W_i - W_f}{W_i} \times 100$$

Where W_i = initial weight of the samples

W_f = final weight of the samples after degradation period

3.0 RESULTS AND DISCUSSION

Tensile strength and modulus

The effect of filler loading on the tensile strength and modulus of the CNSP and CNSP-ESP filled compositesareillustrated in figures(1) and (2). It was observed that the tensile strength and modulus reduced as theamount of CNSP filler in the composite increased. This trend was noticed in both the ESP andnon-ESP filled composites and the results were similar to the studies reported previously by (Nwanonenyi& Chike-Onyegbula,2013,352-358; Ardhyananta, Ismail & Takeichi,2007, 789 and Lumlong,et al,2007,789).This decrease in tensilestrength may be due to the poor adhesion of the filler-matrix and the agglomeration of the fillerparticles. The decreasing modulus with increasing filler, despite exhibiting high stiffness may be due to the incompatibility of the fillers with the LLDPE. This decreases its ability to withstand greater loads thus the composites break apart more easily under tension. Another reason may be due to interfacial voids created when composites are subjected to tension. The voids acted as stress concentrators and thus propagated more rapidly, leading to deformation at a reduced tensile stress. The tensile strength and modulus of non ESP composites were higher than those of the ESPcomposites; this may probably be due to better compatibility and interfacial adhesion of CNSP filler and LLDPE whencompared to CNSP-ESP fillers and LLDPE. Previous studies have shown that the decrease in tensile strength ofcomposites is due to poor interfacial adhesion of the filler-matrix of the polymeric material while that of tensile modulus is due to creation of interfacial voids which act as stress concentrators (Salmah,Ismail& Bakar,2018,12-15).The increased tensile strength and modulus of (17:3) ESP composite when compared to same ratio of CNSP composite may be because ESP had better interfacial adhesion to LLDPE (i.e the force of adhesion) was greater when compared to CNSP. There was also drastic drop in the tensile strength and modulus of the 20g-CNSPcomposite when compared to that of other formulations. This may be attributed to poor mixing or unevendispersion of the filler in the polymermatrix.

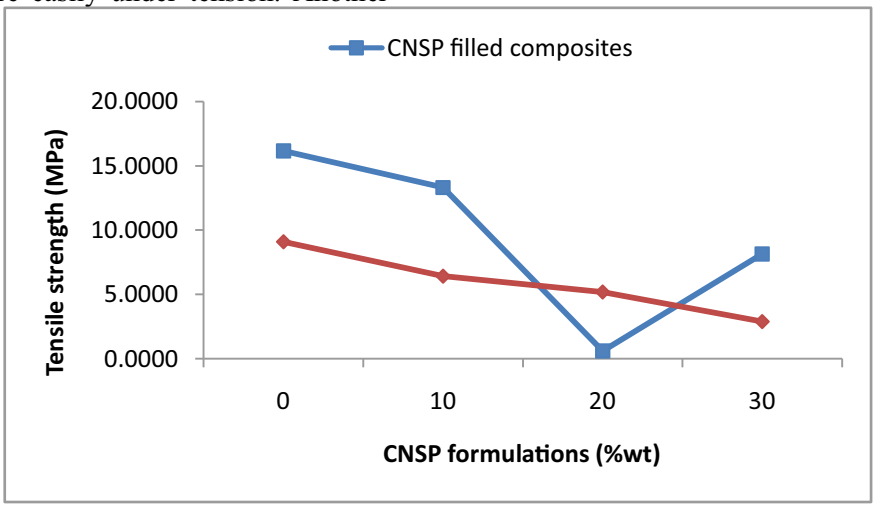

Figure 1: The tensile strength of CNSP and CNSP-ESP filled composites at different filler loadings(P-value for both the CNSP and ESP were less than 0.05)

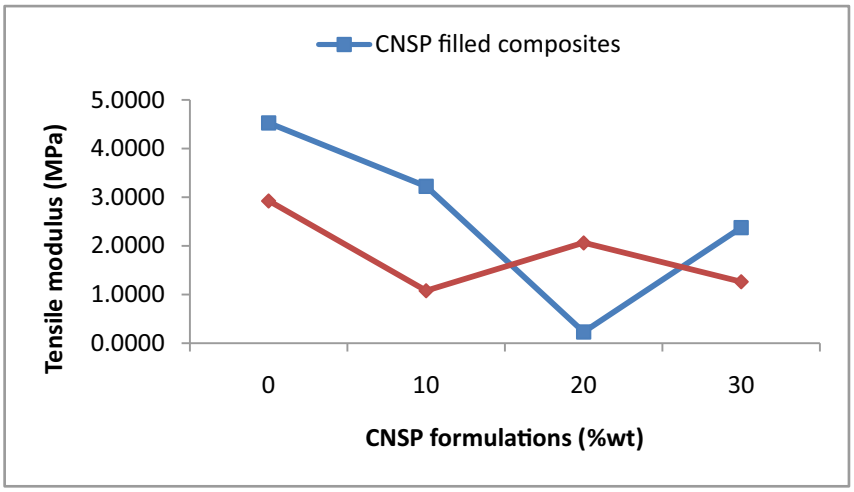

Figure 2: The tensile modulus of CNSP and CNSP-ESP filled composites at different filler loadings (P-value for both the CNSP and ESP were less than 0.05)

Elongation at -break

The effect of filler loadings on the elongation at break of the CNSP and CNSP-ESP filled composites is shown in figure 3; it expresses the capability of a material to resist changes without crack formation. It was observed that the elongation at break decreased as the amount of CNSP filler in the composite increased for both the ESP and non-ESP composites. This behavior is also similar to the trend reported byNwanonenyi&Chike-Onyegbula,2013,352-358 and Lumlong,*etal,* (2007,789). This is probably because increased filler loading in the LLDPE matrix resulted in the stiffening and hardening of the composite which reduced its resilience and toughness and led to lowerelongation at break. Thus, the decreasing elongation at break indicates the incapability of thefiller to support the stress transfer from filler to polymer matrix. The elongation at break of theCNSP composites were higher than those of the CNSP-ESP composites, this is probably due to the fact that CNSP filler had better interfacial adhesion to LLDPE than CNSP-ESP filler to LLDPE. Previous studies have reportedsimilar trend to be attributed to the incapability of the filler to support the stress transfer from polymer filler to the matrix (Lumlong, *et al*,2007,789 and Jacob, Thomas &Varughese, 2004, 955-965).

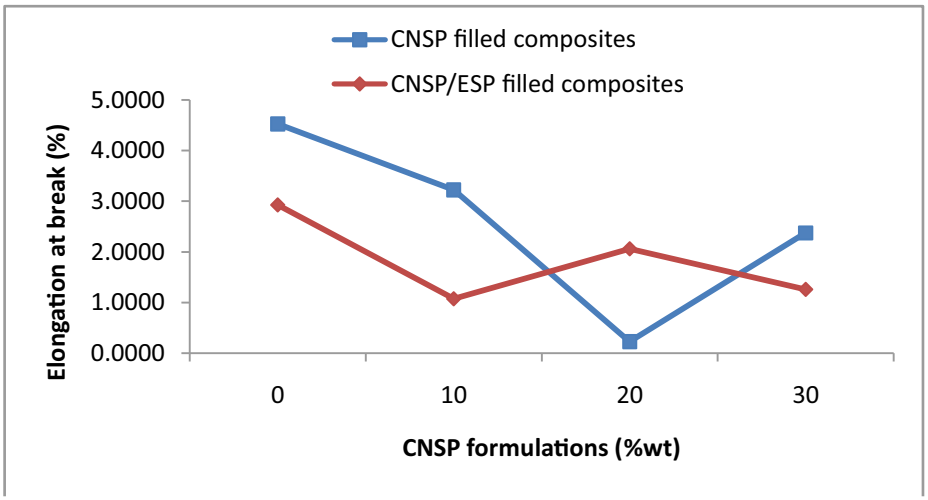

Figure 3: The elongation at break of CNSP and CNSP-ESP filled composites at different filler loadings (P-value for both the CNSP and ESP were less than 0.05)

Flexural strength and modulus

The flexural strength and modulus of the CNSP and CNSP-ESP filled composites at different filler loadings are represented in figures(4) and (5). Flexural strength is the maximum bending stress that can be applied to a material before it yields while flexural modulus is the tendency for the material to resist bending. It was observed that the flexural strength and modulus reduced as the amount of CNSP filler in the composites increased for both the ESP and non-ESP composites. These results were similar to the trend reported by Ardhyananta,Ismail&Takeichi,(2007,789) which is probably due to the fact that as the amount of filler in the composite increases, the composite becomes highly non-homogenous which leads to defects. Therefore, when the composite material is subjected to bending force, these defective sites tend to localize the stress potentially creating localized weakness, the material therefore fractures (snaps) at these sites. This shows that as the filler content in the composite increases, the ability of the composites to resist bending reduces.The flexural strength and modulus of the CNSP composites were higher than those of the CNSP-ESP composites; this is attributed to increased non-homogeneity of CNSP and ESP used together as fillers in compositing. According to Salmah,Ismail& Bakar,2018,12-15, this is due to the non-homogeneity of the polymer/filler matrix can affect the flexural strength and modulus of composites. The results of the (17:3) ESP composite was higher than that of the (17:3) CNSP composite and this may probably be due to better adhesion between the ESP and LLDPE when compared to CNSP and LLDPE. The drastic drop in the flexural modulus and strength of the 20g-CNSP composite whencompared to that of other formulations could be attributed to random orientation or uneven dispersion of the fillerin the polymer matrix.

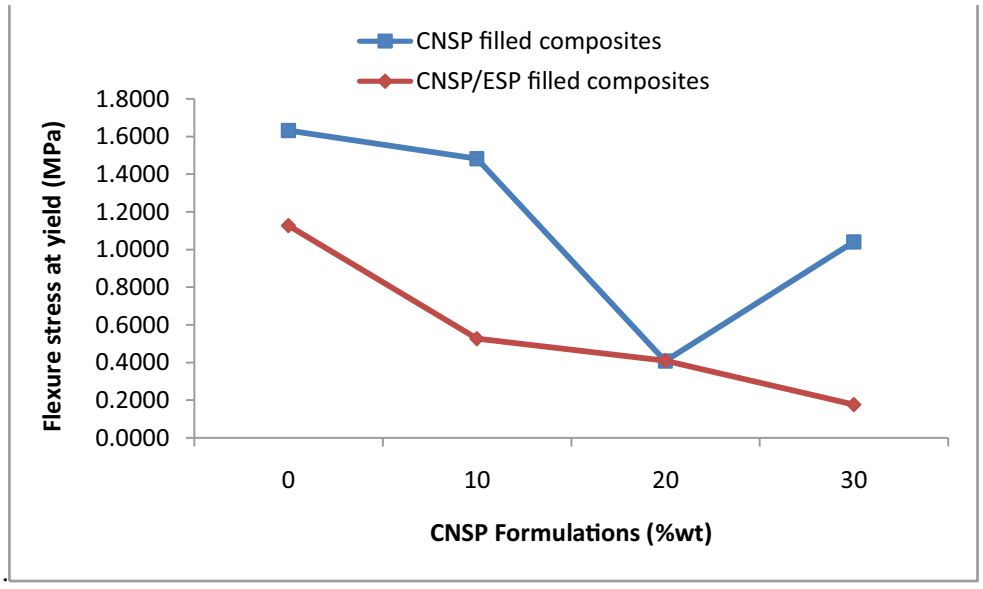

Figure 4: The flexural strength of CNSP and CNSP-ESP composites at different filler loadings (P-value for both the CNSP and ESP were less than 0.05)

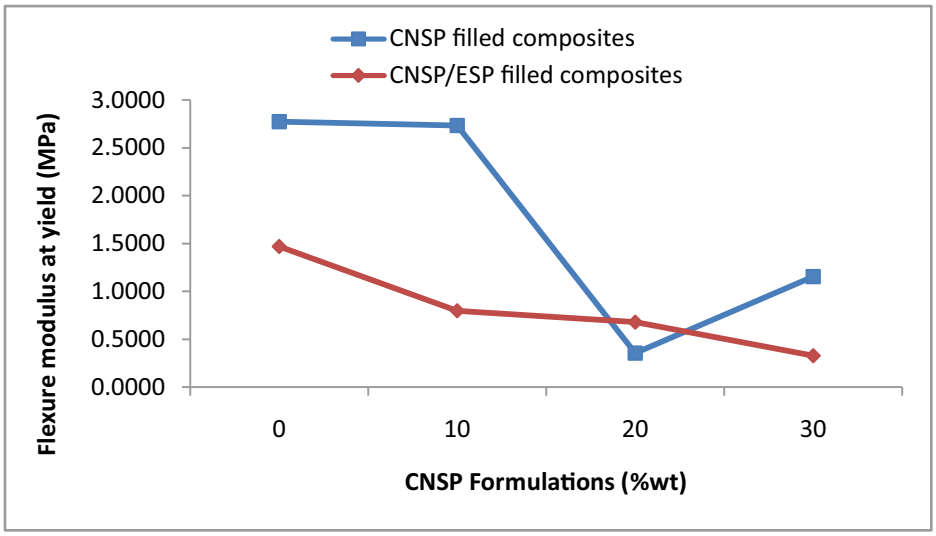

Figure 5: The flexural modulus of CNSP and CNSP-ESP composites at different filler loadings (P-value for both the CNSP and ESP were less than 0.05)

Impact strength

The effect of filler loadings on the impact strength of the CNSP and CNSP-ESP filled compositesis shown in figure 6. It is the amount of energy a material can absorb before it fractures. Results showed that the impact strength reduced as the amount of CNSP filler in the composite increased for both the ESP and non-ESP composites, this trend was similar to the study byLumlong*et al, (*2007, 789*).* This is attributed to the poor interfacial adhesion between the polymer/filler matrix, thus reducing the ability of the composites to withstand shock with increasing filler content. The result of the 30g-ESP composite was higher than same ratio of CNSP composite, and this may be because ESP had better interfacial adhesion to LLDPE when compared to CNSP. Futhermore, the drastic drop in the impact strength of the 20g-CNSP composite when compared to that of other formulations may be attributed to uneven dispersion in the compound mix.

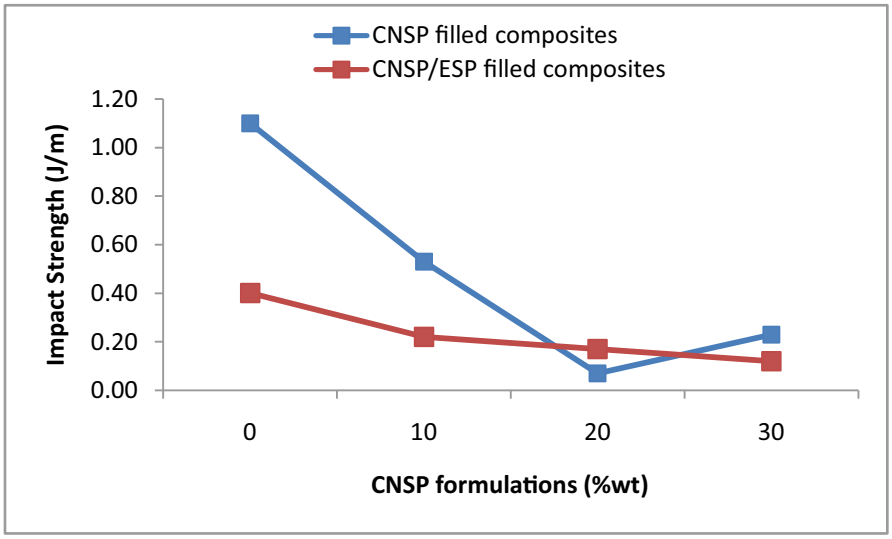

Figure 6: The impact strength of CNSP and CNSP-ESP composites at different filler loadings (P-value for both the CNSP and ESP were less than 0.05)

Water absorption

The effect of filler loadings on the water absorption properties of the CNSP and CNSP-ESP filledcomposites is represented in figure 7. It was observed that the water absorption increased as the amount of CNSP filler in the composite increased for both the ESP and non-ESP composites. According to Farahana,Supri& Teh,2015,1-9, it may be attributed to the fact that biomaterial which are used as fillers are hydrophilic in nature. The water absorption of the CNSP-ESP filled composites was higher than those of the CNSP filled composites.This may be due to the presence of high level of $CaCO_3$ in the eggshell powder which is able to absorb more water, thus increasing the water absorption. Another reason is the incorporation of different fillers stemming from theincreased amount of filler which lead to the agglomeration of the fillers thus increasing the water absorption of the composites.According to Abdullah*et al*., 2011,36-42, as the filler contentincreases, the formation of agglomerations increases due to the difficulties of achieving a homogeneous dispersion of filler at high filler content. The 30g-ESP composite has a higher rate of water absorption when compared to the 30g-CNSP composite; this is most likely because ESP has a greater propensity to absorb more water when compared to CNSP, thus apparently aiding in more water absorption properties of CNSP-ESP filled composites when compared to neat LLDPE and CNSP composites.

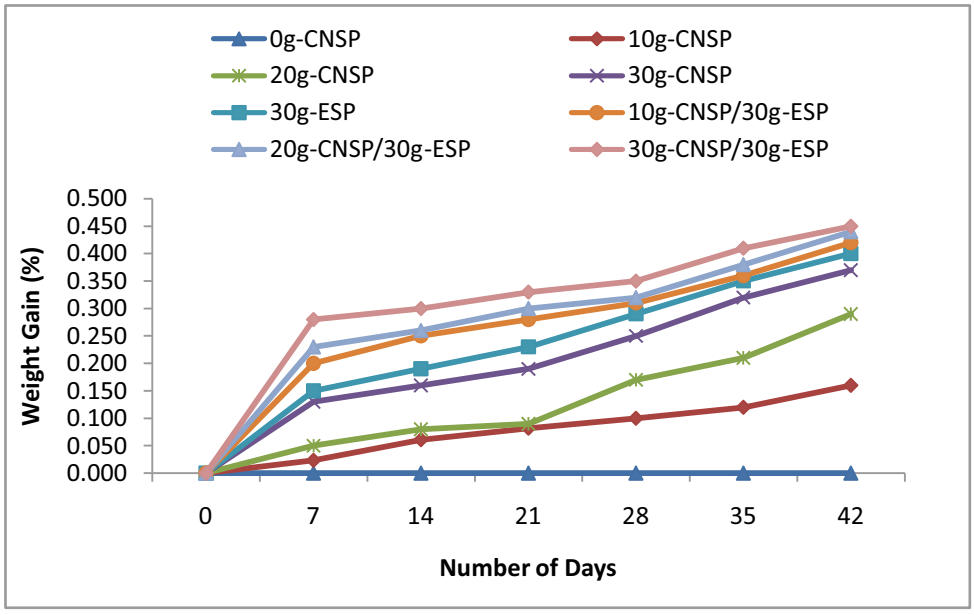

Figure 7: Effect of exposure time on the percent weight gain of water absorption of the composites(P-value for both the CNSP and ESP were less than 0.05)

Biodegradation

The effect of filler loadings on the biodegradation of the CNSP and CNSP-ESP filled composites is represented in figure 8. It was observed that the rate of biodegradation increased as the amount of CNSP filler in the composite increased for both the ESP and non-ESP composites. Similar trend was reported by Farahana,Supri& Teh,2015,1-9, and can be attributed to the fact that ESP sand CNSP are non-plastic materials and thus are readily biodegradable, hence its composites would show increased biodegradability with increased filler loadings. Generally, unlike the neat LLDPE, all the composites underwent a certain degree of biodegradation within the 100days period, with the rate of biodegradation increasing with increasing amount of CNSP filler and duration. The biodegradation was further increased with the incorporation of ESP filler. According to Muller,2015,366-388,certain fillers are more water absorbent and thus experience swelling

(due to water intake)when there are still in the intricate pores of the parent polymer. At the point when these fillers have achieved maximum water retention, they burst, thereby creating greater number of sites for biodegradability to occur. From the water absorption results in figure 6, the ESP filled composites absorbed more water when compared to non-ESP filled composites and neat LLDPE, thus the former composites have great propensity to create more sites for biodegradation which inadvertently aided its high rate of biodegradation. Similarly, 30g-ESP composite has a higher rate of biodegradation when compared to the 30g-CNSP composite. This is most likely because the ESP filler has high tendency to absorb more water than the CNSP filler, thus helps in creating more sites for biodegradation to take place.

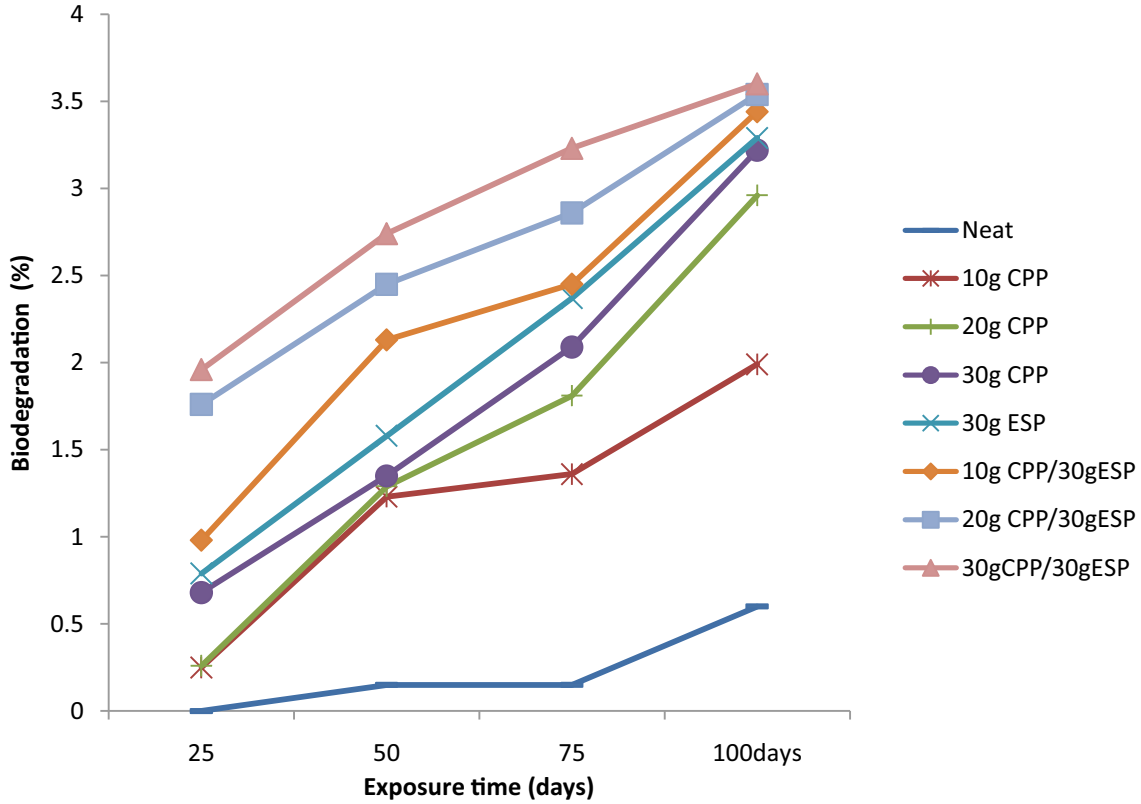

Figure 7: Effect of exposure time on the rate of biodegradation of the composites (P-value for both the CNSP and ESP were less than 0.05)

CONCLUSION

The study has shown that the mechanical properties generally showed a negative trend for both the ESP composites and non-ESP composites. However, the non-ESP composites have better mechanicalproperties when compared to ESP filled composites while the ESP-filled composites have better water absorption and biodegradation properties when compared to neat LLDPE and non-ESP filled composites. Futhermore, the mechanical properties of the (17:3)ESP-filled composite having similar ratio with the CNSP was higher than its CNSP-counterpart. All the composites had a better rate of biodegradation and water absorption when compared to the neat LLDPE, with the propensity of biodegradation and water absorption increasing with increasing filler content and duration. A two-way ANOVA with replication showed that P-value for both the CNSP and ESP were less than 0.05 (margin for error) which indicated the significant increase in their rates of biodegradation and water absorption.ESP and CNSP wastes have now proved to be a valuable contribution to the plastic industry.

DECLARATION OF CONFLICTING INTERESTS

The author(s) have declared no conflict of interests.

FUNDING

The author(s) received no financial support for the research,authorship, and/or publication of this article.

4.0 REFERENCES

Abdulah, A. H.; Ruse, D. S. and Abdulwahab, A. S. (2011). Water Absorption and Mechanical Properties of High-Density Polyethylene/Egg shell Composite,
Journal of Basrah Researches (sciences), 37(3A), 36-42.

Abubakar,S.M.(2016). Studies on the Impact Resistance of Cashew Nutshell Powder and Calcium Carbonate Filled Polypropylene.Dissertation Polymer Science and Technology, Department of Chemistry, Faculty of Science, Ahmadu Bello University, Zaria,Nigeria.

Ardhyananta,H.;Ismail,H. and Takeichi,T.(2007). Effect of Organoclay Loading and Ethylene Glycol on Mechanical, Morphology and Thermal Properties of Ethylene Vinyl Acetate/Organoclay Nano composite.*J.Reinforced plastics and composites,*26,789.

Boran,S(2016). Mechanical, Morphological and Thermal Properties of Nutshell and Microcrystalline Cellulose Filled High-Density Polyethylene Composites. *Biores,* 11(1).1741-1752.

Carraher,C.E.(2014). Carraher's Polymer Chemistry. CRC Press Taylor &Francis Group, Boca Eaton. 231-232.

Daengprok,W; Garnjanagoochorn,W. and Mine,Y.(2002). Fermented Pork Sausage Fortified with Commercial or hen eggshell Calcium Lactate. *Meat Science.* 62(2).199-204.

Elhajjar,R.; LA Sasaponara,V.andMuliana,A.(2017). Smart Composites: Mechanics and Design. CRC Press. 1-430.

Farahana,R.N.;Supri,A.G.andThe,P.L.(2015). Tensile and Water Absorption Properties of Egg Shell Powder Filled Recycled Density Polyethylene/Ethylene Vinyl Acetate Composites: Effect of 3-Aminopropyltriethoxysilane.*J.Adv.Red.Mater. Sci.* 5(1):1-9.

Fazeli,M.; Keley,M.andBiazar,F.(2018). Preparation and Characterization of Starch-based Composite Films Reinforced by Cellulose Nanofibers. *International Journal of Biological Macromolecules,* 116, 272-280.

Ferri,E.(2011). Bioresins from Cashew Nutshell Oil.*Reinforced Plastics.* 55(3).29-31.

Igwe,I.O.andOnuegbu,G.C.(2012). Studies on Properties of eggshell and Fish Bone Powder Filled Polypropylene.*AmericanJ.PoymCarbon* 2(4).56-61.

Ilavbare,O.A.;Emmanuel, G.C.; Ptileri,M.P.andHamza,A.(2018).Hybridisation of Carbon black: Cashew Nutshell Powder as Fillers on the Mechanical Properties of Natural Rubber Materials*Composite Materials.* 2(2), 49-54.

Jacob,M.; Thomas,S.andVarughese,K.T.(2004). Mechanical Properties of Sisal Oil Palm Hybrid Fiber Reinforced Natural Rubber Composites. *Composites Sci. Techn, 64, 955-965.*

Lumlong,S.; Pungpo,P.; Khamsri,B.; Saenglam,I.andKongkaew,C.(2018). Study on the Effect of Calcium Carbonate from Egg Shell as a Filler in Natural Rubber. *Intern.J.Adv.Sci. Eng.Techn,* 6(1,2),12-15.

Matson,L.E.;andHecht,N (1999). Microstructural Stability and Mechanical Properties of directionally Solidified Alumnia/YAG eutectic Monofilaments.
Journal of European Ceramic Society, 19, 2487-2508.

Muller, R.(2005). Biodegradability of Polymers. Regulations and Methods for Testing Biopolymers online. 10, 366-388.

Najafi,S.K.; Hamidinia,E.andTajvidi,M.(2006). Mechanical Properties of Composites from Sawdust and Recycled Plastics.*J.App. Polym. Sci.* 100(5),3641-3645.

Nitin,S.andSingh,V.K.(2012).Mechanical Behaviour of Walnut Reinforced Composite. *J.Mater. Environ Sci. 4(2), 233-238.*

Nwanonenyi,S.C.andChike-Onyebula,C.O.(2013). Water Absorption, Flammability and Mechanical Properties of Linear Low Density Polyethylene/Egg Shell Composite. *Academic Red. Intern.* 4(1),87-98.

Salmah,H.; Ismail, A.andBakar,A.(2003).Dynamic Vulcanization of Paper Sludge Filled Polypropylene(PP) ethylene propylene dieneTerpolymer (EPDM). *Malaysian Journal of Microscopy.*
2,15-22.

Shuhadah,S.andSupri,S.G.(2009).LDPE-Isophthalic Acid-Modified Egg Shell Powder Composites (LDPE/ESPI).20(1), 87-98.

Nigerian Journal of Polymer Science and Technology, 2020, Vol. 15, pp77-87
Received: 22/08/2020 Accepted: 04/10/2020

Effect of Acetylation on the Viscoelastic and Creep Properties of Orange Peel Reinforced Polypropylene Composites

Okpanachi, C.B[1], Agbaji, E.B.[2], Mamza, P.A.P.[2] and Yaro, S.A[3]

[1]*Department of Pure and Industrial Chemistry, Kogi State University, Anyigba*
[2]*Department of Chemistry, Ahmadu Bello University, Zaria*
[2]*Department of Chemistry, Ahmadu Bello University, Zaria*
[3]*Department of Metallurgical and Materials Engineering, Ahmadu Bello University, Zaria*

Corresponding Author: cliffordokpanachi@yahoo.com

Abstract

O*range Peel fibers were treated by acetylationto increase its compatibility with the polymer matrix, and its reinforcement with polypropylene was developed via compression mouldingtechnique which waslater subjected to thermal characterization. Results obtained from the dynamic mechanical analysis showed an increase in the storage and loss modulus of the composites with weight fraction of orange peel fibers, with the chemically treated (acetylated) composites having higher storage and loss moduluscompared to the untreated composites.Lower damping peaks (Tan ∂) values were generally found at higher filler loadings implying an improvement in thermal stability and load bearing capacity of the composites. Results for the creep behaviour of the composites revealeda decrease in the creep strain of the composites with filler loading of the orange peel fibers and an increase in the creep strain as the time was varied. The treated composites had lower creep strain than the untreated composites which confirmed the presence of the acetylation in improving the interfacial bonding between the fibers and the matrix.*

Keywords: *Acetylation, Composites, Creep, Dynamic mechanical analysis, Orange peel, Polypropylene*

1. Introduction

Agricultural wastes residues during harvest seasons in most African countries are enormous and often constitute environmental menace (Adeosun, *et al*., 2015). And as far as environment is concerned, researchers are focused on biodegradable and renewable natural fibers as the most promising material for economic growth (Bambach, 2017; Petrone and Meraune, 2017). Natural fibers have many advantages over synthetic fibers such as high biodegradability, non-abrasive nature, low energy consumption, low densities/cost and high specific mechanical properties(Rojo*et al*., 2015; Cordeiro*et al*., 2017).Hence, researchers have viewed that natural fibers can effectively be used as filler/reinforced material in varieties of thermoplastic and thermoset polymer composites for construction and automotive applications (Saba*et al*., 2015;Asim*et al*., 2018; Supian*et al*., 2018).Several factors are likely to influence the properties of cellulosefiber-reinforced composites, with the effect of the filler–matrix adhesion on the composite performance particularly significant. Variety of fiber modifications have been reviewedin literature for improvement on such adhesion(Kabir*et al*., 2012; Rojo*et al*., 2015), andmodification of the fibers by acetylation have been selected in this work as a result of having proven efficacy for treating cellulose fibers (Loong and Cree, 2018; Kusumaningrum*et al*., 2018; Latif*et al*., 2019).

Dynamic mechanical analysis is an indispensable and effectivetool for determining the viscoelastic propertiesof polymer and composite materials related to primaryrelaxations (Saba *et al*., 2016). It is a

sensitive technique that characterizes the mechanical responses of materials by monitoring property changes with respect to the temperature and/or frequency of oscillation (Palanivel*et al*., 2017). The technique separates the dynamic response of materials into two distinct parts: an elastic part (E') and a viscous or damping component (E"). The elastic process describes the energy stored in the system while the viscous component describes the energy dissipated during the process (Shedbale and Muley, 2017). Creep behaviour is the permanent deformation that occurs when a material is under constant stress and is a function of time, temperature and material properties (Yanjun, 2009). It is a critical factor in the long-term performance and reliability of materials such as polymer composites which are often exposed to various types of stress applications (Daver*et al*., 2016). A proper understanding, measurement and long-term prediction of the creep resistance of natural fiber reinforced polymer composites are required in order to design a component for an adequate long term performance.

Polypropylene (PP) is a thermoplastic polymer widely used as an engineering because it possesses several vital and useful properties such as transparency, dimensional stability, flame resistance, high heat distortion temperature and high impact strength (Khan *et al*., 2010). It is also very suitable for filling, reinforcing and blending. PP with fibrous natural polymers of biomass origin is one of the most promising routes to create natural–synthetic polymer composites (Motaleb*et al*., 2018).Orange remains one of the most economically important fruits in Nigeria and a preferred choice compared to other fruits due to its sweet taste and relatively cheap price. Its peel could be used for composite fabrication and hence potentially reducing the environmental hazard it causes to communities. Since the "eco-green" initiative of environmental agencies worldwide has encouraged the use of wastes for wealth-convertible materials, orange peels are therefore a good option to utilize for composite fabrication (Ajibade*et al*., 2015).

Orange peels have been explored by a number of researchers in the fiber reinforced composites;therefore the aim of this study is to study the effect of acetylation on the viscoelastic and creep properties of the orange peel / polypropylene composite and also to vary its filler loading withthese properties.

2. Materials and Methods

2.1. Material Collection and Preparation

Orange peel fibers were obtained from fruit sellers located within Zaria metropolis in SabonGari local government area of Kaduna state, Nigeria.The samples were thoroughly washed with distilled water to remove foreign materials and water-soluble components. The washed samples were initially air dried for 12 hours and then oven-dried to a constant weight at 65 °C for 36 hours. After drying, the samples were cut, ground then sieved with laboratory sieves to obtain homogenous particle sizes using a mechanical sieve shaker which was used to separate the fibers into the desired particle size of 300 µm.To reduce the influence of the fiber extract on acetylation, the sieved materials were extracted with a mixture of acetone and n-hexane (4:1, v/v) as solvents for 5 hours. The extraction was carried out to remove extractible components from the fibers. After extraction, the samples were dried in a laboratory oven for 16 hours (Nwadiogbu*et al*., 2016).

2.2. Treatment of the fibers by Acetylation

The fibers were placed in a 250 mL conical flask containing 120 mL of acetic anhydride and 6 g (1% of the solvent) N-bromosuccinimide (NBS). The flask was placed in a temperature-controlled water bath set at 70 °C for 90 minutes, under atmospheric pressure after which it was removed from the water bath and the hot reagent decanted. The fibers were thoroughly washedwith ethanol and acetone to remove unreacted acetic anhydride and acetic acid by-product. The products were allowed to dry in an oven set at 60 °C for 16 hours, later cooled in a desiccator and stored in a plastic container prior to analysis (Onwuka *et al*., 2016).

2.3. Preparation of the treated and untreated orange peel composites

The polypropylene composites were prepared by melt mixing and compression moulding on a two roll mill and compression moulding machine respectively. The composite samples were produced by the addition of the polypropylene pellets while the rolls were in counter clockwise motion for a period of 10 minutes at a temperature of 170℃. Upon achieving a paste like matrix; the filler material (raw / treated orange peel powder) was introduced by gently applying manually as the rolls rotated at a rate of 500 rpm (Chike*et al*., 2014). The percentage filler loading was varied at 0, 5, 15, 25 and 30 wt%for the DMA and Creep analysis.The compounded samples were cured on a hydraulic machine 12000 model with electrically heated platens. The temperature of the platens was set at 150℃ and when the temperature was attained, the moulds were preheated to attain the platen temperature. The material was then cut to take the shape of the mould and was placed in between the platens with a pressure of 4 MPa for 10 minutes, and finally the cured samples were removed from the mould after cooling (Jacob *et al*., 2018).

2.4. Dynamic Mechanical Analysis

DMA was carried out using DMA 242E machine according to ASTM (2015). Instrument set up included the sample holder (3-point bending), furnace temperature range of 26 - 120 °C, dynamic load of 4 N, frequency of 10 Hz and heating rate of 6 K/min were configured. Sample dimension of 60 x 12 x 3 mm were produced for each test. The test specimens were loaded into the machine using a three-point bending and locked into the furnace.

2.5. Creep Test

Creep Test was also done on a DMA-242 analyzer. Sample dimension of 75 x 13 x 3 mm were produced for this test.The test specimens were loaded into the machine using a three- point bending and locked into the furnace. The samples were run for the displacement portions of the experiment with the strains being individual to each sample. The test was conducted for 60 minutes at a loading force of 2 N at 80^{o}C.

3. RESULTS AND DISCUSSION

3.1. Storage modulus

Results shown in Figure 3.1 below depicts the variation of the storage modulus (E') with temperature for the control (PP), untreated and treated composites. Storage modulus (E') represents the elastic portion of materials and is defined as the maximum amount of energy stored by a material during one cycle of oscillation (Gupta, 2017; Rana*et al*., 2017). It also gives an estimate of temperature-dependent stiffness behaviour and load-bearing capacity of the polymer composites (Kehrer*et al*., 2018).It was observed that the E' of the composites increased with higher filler loading of reinforcement, this is as a result of enhanced stiffness which could be attributed to the fact that when the fillers were incorporated as a rigid reinforcement, it was embedded in the holes of the PP making them more closely connected and thus improving the deformation resistance of the composites (Zhang *et al*., 2017; Jacob *et al*., 2018).Highest values of storage modulus were obtained at 30% wt meaning the composite at that filler loading had better interfacial bonding compared to other composites while lower storage modulus at 5% wt and 15% wt may be attributed to the low stiffness which tends to reduce the viscoelasticity of the polypropylene matrix (Gupta, 2018). A decrease in the storage modulus was observed at elevated temperatures for all the composites, this could be attributed to the increase in the molecular mobility of the polymer chains leading to its loss in stiffness (Palanivel*et al.,* 2017).

The storage modulus ofthe treated fiber composites was higher than the untreated fiber composites. In case of the untreated fiber composites, the hydrophilic nature of orangepeel fibers showed poor wettability causing the formation of voids at the fiber/ polypropylene interfacewhich produced composites of lower stiffness and strength. Acetylation treatment improved the compatibility of the fillers with polypropylene matrix leading to better wettability which produced strong filler/matrix interface bonding (Al-Mahama and Al-Huniti, 2019). The improved interaction and adhesion between the fillers and matrix led to better stress

transfer giving rise to a much stiffer composite with higher storage modulus.

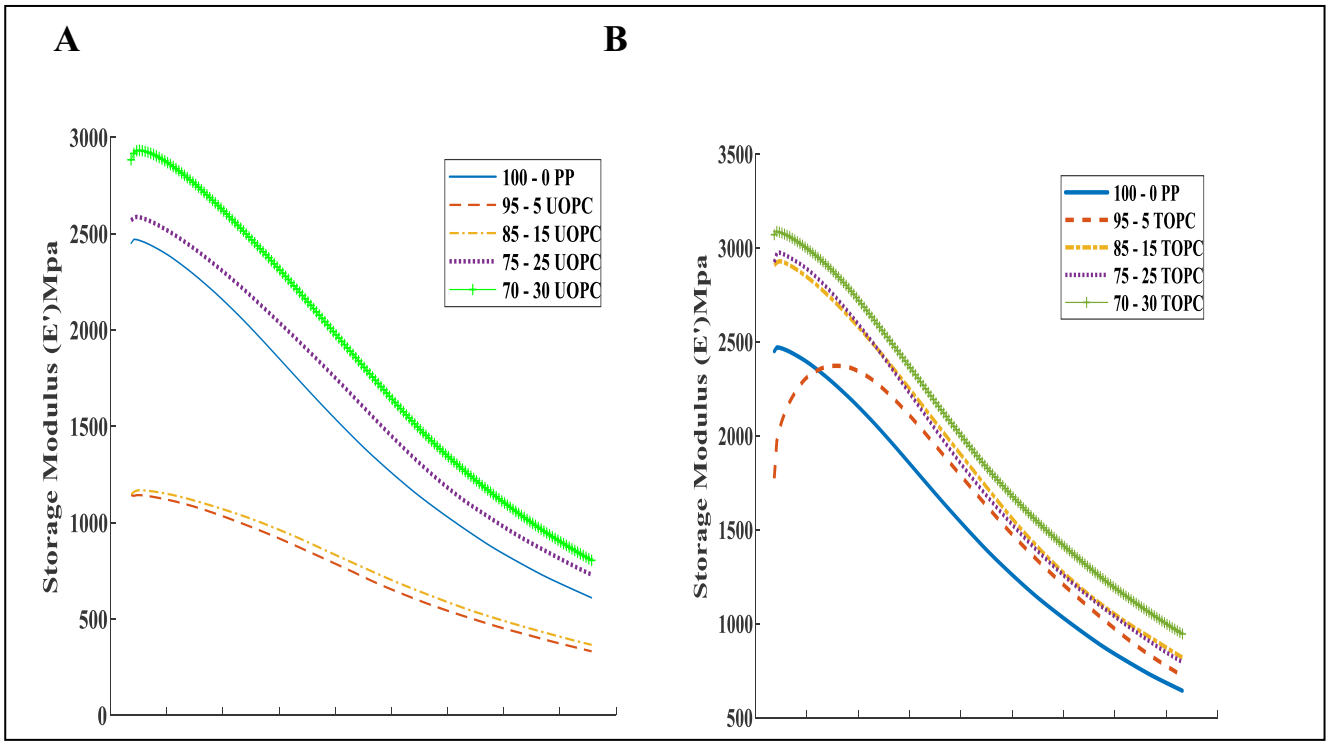

Figure 3.1: Variation of the Storage Modulus with Temperature for (A) Untreated and (B) Treated Orange Peel Polypropylene Composites

3.2. Loss Modulus

The result of the loss modulus of the pure polypropylene, treated and untreated orange peel polypropylene composites and their variations at 5%, 15%, 25% and 30 % filler loading is shown in Figure 3.2. Loss modulus (E") is defined as the maximum energy dissipated by composite materials during deformation. It characterizes mechanical losses and determines the amount of energy that was converted to heat during one deformation period. It represents the viscous response of the materials which depends upon motion of polymeric molecules in the composites (Jawaid*et al*., 2013).

Results showed that the loss modulus generally increased with filler loading resulting in a higher efficiency in dissipation of external energy which showedan increase in the thermal stability with filler loading. The higher thermal stability could be associated with the decrease in mobility of matrix due to the incorporation of fillers and probably due to the change in physical state of the matrix by the addition of the fillers surrounding the matrix (Asim*et al*., 2017).The effect of increasing filler loading creates a high internal friction at the filler/matrix interface that enhances the dissipation of energy.This trend depicts an increase in the thermal stability of the composite materials of higher filler loading compared to the pure polypropylene.There was a general drop in the loss modulus for all samples as the temperature was increased; this reflects an increase in the molecular motion of the polypropylene molecules leading to its disentanglement of the polymer chain. The drop was alsoas a result of the weakening effect of filler/matrix interface as the temperature increased which reduces the tight packaging of filler/matrix interface as well

as frictional resistance at the interface (Yang *et al*., 2016).

Results also showed the variation of loss modulus (E'') curve of the treated and untreated orange peel polypropylene composites at different filler loadings. The effect of chemical modification on loss modulus showed that the treated fibers composites had higher loss modulus (E'') compared to the untreated fiber composites. This was as a result of decreased mobility of the matrix chains which indicated enhanced interfacial adhesion between the fibers achieved by the effect of the acetylation.

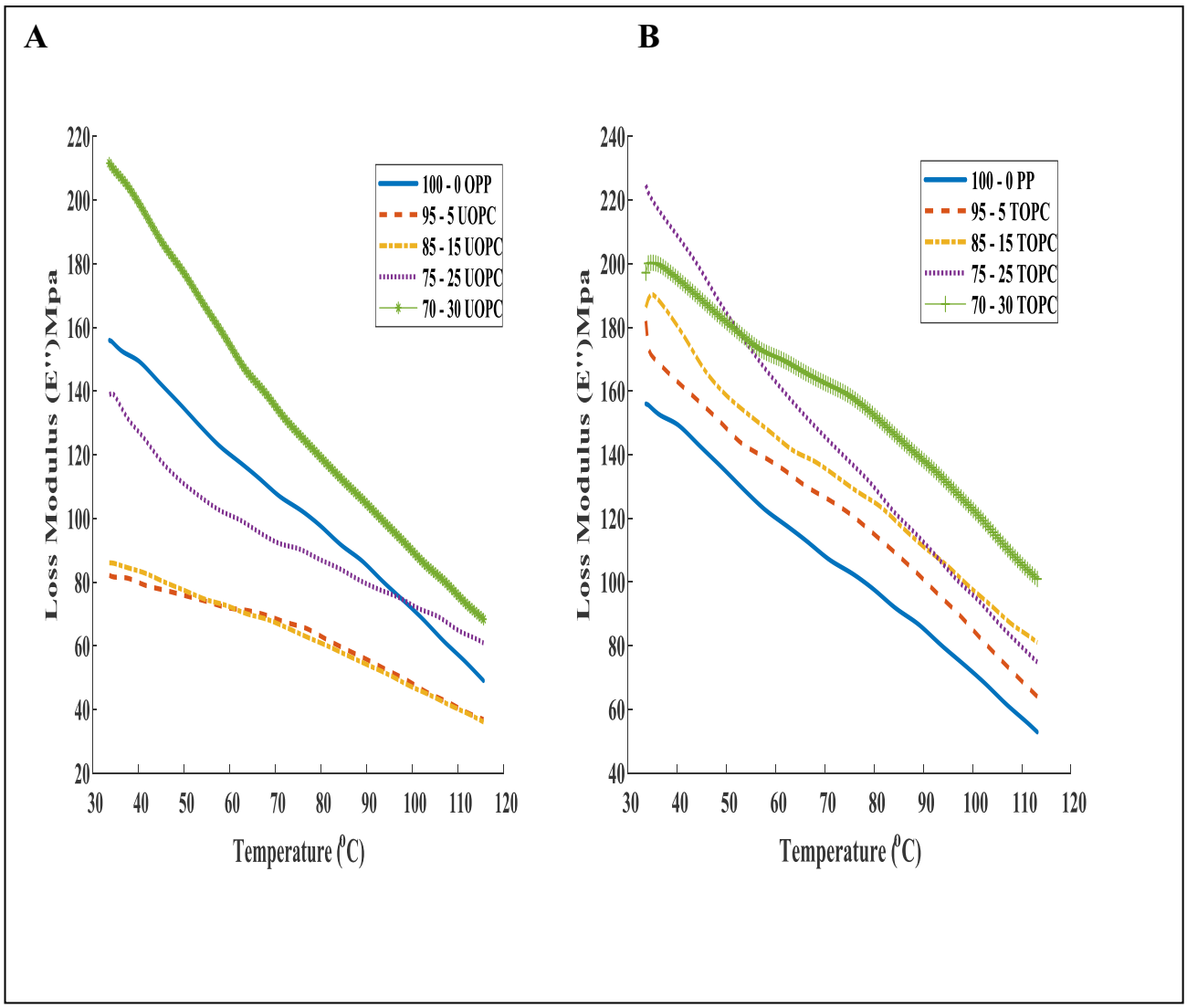

Figure 3.2: Variation of the Loss Modulus with Temperature for (A) Untreated and (B) Treated Orange Peel Polypropylene Composite

3.3. Damping

Damping or loss factor is a ratio of the loss to storage modulus, otherwise known as tan δ. The damping properties of the material give the balance between the elastic and viscous phases in a polymeric structure (Jacob *et al*., 2018).A high value of damping is indicative of a material with high non-elastic strain behavior while low value of damping indicates that the material is more elastic.

Figure 3.3showed the effect of filler loading on the damping factor as a function of temperature for treated and untreated orange peel polypropylene composites. Results showed

that the dampingvalue for both treated and untreated composites generally reduced with the increment of filler contents, this could be owed to the reduced energy-loss rate and limited degree of molecular displacement during heating, The increased stiffness of thecomposites could limit the degree of freedom of the polymer chain at an atomic level and increase the filler/matrix interfacial bonding resulting in the reduction in the damping factor since mobility of the molecular chains at the fiber/matrix interface decreases (Pawar*et al*., 2015).Among the composites, the damping factor of 25%wt for the untreated OPC was the lowest, while for the treated OPC it was lowest at 30% wt. This could be due to better compatibility and reinforcing effect of the orange peel fibers in the polymer matrix. Lower value of damping shows the good load bearing capacity of the composites

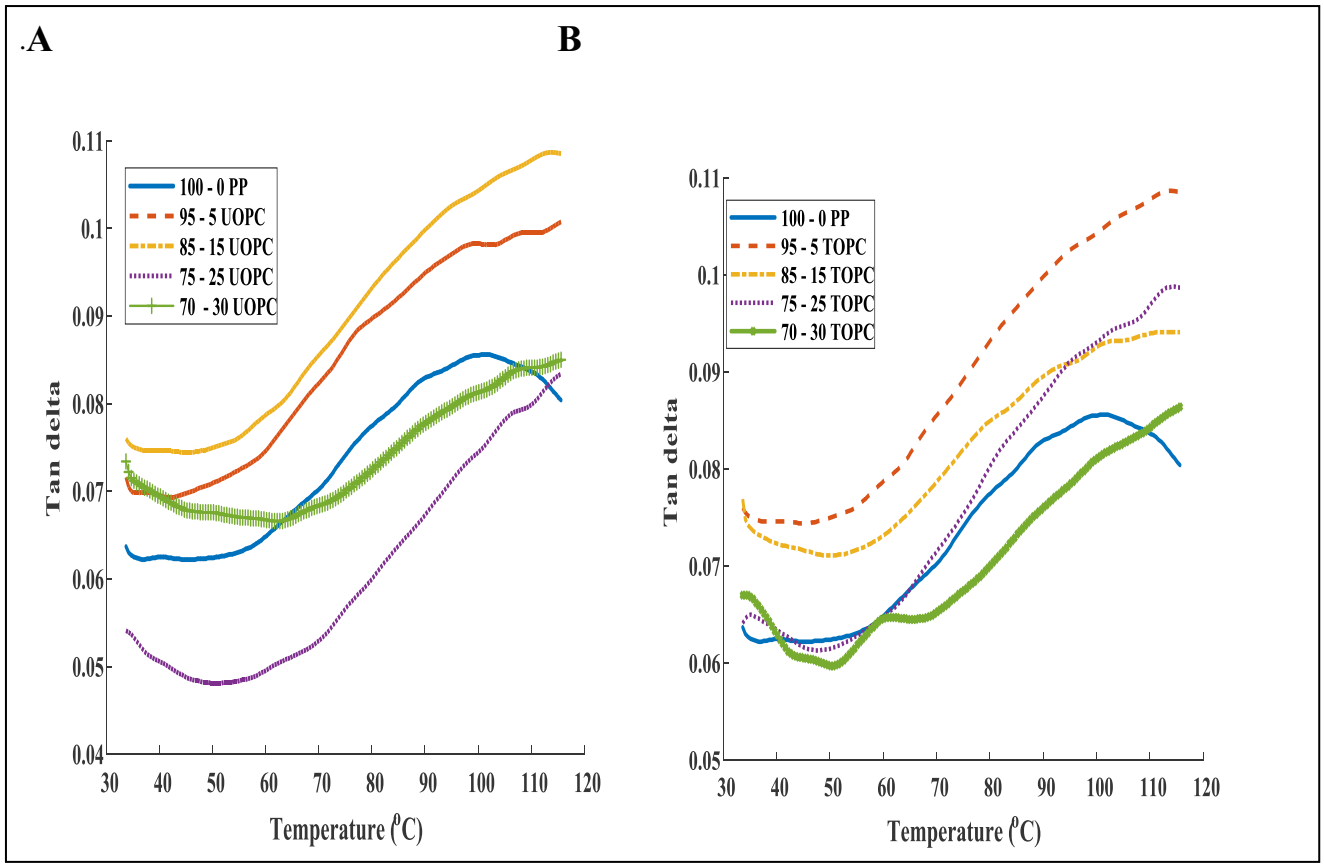

Figure 3.3: Variation of the Damping factor with Temperature for (A) Untreated and (B) Treated Orange Peel Polypropylene Composites

3.4 Creep Studies

The creep behaviour of the orange peel polypropylene composites was investigated in Figure 4. Results showed a decrease in the creep strain with an increase in filler loading. This could be as a result of higher stiffness of the composites which contributes in hindering the polymeric chain mobility by forging strong interfacial interactions with the polymer matrix (Kumar *et al*., 2017). Composites on 5% filler loading showed the highest creep strain, this could be due to the fact that the composite possessed much interfacial cracks and these cracks affect the creep behaviour which coalesce and propagate through the matrix on application of load, causing it to show higher creep strain compared to others (Dan and Dirk, 2018).

Composites on 15% filler loading showed a lower creep strain compared to 5 wt% filler loading, this was probably due to better dispersion of the fillers which is directly related to the creep and recovery nresponses of polymers. Effective dispersion of the fillers can result in better interaction with the polymer matrix and cause restrained movement of polymer chain segments on application of load (García*et al*., 2010). Higher filler loadings of 25% and 30% for both treated and untreated composites showed the lowest creep strain values. This may be attributed to effective dispersion of fillers, greater inhibition of slippage and better reorientation of polymer chain with increasing filler contents (Jabbar*et al*., 2016).

With respect to time, there was an increase in the creep deformation as the time was varied, this is because with time more dislocations develop producing increasing interference with each other's movement thus causing creep rate to increase. Also over time, the creep compliance at a particular temperature increases due to prolonged thermal energy which allows for rotational and translational motions of the polymer chains causing increased deformation and higher creep strain (Wang *et al*., 2014). The creep strain deformation for the treated composites were lower than the untreated ones, this can be ascribed to an improved filler-matrix bonding which gives better constraints on the deformation of fillers caused by slippage effects (Shanmugam and Thiruchitrambalam, 2013). The effect of acetylation tends to separate elementary fibers from their fiber bundles thus increasing the effective surface area for bonding with a matrix material and improving the filler dispersion within the matrix.

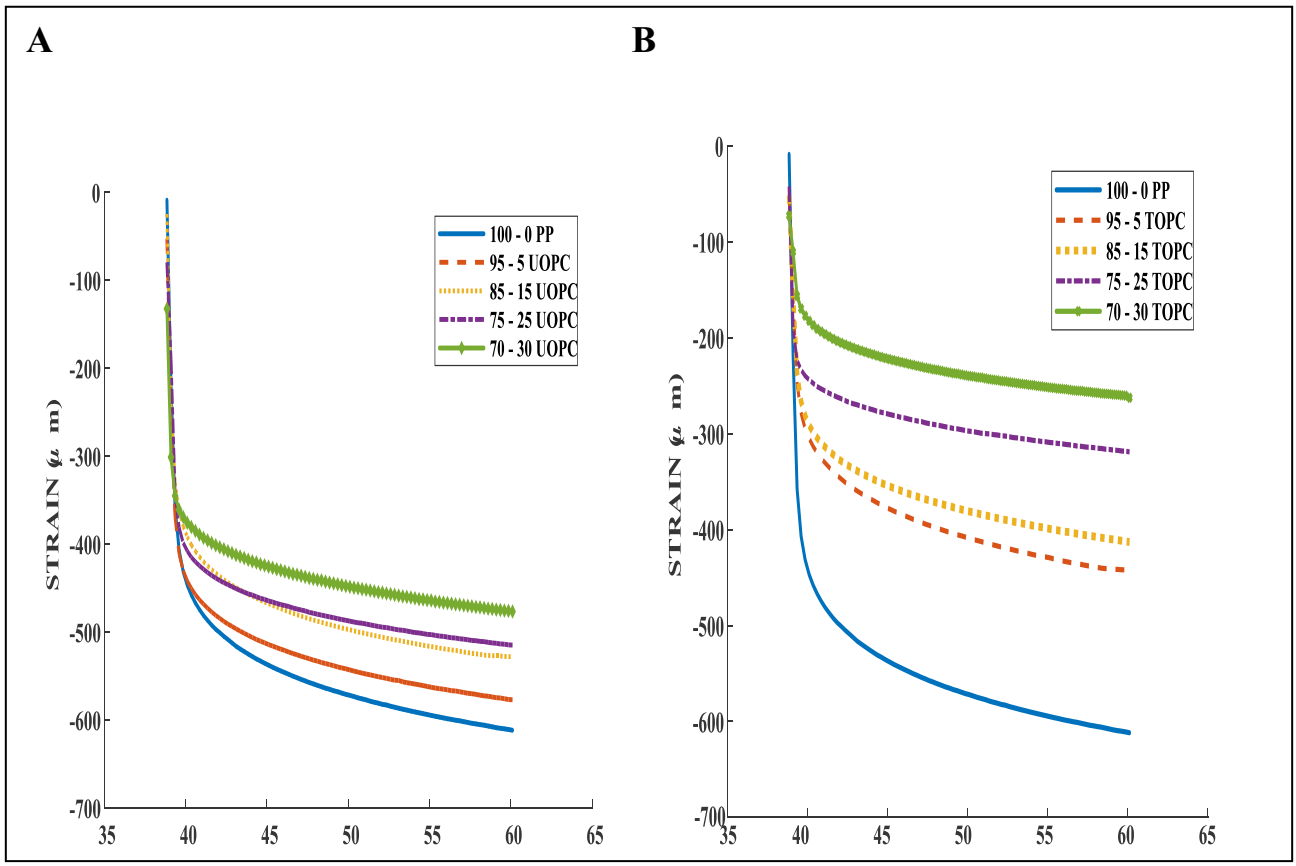

Figure 3.4: Variation of Creep Strain with Time for (A) Untreated and (B) Treated Orange Peel Composites

Conclusion

The utilization of orange peel fiber in composite application is economic and ecofriendly. It was found that its incorporation into the polypropylene matriximproved the dynamic mechanicalproperties of composite,with better thermal propertiesobserved with the increase in fiber loading and chemical treatment by acetylation. Highest values of the storage and loss modulus were obtained at 30wt% for both treated and untreated fiber composite. Results also showed that the composites had better creep properties compared to the pure polypropylene and that the creep strainof the composites decreased with filler loading of the orange peel fibers. The highest creep strain was obtained at 5wt% while the lowest creep strain was at 30 wt%. A comparison of creep behaviour of the composites showed that the treated fiber composites had lower creep strain than the untreated fiber composites which confirmed the presence of the acetylation in improving the interfacial bonding.Results have thus showed that orange peelscould be used in fabrication of ecofriendly composite products for diversified applications andcould also be used as a substitute to synthetic fibers.

References

Adeosun, S. O., Akpan, E. I. andAkanegbu, H. A.(2015).Thermo-Mechanical Properties of Unsaturated Polyester Reinforced with Coconut and Snail Shells, *International Journal of Composite Materials,* 5(3), 52 – 64.

Ajibade, O. A., Agunsoye, J. O. and Oke, S. A. (2015). Experimentation and Prediction of Moisture Characteristics and Density of Sweet Orange Peels Used for Epoxy-based Composite Fabrication, *The Journal of the Association of Professional Engineers of Trinidad and Tobago*, 43 (2),44 - 52.

Al-Maharma, A. Y. and Al-Huniti, N. (2019). Critical Review of the Parameters Affecting the Effectiveness of Moisture Absorption Treatments Used for Natural Composites, *Journal of composites science*, 3(27), 1 – 38.

Asim, M., Jawaid, M., Nasir, M. and Saba, N. (2017). Effect of Fiber Loadings and Treatment on Dynamic Mechanical, Thermal and Flammability Properties of Pineapple Leaf Fiber and Kenaf Phenolic Composites.*Journal of renewable composites*, 6 (4), 383 - 393.

Asim, M., Saba, N., Jawaid, M. and Nasir, M. (2018). Potential of natural fiber/biomass filler-reinforced polymer composites in aerospace applications. *Sustainable Composites for Aerospace Applications,* 12, 253 – 268.

ASTM D7028 (2015). Standard Test Method for Glass Transition Temperature (DMA Tg) of Polymer matrix composites by dynamic mechanical analysis (DMA). American Society for Testing and Materials International West Conshohocken, PA West Conshohocken. PA.

Bambach. M. (2017). Compression strength of natural fibre composite plates and sections of flax, jute and hemp.*Thin Walled Structures*, 119, 103 – 113.

Chike, V. C., Anthony, I. O., Danjuma, S. Y., Aigbodion, V. S., Obada, D. O. and Samotu, I.A.(2014). Effects of Reinforcement Loading on Physical and Mechanical Properties of Developed Recycled Low Density Polyethylene / Maize Cob Ash Particulate (PLDP / MCAp) composite. *Advances in Applied Science Research*, 5 (2), 286 – 291.

Cordeiro, E.P., Pita, V.J. and Soares, B. G. (2017). Epoxy–fiber of peach palm trees composites: the effect of composition and fiber modification on mechanical and dynamic mechanical properties.

Journal of Polymers and the Environment, 25(3), 913 – 924.

Dan, L. and Dirk, J. P. (2018). Crack Propagation Mechanisms for Creep Fatigue: A Consolidated Explanation of Fundamental Behaviours from Initiation to Failure, *Metals,* 8 (623), 1 – 32.

Daver, F., Kajtaz, M., Brandt, M. and Shanks, R. (2016). Creep and Recovery Behaviour of Polyolefin-Rubber Nanocomposites Developed for Additive Manufacturing. *Polymers,* 8 (12), 437 - 449.

García, M. G., Marchese, J. and Ochoa, N. A. (2010). Effect of the particle size and particle agglomeration on composite membrane performance. *Journal of Applied Polymer Science,* 118, 2417 – 2424.

Gupta, M. K. (2017). Effect of frequencies on dynamic mechanical properties of hybrid jute/sisal fibre reinforced epoxy composites. *Journal of Materials and Environmental Sciences*, 9 (1), 100 – 106.

Gupta, M. K. (2018). Effects of variation in frequencies on dynamic mechanical properties of jute fibre reinforced epoxy composites. *Journal of Materials and Environmental Sciences*, 9(1), 100 – 106.

Jacob, J., Mamza, P. A. P., Ahmed, A. S., and Yaro, S. A. (2018). Mechanical and Viscoelastic Properties of Plantain Peel Powder Reinforced Recycled High Density Polyethylene Composites, *Nigerian Journal of Polymer Science and Technology*, 13, 55 - 66.

Jabbar, A., Militký, J., Madhukar Kale, B., Rwawiire, S., Nawab, Y. and Baheti, V. (2016). Modeling and analysis of the creep behavior of jute/green epoxy composites incorporated with chemically treated pulverized nano/micro jute fibers. *Industrial Crops and Products,* 84, 230 – 240.

Jawaid, M., Khalil, H. P. S. A., Hassan, A., Dungani, R. and Hadiyani, A. (2013). Effect of Jute fibre loading on tensile and dynamic mechanical properties of oil palm epoxy composites, *Composites Part B*, 45, 619 – 624.

Kabir, M. M., Wang, H., Lau, K.T. and Cardona, F. (2012). Chemical treatments on plant-basednaturalfibre reinforced polymer composites: an overview. *Composite Part B: Engineering Journal*, 43(7), 2883 – 2892.

Kehrer, L., Wicht, D., Wood, J.T., Bohlke, T. (2018). Dynamic mechanical analysis of pure and fiber-reinforced thermoset- and thermoplastic-based polymers and free volume-based viscoelastic modeling, *Experimental Solid Mechanics,* 41: 1, 1 – 16.

Khan R. A., Khan M. A., Sultana S., Nuruzzaman Khan M., Shubhra Q. T. H. and Noor F. G. (2010). Mechanical, degradation, and interfacial properties of synthetic degradable fiber reinforced polypropylene composites. *Journal of Reinforced Plastics and Composites*, 29 (3), 466 – 476.

Kumar, G. S., Prusty, R. K., Rathore, D. K. and Ray, B. C. (2017). Creep behaviour of graphite oxide nanoplates embedded glass fiber/epoxy composites: Emphasizing the role of temperature and stress. *Composites Part A: Applied Science and Manufacturing,* 102, 166 – 177.

Kusumaningrum, W., Syamani, F., Desiana, D., Suryanegara, L., and Subyakto1, S. (2018). Characterization of acetylated cellulose from oil palm frond fiber (ElaeisguineensisJacq.) for composites application. *Journal of*

Lignocellulose Technology, 2(1), 18 - 23.

Latif, R., Wakeel, S., Khan, N. Z., Siddiquee,A. N., Verma, S. L. and Khan, Z. A. (2019). Surface treatments of plant fibers and their effects on mechanical properties of fiber-reinforced composites: A review.*Journal of Reinforced Plastics andComposites*, 38 (1), 1 - 16.

Loong, M. L. and Cree, D. (2018). Enhancement of Mechanical Properties of Bio-Resin Epoxy/Flax Fiber Composites using Acetic Anhydride. *Journals of Polymers and the Environment.* 26 (1), 224 – 234.

Motaleb, K., Shariful Islam, M. andHoque, M. B. (2018). Improvement of Physicomechanical Properties of Pineapple Leaf Fiber Reinforced Composite. *International journal of biomaterials*, Article ID 7384360, doi: 10.1155/2018/7384360.

Nwadiogbu, J. O., Ajiwe, V. I. E. and Okoye, P. A. C. (2016). Removal of Crude Oil from Aqueous Medium by Sorption on Hydrophobic Corncobs: Equilibrium and kinetic studies. *Journal of Taibah University for Science,* 10 (1), 56 – 63.

Onwuka, J. C., Agbaji E. B., Ajibola, V. O. and Okibe, F. G. (2016). Kinetic Studies of Surface Modification of LignocellulosicDelonixregia Pods as Sorbent for Crude Oil Spill in Water. *Journal of Applied Research and Technology*, 14, 415 – 424.

Palanivel A., Veerabathiran, A., Duruvasalu R., Iyyanar, S. and Velumayil, R. (2017). Dynamic mechanical analysis and crystalline analysis of hemp fibre reinforced cellulose filled epoxy composite. *Polimeros*, 27(4), 309 - 319.

Pawar, M. J., Patnaik, A. and Nagar, R. (2015). Investigation on mechanical and thermo-mechanical properties of granite powder filled treated jute fiber reinforced epoxy composite. *Polymer Composites,* 38(4), 736 – 748.

Petrone, G. and Meruane, V. (2017). Mechanical properties updating of a non-uniform natural fibre composite panel by means of a parallel genetic algorithm, Composte A: *Applied Science and Manufacturing*, 94, 226 – 233.

Rana, S. S., Gupta, M. K. and Srivastava, R. K. (2017). Effect of variation in frequencies on dynamic mechanical properties of short sisal fibre reinforced polyester composite. *Materials Today: Proceedings*, 4 (Part A): 3387 – 3396.

Rojo, E., Alonso, M. V., Oliet, M., Saz-Orozco, B. D. and Rodriguez, F. (2015). Effect of fiber loading on the properties of treated cellulose fiber-reinforced phenolic composites, *Composite Part B: Engineering Journal*, 68, 185 - 192.

Saba, N., Paridah, M. and Jawaid, M. (2015). Mechanical properties of kenaf fiber reinforced polymer composite: a review. Construction and Building Materials, 76, 87 – 96

Saba, N., Jawaid, M., Alothman, O. Y. andParidah, M. T. (2016). A review on dynamic mechanical properties of natural fibre reinforced polymer composites, *Construction and Building Materials*, 106, 149 – 159.

Shanmugam, D. and Thiruchitrambalam, M. (2013). Static and dynamic mechanical properties of alkali treated unidirectional continuous Palmyra Palm Leaf Stalk Fiber/jute fiber reinforced hybrid polyester composites. *Materials & Design,* 50, 533 – 542.

Shedbale, N. and Muley, P. V. (2017). Review on Viscoelastic Materials used in

Viscoelastic Dampers. *International Research Journal of Engineering and Technology*, 4 (7), 3375 – 3381.

Supian, A. B. M., Sapuan, S. M., Zuhri, M. Y. M., Zainudin, E. S. andYa, H. H. (2018). Hybrid reinforced thermoset polymer composite in energy absorption tube application: A review. *Defence Technology*, 14(4), 291– 305.

Wang, W.-H., Huang, H.-B., Du, H.-H., and Wang, H. (2014). Effects of fiber size on short-term creep behavior of wood fiber/HDPE composites. *Polymer Engineering & Science,* 55(3), 693 – 700.

Yang, W., Luo, R. and Hou, Z. (2016). Effect of Interface Modified by Graphene on the Mechanical and Frictional Properties of Carbon/Graphene/Carbon Composites. *Materials (Basel, Switzerland)*, *9*(6), 492.

Yanjun, X. (2009). Creep Behaviour of natural fiber reinforced composites, Doctoral Dissertations, Louisian State University.

Zhang, Q., Cai, H., Ren, X., Kong, L., Liu, J. and Jian, X. (2017). The Dynamic Mechanical Analysis of highly filled rice husk biochar/ high density polyethylene composites. *polymers,* (11), 628. DOI: 10.3390/polym9110628.

Nigerian Journal of Polymer Science and Technology, 2020, Vol. 15, pp88-98
Received: 02/10/2020 Accepted: 13/12/2020

Graft Copolymerization of Methylmethacrylate Onto Cellulosic Cotton Fabric: Effects of Preteatments and Monomer Concentration

Yusuf Bako Taura[1*], Shehu Habibu[2], Sani Muhammad Gumel[3], Muhammad Kabiru Yakubu[4] and Abba Musa Ya'u[1]

[1]*Department of Fashion and Clothing Technology, Hussaini Adamu Federal Polytechnic, Kazaure Jigawa State - Nigeria*

[2]*Department of Chemistry, Faculty of Science, Federal University, Dutse, P. M. B. 7156, Jigawa State - Nigeria*

[3]*Department of Pure and Industrial Chemistry, Bayero University, Kano P. M. B. 3011, Kano State - Nigeria*

[4]*Department of Textile Science and Technology, Ahmadu Bello University Zaria, Kaduna State – Nigeria*

*Corresponding Author: yusufbakotaura@yahoo.com

ABSTRACT

Graft polymerization of methylmethacrylate (MMA) on to enzyme desized, scoured, bleached, and mercerized cellulosic cotton fabric was studied in 0.1M nitric acid using ceric ammonium nitrate (CAN) as an initiator. The investigation was carried out to study the possibility of grafting methylmethacrylate on to cellulosic cotton fabric at various stages of processing. Two sets of five different samples were used, four of them passed through the pretreatment stages of desizing (D), desizing and scouring (DS), desizing, scouring and bleaching (DSB), desizing, scouring, bleaching and mercerizing (DSBM) and one was kept as grey (G). The first set of the samples including the grey were grafted with 3.5 ml of MMA and 0.05 M of CAN at 50 °C for 3 hrs. In the second set of samples the graft polymerization was carried out under varying concentrations of monomer, while keeping all other factors constant. The second set has all passed through the final stages of pretreatment (DSBM). The results of FTIR (Infrared spectroscopy), water absorption, dimensional stability, crease recovery properties, tearing strength indicated that there was improvement in the physical and chemical properties of the cellulosic cotton fabric as a result of the graft polymerization. Tearing strength and water absorption of the grafted sample showed considerable decrease. The dimensional stability and crease recovery characteristics of the cotton fabric were generally improved.

Key words: ***cellulose, graft copolymerization, methylmethacrylate, pretreatments***.

1. INTRODUCTION

Modification of polymers has received much attention recently. Graft co-polymerization is an attractive method through which a variety of functional groups can be introduced into the cellulosic polymer. This results in the modification of its physical and chemical properties (Haruna, 1998). Grafting allows the introduction of vinyl

monomers on to the cellulose backbone thus incorporating the properties of the added polymers while retaining the basic traits of the cellulosic material. It also allows the development of a material with a tailor made properties for a variety of applications (Amar *et al.,* 2012). Cellulose is a renewable biodegradable product which can be modified through chemical reactions in a variety of ways to obtain novel characteristics (Kulicke *et al.,* 1996). This is made possible through the creation of grafts (branches) of polymers on the cellulose backbone that imparts the desired properties without destroying its basic characteristics (Hebeish, 1981).

Modification of cellulose through graft co-polymerization has been conducted over the years using different methods. Typical of these methods include ionic and ring opening polymerizations, living radical and free radical polymerizations (Habibu, Sarih, & Mainal, 2018). Among these methods free radical polymerization received the greatest attention (Sebenik, 1998). In this technique free radicals are created through reaction with initiator on the cellulose backbone. The free radical thus formed can add to the monomer to create a covalent bond between the monomer and the cellulose. This reaction is then followed by propagation leading to the formation of macromolecules and subsequently termination. The process is usually carried out by a combination of two growing radical chains (Athawale, 1999; Berlin, 1992). Graft polymerization of cellulose using vinyl monomers is one of the most extensively studied using a wide range of initiators such as $KMnO_4$-HNO_3 redox system, $KMnO_4$/Citric acid redox system, and CAN initiation (Deo, 1999; Vijay, 2009; Khullar et al., 2008). Ceric ammonium nitrate (CAN) initiation technique was favored because of its simplicity, availability, and better yield. Modification of cellulose through graft co-polymerization has a bright future and their development is practically boundless. The use of ceric ammonium nitrate to initiate graft copolymerization of vinyl monomers on to various cellulosic materials such as cotton, jute, flax, rayon, wood pulp and paper has gained considerable attention. Ceric ion is a powerful oxidizing agent and possess high efficiency on both grafting and oxidation of cellulose (Neetu *et al.*, 2011). In the presence of nitric acid, ceric ammonium nitrate (CAN) is an efficient initiator for graft polymerization of vinyl monomers on to cellulose. A number of scholars have worked on the prospects of graft co-polymerization on natural cellulosic fibers applying advance techniques of characterization to evaluate their properties, (Kumar *et al.*, 2005). A wide variety of monomers either hydrophobic or hydrophilic has been grafted on to cellulose (Zahran *et al.,* 2003), but generally acrylic monomers are the most widely used. Few of the recent areas of applications of cellulose graft copolymers are wood plastic composites, dispersion stabilizers, and film development etc. (Gürdağ & Sarmad, 2013; Jiang, Pan, Zhang, & Fang, 2019; Kumar, Sharma, & Singh, 2018). At this point, you need to state briefly, what the paper is reporting.

2. EXPERIMENTAL

All the chemicals used in this investigation were of laboratory grade. The cellulosic cotton fabric was procured from Kwari market in Kano Nigeria and was analyzed at the African Textile Manufacturers Limited; Challawa Industrial Estate, Kano, to have the following specifications: Fabric width 51.1inches; picks/inch 68 and ends/inch 72: warp count 24.6 and weft count 28.1: weight/meter 168.79 g.

2.1 Pretreatment of the cotton fabric

The cotton fabric was thoroughly treated prior to the graft polymerization reaction.

2.1.1 Desizing

A 10gm of the sample was treated at 45 °C with 5 g/l of enzyme, 3 g/l common salt, and 2 g/l wetting agent. The process involved soaking the fabric in the prepared solution for 3 mins. It was then removed folded and

wrapped in a polythene bag for 24 hrs. The fabric was removed, washed thoroughly with hot, warm, then cold water respectively and finally dried.

2.1.2 Scouring

The scouring was carried out on a 10 g sample of fabric using a programmable electrical thermostatic water bath with NaOH 4 g/l/, Na_2CO_3 2 g/l and liquor to material ratio of 1:30. The temperature was raised to 90 °C and kept for 2hrs. The fabric was removed, washed thoroughly with hot, warm, then cold water respectively and finally dried (Kathirvelan *et al.,* 2000).

2.1.3 Bleaching

The scoured fabric was treated for 60 minutes in a solution containing 5g/l hydrogen peroxide, caustic soda 1g/l, sodium silicate 3g/l, and wetting agent 2g/l at 90 °C using a liquor ratio of 1:30 (Nkeonye, 2009). The fabric was properly washed with hot, warm, then cold water respectively and finally dried.

2.1.4 Mercerization

In this process 10g sample was passed through a 27 % solution of caustic soda at room temperature for a period of 60 seconds. The fabric was washed thoroughly with hot, warm, then cold water respectively and finally dried after neutralization with acetic acid (Remzi, 2010).

2.2 Graft copolymerization

The graft co-polymerization was conducted using the procedure adopted by Kazaure M.A., (1996) and Danbatta M.H. (1998). The ceric ammonium nitrate (CAN) solution was prepared by dissolving the required amount in 0.1 M nitric acid. The material was introduced into the 250 ml conical flask and kept in a thermostat water bath at a temperature of 50 °C for 15mins; the material to ceric solution ratio was 1:50. Samples of both grey and treated samples were placed inside the solution and after a period of 15mins the required amount of the monomer was added. The flask was covered with a stopper and the contents stirred at intervals during the polymerization period of 3hrs. The samples were then removed, washed thoroughly in acetone, and the occluded homopolymer was removed using Soxhlet extraction in methanol for 24hrs . The co-polymer was then dried at 40 °C under vacuum to constant weight. This procedure was repeated on the mercerized cotton fabric with varying concentrations of monomer.

2.3 Analyses of the grafted cotton fabric

2.3.1 Fourier Transform Infra-Red Spectroscopy (FTIR)

The FTIR spectra of the grafted and ungrafted cellulose cotton fabrics were recorded on 8400-S Fourier Transform Infrared Spectrophotometer using KBr pellet technique in the range 4500 – 400 cm^{-1} with a resolution of 2 cm^{-1}.

2.3.2 Determination of dimensional stability

The length of the samples was taken in both warp and weft direction before the test. The samples one after the other was immersed in boiling water each for 3 mins, they were then removed without squeezing and dried. The measurement was again taken in both warp and weft direction.

2.3.3 Determination of crease recovery angle

The test samples of 40 mm x 15 mm dimensions with ten samples cut in warp direction and ten in weft were conditioned for 24 hrs at 20 °C ± 2 °C and RH (Relative Humidity) of 65 % ± 2 %. Half the number of the test specimens in the warp direction were folded face to face and the other half back to back, same applied for those in the weft direction. The crease recovery angle was measured across the length (warp direction) face to face and back to back and the angle was also measured along the width

(weft) of the fabric face to face and back to back according to (ISO/R 2313) standard.

2.3.4 Determination of tear strength

Five samples of 10.5 cm x 7.5 cm in both warp and weft directions were prepared. The machine has upper and lower jaws. A cut was made in the sample to form two tongues and lines were marked indicating the point where the tear should reach, one tongue was fixed to the upper jaw and the other to the lower. The machine was then put on to tear the fabric up to the reference point. The reading was taken for each of the five samples in both warp and weft directions. The average tearing strength was then recorded.

3. RESULTS AND DISCUSSION

3.1 Analyses of the pre-treated cotton fabric

The size mixtures present on the cellulosic cotton fabric has been removed as a result of the desizing process carried out. This was further confirmed through testing with iodine solution. When a drop of iodine solution was placed on the desized cotton fabric a yellow color was observed indicating that the size had been degraded and removed. The impurities both natural and added present on cotton fabric prior to scouring had been removed. This is evident from the increased absorbency observed on the fabric. The natural coloring matter had been degraded and decolorized during the bleaching operation and removed in the subsequent washing treatment. Increased water absorbency, strength, and luster has been observed indicating proof of mercerization.

After the copolymerization reaction (Scheme 1), the graft percent yield was calculated using the relationship:

$$\%\ GY = \frac{final\ cellulose\ wt. - initial\ cellulose\ wt.}{initial\ cellulose\ wt.}\ x\ 100$$

And the result is presented in Table 1 and 2 below:

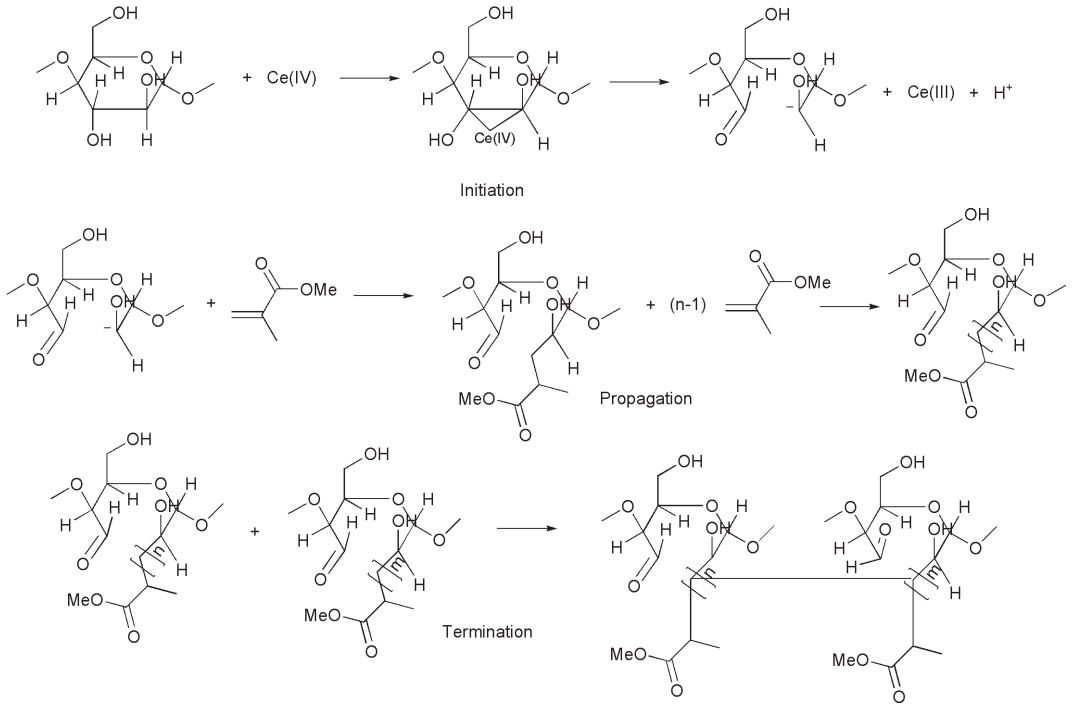

Scheme 1: *Mechanism of graft copolymerization of MMA onto cellulose*

Table 1: *effect of pretreatments on the percentage yield of cotton cellulose grafted-co-MMA.*

Sample	MMA(ml)	*Graft % Yield*
G	„“	8.26
D	„“	9.46
DS	„“	11.17
DSB	„“	13.33
DSBM	„“	14.34

Table 2*: Effect of Monomer Concentration on the yield cotton cellulose grafted-co-MMA.*

Sample	MMA(ml)	*Graft % Yield*
DSBM	0.0	0.00
DSBM	1.0	9.06
DSBM	2.5	12.11
DSBM	3.5	14.34
DSBM	4.0	15.52
DSBM	5.0	13.93

From Table 2, the grafting reaction was studied under varying concentrations of monomer keeping all other factors constant. The mercerized (DSBM) sample was used as such the natural and added impurities which might affect the grafting process have been removed. The graft percent yield increased up to a monomer concentration of 4.0 ml. In addition to the pretreatment this may be attributed to the generation of more monomer radicals to react on to the reactive sites on the cellulose backbone. After reaching the optimum value, the percent graft yields decreased and this may not be unconnected with the predominance of homopolymer over graft polymerization, (Kumar *et al.*, 2005). The highest graft percent yield was obtained on the DSBM samples. This happened as a result of the mercerization and removal of all the impurities present on the cotton fabric prior to the grafting reaction. The graft percent yield increased with increasing accessibility due to greater availability of physically absorbed monomer on the more accessible sites on the substrate, (Hebeish, 1981). It is therefore evident that the graft percent yield obtained on grafting (MMA) on to mercerized cotton fabric is higher.

3.2 Water absorbency

The water absorbency test result is presented in Table 3 below. It was observed that there is a considerable decrease in water absorption of the methyl methacrylate grafted cotton fabric.

Table 3: *Effect of Pretreatments on Water Absorbency of Cotton cellulose grafted-co-MMA.*

Sample		Water Absorbency (s)
	Control	3.5 ml MMA
G	20 x 60	22 .11 x 60
D	10 x 60	23.09 x 60
DS	5 x 60	22.67 x 60
DSB	12	24.31 x 60
DSBM	06	29.81 x 60

It can be observed from the above table that the more the number of pretreatments on the fabric, the higher the water absorption; The best result of 6 seconds; was obtained with the DSBM samples, which is attributed to the mercerization and efficient removal of impurities present on the fabric prior to grafting. Before grafting, a wetting time of 6 seconds was recorded, but after grafting with methylmethacrylate, a wetting time of 29.81 minutes was observed with the mercerized (DSBM) sample. This clearly indicates that the absorption of water by methylmethacrylate grafted samples had greatly decreased.

Table 4: *Effect of Monomer concentration on Water Absorbency of Mercerized Cotton cellulose grafted-co- MMA.*

Monomer Concentration		Water Absorbency (secs)
DSBM	1.0	22 .60 x 60
DSBM	2.5	22.60 x 60
DSBM	3.5	29.81 x 60
DSBM	4.0	32.07 x 60
DSBM	5.0	26.60 x 60

Further decrease of water absorption was also recorded with DSBM of the varying concentrations of monomer grafted samples as can be seen from Table 4, above. The graft copolymerization carried out on the fabric has made it more hydrophobic resulting in decrease water absorption (Negishi *et al.*, 1965).

3.3 Results of the analyses carried out on the Unmodified and grafted cotton fabrics

3.3.1 FTIR Spectroscopy

The result for the FTIR spectra of the raw cellulose as well as the grafted cellulose is presented in Figure 1 and Table 6.

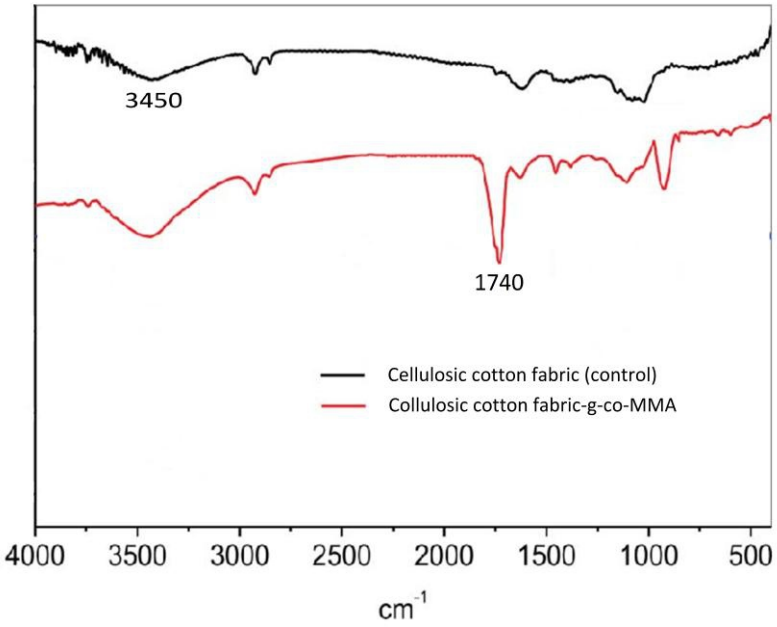

Figure 1: FTIR spectrum of cellulosic cotton fabric and cellulosic cotton fabric

Table 65: *FTIR Absorption Frequencies (cm^{-1}) of Cellulosic Cotton Fabric (Control) and Cellulosic Cotton Fabric – g -co-MMA*

Control Sample		Grafted Sample	
Assignment	**Functional Group**	**Assignment**	**Functional Group**
3500-3200	O-H (H-bonded)	3500-3200	OH(H-bonded)
-	C-H(Stretch)	2899	CH(Stretch)
-		1703	C=O(Esther)
-		1709	C=O(Esther)
-		1708	C=O(Esther)
-		1708	C=O(Esther)

Control Sample		Grafted Sample	
Assignment	Functional Group	Assignment	Functional Group
-		1430	C-CH_3(Bending)
1315	CH_2(rocking)	1130	CH_2(Bending)

From the results it can be seen that both control and grafted cellulosic cotton fabrics have a common –OH stretching vibration in the region 3500-3200 cm^{-1} corresponding to hydrogen bonded substances and 2890-2899 cm^{-1} of C-H stretch. This is regardless of the stage of pretreatment at which the cotton fabric was grafted. This clearly suggests that not all the OH groups of the cellulosic cotton fabric have been replaced by methylmethacrylate groups. However, in the case of methylmethacrylate grafted cotton fabric an additional peak appears at 1703.2, 1709.95 cm^{-1}, 1708.02 and 1708.99 cm^{-1} which is peculiar to the Carbonyl group (>C=O) of ester stretching. This suggests that MMA has been grafted on to the cellulosic cotton fabric through covalent linkages. Other peaks at 1430.26 (O-CH_3 bending of MMA), 1329.96 (C-CH_3) and 1132.25 - (CH_2) bending of MMA support this assumption (Kazaure et al., 1999).

3.3.2 Dimensional Stability

After drying, the samples were measured again and the length in both warp and weft directions remained unchanged. The test was conducted for both the control and the grafted samples and the results are presented in the Table 7 below:

Table 7: *Effect of pretreatment on the dimensional stability of Cotton cellulose grafted-co-MMA.*

Sample	Dimensional Stability			
	Control		3.5 ml MMA	
	Warp	Weft	Warp	Weft
G	4.30	9.80	0.00	0.00
D	6.10	11.40	0.00	0.00
DS	7.20	17.80	0.00	0.00
DSB	10.00	21.60	0.00	0.00
DSBM	11.80	27.10	0.00	0.00

Table 8: *Effect of Monomer concentration on Dimensional Stability of Mercerized Cotton cellulose grafted-co-MMA.*

Concentration	Shrinkage (%)	
	Warp	Weft
1.00	0.92	1.76
1.00	0.16	1.02
1.00	0.00	0.00
1.00	0.00	0.00
1.00	0.00	0.00

It can be observed from tables 7 and 8 that the methyl methacrylate-grafted cotton fabric has a satisfactory dimensional stability.

3.3.3 Tearing Strength

This is the force required to tear the fabric. It is the average force required to continue a tear previously initiated in a fabric by twice the length of tear. Graft co-polymerization of methyl methacrylate produced a marked increase in some desirable properties such as dimensional stability, crease recovery, and thermal stability of the grafted cellulosic cotton fabric, (Hebeish and Guthrie, 1981). However certain undesirable effects such as reduction in tearing strength are also observed. The grafted fabric samples were arranged according to the sequence of processing; desized (D), desized and scoured (DS), desized, scoured and bleached (DSB), desized, scoured, bleached and mercerized (DSBM), the result is presented in the Table 9.

Table 9: *Effect of pretreatment on the Tear Strength of Cotton cellulose grafted-co-MMA.*

Sample	Tear Strength (kg)			
	Control		3.5 ml MMA	
	Warp	Weft	Warp	Weft
G	16.21	134.4	111.8	87.2
D	154.2	126.1	125.2	80.8
DS	155.9	125.7	97.6	71.2
DSB	149.2	125.7	97.6	71.2
DSBM	157.7	125.7	118.7	93.6

It could be observed from Table 9 that the tearing strength remained fairly stable prior to grafting, but after grafting a considerable reduction in the tearing strength was recorded. The tearing strength of the control samples seemed to be good and this might be connected with the mercerizing and efficient removal of size mixtures from the fabric following enzyme desizing. It can also be observed that the grafted samples show a considerable reduction in tearing strength when compared to control samples. This was due to the increase in stiffness of the fabric as a result of grafting with MMA (Masazo, 1964).

Table 10: *Effect of Monomer concentration on the Tear Strength of Mercerized Cotton cellulose grafted-co-MMA.*

Concentration (ml)	Tear Strength (kg)	
	Warp	Weft
0.00	157.7	125.8
1.50	118.7	93.6
2.50	126.4	74.4
3.50	116.4	87.6
4.00	101.2	64.6
5.00	91.2	57.6

From Table 10, it could be observed that the tearing strength of the grafted samples continued to decrease progressively reaching its lowest level. The tearing strength of the grafted samples decreased progressively as the monomer concentration was increased. The overall reduction in the strength of all the treated samples was believed to be as a result of the stiffening of the cloth following methylmethacrylate grafting. A similar decrease of the tearing strength of the grafted cellulosic fabric was reported by Hebeish and Guthrie, (1981).

3.3.4 Crease recovery angle

Crease recovery denotes that property of fabric to go back to its original shape or position after creasing. It is a measure of crease resistance specified in quantitative terms of crease recovery angle. If the angle is 0° then recovery is zero and if the angle is 180° recovery is full. The results are given in the following tables:

Table 11: *Wrinkle Recovery Angle (WRA), deg. of the Control Samples*

Sample	Warp		Weft		Total WRA	
	Face to Face	Back to Back	Face to Face	Back to Back	Warp	Weft
G	6.40	5.20	7.20	6.80	11.6	14.0
D	19.0	17.6	17.6	18.0	36.4	35.6
DS	18.7	21.1	20.3	19.6	39.8	39.9
DSB	19.4	19.0	19.8	19.2	38.4	38.6
DSBM	19.1	20.0	22.4	21.5	39.1	42.4

Table 6: *Wrinkle Recovery Angle (WRA), deg. of the Constant Concentration of Monomer Grafted Samples (3.5ml)*

	Warp		Weft		Total	
Sample	**Face to Face**	**Back to Back**	**Face to Face**	**Back to Back**	**Warp**	**Weft**
G	22.8	22.6	23.2	22.6	45.4	45.8
D	24.2	22.2	22.4	24.2	46.4	46.6
DS	24.6	23.2	23.0	23.0	47.8	46.0
DSB	24.1	24.0	23.8	23.3	41.1	47.1
DSBM	26.0	25.6	23.8	23.8	51.6	47.6

Table 13*: Wrinkle Recovery Angle (WRA), deg. of the Varying Concentrations of Monomer Grafted samples*

	Warp		Weft		Total	
Monomer Concentration	**Face to Face**	**Back to Back**	**Face to Face**	**Back to Back**	**Warp**	**Weft**
1.0	21.2	19.0	21.6	17.4	43.8	39.0
2.5	25.0	24.8	24.9	19.8	49.8	44.7
3.5	20.8	28.8	23.2	20.6	49.6	43.8
4.0	25.0	25.6	26.2	23.8	50.6	50.0
5.0	20.8	19.0	23.2	17.4	43.8	39.0

It can be seen from the control (Table 11) that the crease recovery angle was low compared to that of the grafted samples. It was observed that the crease recovery angles increased with the increase in the number of pretreatments reaching its optimum value on the mercerized (DSBM) cotton fabric as can be seen on Table 12. The second set of samples in their final stages of pretreatment were grafted using varying concentrations of monomer (1 ml, 2.5 ml, 3.5 ml, 4.0mls and 5.0 ml) keeping all other factors constant (Table 13). The crease recovery angle (WRA) was fairly good for all the samples reaching maximum at monomer concentration of 4.0 ml. The pretreatments given to the fabric have effectively removed all the natural and added impurities from the fabric which might otherwise interfere with the grafting process.

4. CONCLUSIONS

Modification of the cellulosic cotton fabric through graft copolymerization allows the elimination of several drawbacks associated with cotton fabrics, and brings about improvement in comfort, ease of maintenance, dimensional stability, crease recovery, and water repellency. The present study was carried out with these aims in mind and the results of experimental analyses proved that the objectives had been achieved. In addition, we were able to prove that graft co-polymerization of methylmethacrylate using ceric ammonium nitrate as initiator can be conducted on cellulosic cotton fabric at various stages of pretreatments. At one stage varying amount of concentrations of the methylmethacrylate was grafted on to the fabric. Infrared spectroscopy (FTIR) was conducted to further establish the proof of grafting. Methylmethacylate (MMA) was grafted on to cellulosic cotton fabric at various stages of pretreatments. The optimum grafting conditions were obtained by studying the effect of pretreatments and varying concentrations of MMA. The effect of these factors was investigated by calculating the graft percent yield. The highest percent yield

of 14.34% was achieved at MMA concentration of 4.0mls on the fabric at its final stage of pretreatment. The result of the study of wrinkle recovery properties, water absorption, dimensional stability, and tearing strength of the grafted samples confirms the grafting of MMA on to the cellulosic cotton fabric. The characterization of the grafted cotton fabric was also confirmed using FTIR Spectroscopy.

ACKNOWLEDGMENT

The Authors wish to acknowledge the support of Hussaini Adamu Federal Polytechnic, Kazaure and Tertiary Education Trust Fund (TETFUND) for sponsoring this research.

REFERENCES

Amar S.S., Raj K. R. and Ashish G. (2012): Functional Polymers from Graft Copolymerization of Binary Monomers Mixture on to Cellulosic Biomas; Synthesis, Characterization and Properties Evaluation."Graft Copolymerization of Monomer". *Lignocellulse* 1(2): 129-132

Athawale Y. D. and Rath S. C. (1999): Graft Polymerization of Starch as a Model Substrate. *J. Macromol Sci. Rev. Chem. Phy*. 39, 445 – 480

Berlin A. A. And Kislenso X.N. (1992). Kinetics and Mechanism of Radical Graft Polymerization on to Polysaccharides. *Prog. Polym, Sci.* 17, 765-825.

Deo H. T. and Gatmare V. D. (1999). Acrylonitrile Monomer Grafting on Cotton to Impart High Water Absorbency. *J. Appl. Polym. Sci*. 72, 887 – 894.

Habibu, S., Sarih, N. M., & Mainal, A. (2018). Synthesis and characterisation of highly branched polyisoprene: exploiting the "Strathclyde route" in anionic polymerisation. Rsc Advances, 8(21), 11684-11692.

Hebeish A. and Guthrie J. T. (1981). The Chemistry and Technology of Cellulosic Copolymers, 32-308. *Springer – Verlag*. Berlin Heidelbers N.Y.

Kathirvelan D., Synthirel S. and Reddy B.S. (2011) Graft Copolym. of 2 – (Dimethylamino) ethylacrylate on to Cellulose (Alkali Scoured cotton) Material. *Int. Journal of Fibre and Textile Research,* 1 (2), 31-38

Haruna M. D.(1998), Preparation and Characterization of Eucalyptus and Cotton Cellulose Graft Copolymers and Cabarnilates. Thesis submitted to the Depart. of Chem. B.U.K., Kano, for award of M.Sc. degree in Chemistry

Kazaure M. A (1996), Preparation and Characterization of Graft Copolymers of Cotton and Tencel Celluloses. PhD Thesis *Bayero University, Kano*

Khullar R. Varshny V.K. and Nathani. P. L. (2008). Grafting of Acrylonitrile on to Cellulosic Material Derived From Bamboo (Dendro Calamus Strictus). *Xpress Polymer Letters* 2, 12 – 18

Kumar V., Bhardway Y.K., Raulat KP and Sabhanwal S, (2005). Radiation Induced Grafting of Vinyl Benzyltrimethyl Ammonium Chloride (VBT) on to Cotton Fabric and Study of its Anti-bacterial Activities. *Radiant phys. Chem*.73, 175 – 182

Kulicke W. M., Kull A. N., Kull W. and Ihelking H., (1996). Characterization of Carboxy Methyl Cellulose Solution in Terms of their Molecular Structure and its Influence on Rheological Behavior. *Polymer* 37, 2723

Gürdağ, G., & Sarmad, S. (2013). Cellulose graft copolymers: synthesis, properties, and applications. In *Polysaccharide based graft copolymers* (pp. 15-57): Springer.

Habibu, S., Sarih, N. M., & Mainal, A. J. R. a. (2018). Synthesis and characterisation of highly branched polyisoprene: exploiting the "Strathclyde route" in anionic polymerisation. *8*(21), 11684-11692.

Jiang, F., Pan, C., Zhang, Y., & Fang, Y. J. A. S. S. (2019). Cellulose graft copolymers toward strong

thermoplastic elastomers via RAFT polymerization. *480*, 162-171.

Kumar, R., Sharma, R. K., & Singh, A. P. J. P. B. (2018). Grafted cellulose: a bio-based polymer for durable applications. *75*(5), 2213-2242.

Negish K. (1997). Personal Product Ltd. Bol. Inst. Prod. Florestais Madeiras Deriv. 3, 31 Negish M., Nakamura Y., Kakinama I. and Huka Y. (1965). Grafting of Acrylate Monomer on Cotton Fabric. *J. Appl. Polym. Sci.* 9. 2227

Neetu B., Gupta P.K. and Sanjay N. (2011). Ceric – Induced Grafting of Acrylonitrile on to ALPH Cellulose Isolated from Lantana Camara. *Cellulose Chem. Technol*., 45 (5-6), 321-327

Remzi G. (2010). Examining the Effect of Mercerization Process Applied Under Different Conditions for Dimensional Stability. Scientific Research and Essays, 5(6), 560-571

Sebenik A., (1998). Living Free Radical Block Copolymerization using thio iniferters, *Prog*. *Polym. Sci.* 23, 875 – 917

Zahran M. K., Marsy M. and Mahmoud R. I. (2003). Grafting of Acrylic Monomers on to Cotton Fabric Using an Activated Cellulose Thiocarbonate AIBN Redox System. *J. App. Polym. Sci.* 26, 149

Zahran M.K.and Magdy K. (2006). Grafting of

\MMA and Other Vinyl Monomers on to Cotton Fabric Using Ce(iv) ion. Cellulose Thiocarbonate Redox System. *Journal of Polymer Research.*13,1,6.